

This is an Open Access document downloaded from ORCA, Cardiff University's institutional repository: <https://orca.cardiff.ac.uk/id/eprint/116448/>

This is the author's version of a work that was submitted to / accepted for publication.

Citation for final published version:

Fantong, Wilson Yetoh, Kamtchueng, Brice Tchakam, Ishizaki, Yasuo, Chi Fru, Ernest, Fantong, Emilia Bi, Wirmvem, Mengnjo Jude, Tongwa AKA, Festus, Nlend, Bertil, Harman, Didier, Ueda, Akira, Kusakabe, Minoru, Tanyileke, Gregory, Ohba, Takeshi and Fru, Ernest Chi 2019. Major ions,  $\delta^{18}\text{O}$ ,  $\delta^{13}\text{C}$  and  $^{87}\text{Sr}/^{86}\text{Sr}$  compositions of water and precipitates from springs along the Cameroon Volcanic Line (Cameroon, West Africa): Implications for provenance and volcanic hazards. *Journal of African Earth Sciences* 150, pp. 12-22. 10.1016/j.jafrearsci.2018.09.025

Publishers page: <http://dx.doi.org/10.1016/j.jafrearsci.2018.09.025>

Please note:

Changes made as a result of publishing processes such as copy-editing, formatting and page numbers may not be reflected in this version. For the definitive version of this publication, please refer to the published source. You are advised to consult the publisher's version if you wish to cite this paper.

This version is being made available in accordance with publisher policies. See <http://orca.cf.ac.uk/policies.html> for usage policies. Copyright and moral rights for publications made available in ORCA are retained by the copyright holders.



Manuscript Number: AES6311R2

Title: Major ions,  $\delta^{18}O$ ,  $\delta^{13}C$  and  $^{87}Sr/^{86}Sr$  compositions of water and precipitates from springs along the Cameroon Volcanic Line (Cameroon, West Africa): Implications for provenance and volcanic hazards

Article Type: VSI:Lake Nyos, 30 years after

Keywords: Bubbling springs. Precipitates. Composition. Provenance. Volcanic activity. Hazards mitigation.

Corresponding Author: Dr. Wilson Yetoh Fantong, Ph.D

Corresponding Author's Institution: Institute of geological and mining research, P.O. 4110, Yaounde

First Author: Wilson Yetoh Fantong, Ph.D

Order of Authors: Wilson Yetoh Fantong, Ph.D; Brice Tchakam Kamtchueng, PhD; Yasuo Ishizaki, Ph.D; Ernest Chi FRU, Ph.D; Emilia Bi Fantong, Ph.D; Mengnjo Jude Wirmvem, Ph.D; Festus Aka Tongwa, Ph.D; Bertil Nlend, M.Sc; Didier Harman, M.Sc; Akira Ueda, Ph.D; Minoru Kusakabe, Ph.D; Gregory Tanyileke, Ph.D; Takeshi Ohba, Ph.D

Abstract: A combined study of major ions,  $\delta^{18}O$ ,  $\delta D$ ,  $^{13}C$ ,  $^{87}Sr/^{86}Sr$  isotopes, X-ray diffraction, scanning electron microscopy, and electron probe microanalyses on springs and spring mineral precipitates along the Cameroon Volcanic Line (CVL) was undertaken to understand water chemistry, and infer the type and origin of the precipitates. The waters are of evaporated Na+K-Cl and non-evaporated Ca+Mg-HCO<sub>3</sub> types, with the more mineralized (electrical conductivity-EC of 13130  $\mu S/cm$ ) Lobe spring inferred to result from interaction of circulating 49°C waters with magmatic volatiles of the active Mt. Cameroon. Water mineralization in the other springs follows the order: Sabga A > Sabga B > Bambui B > Bambui A > Nyos Cave. But for the Nyos Cave spring, all other springs contain fluoride (up to 0.5 - 35.6 mg/l above WHO potable water upper limit). The Sabga spring contains arsenic (up to 1.3 mg/l above the WHO limits). The springs show low fractionation temperatures in the range of 19 - 43 °C. The Lobe and Sabga A springs are precipitating dolomite (CaMg(CO<sub>3</sub>)<sub>2</sub>), while the Nyos Cave, Bambui A, Bambui B and Sabga B springs precipitate trona ((Na<sub>3</sub>H(CO<sub>3</sub>)<sub>2</sub>.H<sub>2</sub>O). Our data suggest a marine provenance for the carbonates, and point to a volcanic input for the Lobe, Nyos, Sabga A, and Bambui A springs. The latter springs are therefore proposed as proxies for monitoring volcanic activity for hazard mitigation along the CVL.

## **NOTE TO EDITOR AND REVIEWERS**

- (1) We modified the title slightly to make it sharper, shorter and punchier (the modified version is in BLUE colour)
- (2) Apart from the review comments, we saw a few editing issues in the text and corrected. Find them in BLUE colour
- (3) Reactions to Editor and Reviewers comments are in RED

## RESPONSE TO EDITOR AND REVIEWERS

L. 28: contained = contains : **Corrected on line 28**

L. 55-56: Order references in chronological order (also L. 84 and check throughout the MS) : **References have been ordered chronologically in the entire MS. Example is shown on line 81**

L. 76: add "." At end of sentence (also for L. 396) : **Added**

L. 78-79. Split this sentence in two sentences for clarity : **Sentence has been modified for clarity on lines 76-79**

L. 97. Warmness = heating : **Corrected on line 93**

L. 100-101. Form of the use of Figure or Fig. (editing issue) : **Form corrected**

L. 138. Impact = impacts : **Corrected on line 131**

L. 150. Delete "very" : **Deleted**

L. 176. Delete ", " after "Fantong et al." **Deleted on line 168**

L. 178. Delete "(...)" in Davies reference : **Deleted on line 169**

L. 189. Stoichiometry? Is this correct + Faure, 1991 (add ",") (same for L. 198 Appelo and Postman, 2005 + L. 222 + L. 348) : **All corrections done**

L. 216. Delete space before "were" (also for L. 374 before "whilst") : **Corrected**

L. 227. Field "of" kaolinite (add "of") : **Corrected on line 218**

L. 262 + 271. Almost absence. Try to find another expression : **Alternative expression used on lines 257 and 267**

L. 285. Mid-1900s : **Corrected on line 282**

L. 298-299. Is T expressed in °C or K, please mention : **°C, mentioned on line 297**

L. 317. Delete "ocean-continental boundary" (as it is already defined before) : **Deleted**

L. 350 Kusakabe (2017): add the "(...)" : **added on line 346**

L. 355. "... when the system". This sentence lost its structure, please check and rephrase. **Has been checked and corrected**

L. 352-357: I don't know if this part is strictly necessary to tell your story, although it is obviously correct to say so. Up to you. It comes a bit out of the blue, as I think "magmatic degassing" sounds "volcanic", too volcanic for the system we have here. **Per the first reviewer comment, i think it is necessary because it gives more justification for monitoring**

L. 359. law = low : **Corrected on line 355**

L. 360. Carbondioxide = **CO<sub>2</sub>** on line 357

L. 373. Fluorine = origin : **Corrected**

Fig. 18. Liotta et al. (2016) = Liotta et al. (2017) : **Corrected on Fig. 18**

Tables. Red colour should be black. **Changed in Table 1**

Specific comment.

I suggest you add the chemical formula for trona and dolomite the first time you use it in the text (or table) : **Chemical formulae of trona and dolomite introduced in abstract (lines 30 and 31)**

- 
- 
- 
- 

- Reply
- ,
- Reply All
- or
- Forward

Send

**Major ions,  $\delta^{18}\text{O}$ ,  $\delta^{13}\text{C}$  and  $^{87}\text{Sr}/^{86}\text{Sr}$  compositions of water and precipitates from springs along the Cameroon Volcanic Line (Cameroon, West Africa): Implications for provenance and volcanic hazards**

Wilson Yetoh FANTONG<sup>1Ψ</sup>, Brice Tchakam KAMTCHUENG<sup>1</sup>, Yasuo ISHIZAKI<sup>2</sup>, Ernest Chi FRU<sup>3</sup>, Emilia Bi FANTONG<sup>4</sup>, Mengnjo Jude WIRMVEM<sup>1</sup>, Festus Tongwa AKA<sup>1</sup>, Bertil NLEND<sup>1</sup>, Didier HARMAN<sup>4</sup>, Akira UEDA<sup>5</sup>, Minoru KUSAKABE<sup>5</sup>, Gregory TANYILEKE<sup>1</sup>, Takeshi OHBA<sup>6</sup>

<sup>1</sup> Hydrological Research Center/ IRGM, Box 4110, Yaounde-Cameroon

<sup>2</sup> Graduate School of Science and Engineering and Research, Environmental and Energy Sciences, Earth and Environmental Systems

<sup>3</sup> School of Earth and Ocean Sciences, Cardiff University, Cardiff, Park Place, Wales-United Kingdom

<sup>4</sup> Ministry of Secondary Education, Cameroon

<sup>5</sup> Laboratory of Environmental Biology and Chemistry, University of Toyama, Gofuku 3190, Toyama 930-8555 Japan

<sup>6</sup> Department of Chemistry, School of Science, Tokai University, Hiratsuka, 259-1211, Japan

Ψ Corresponding author: [fyetoh@yahoo.com](mailto:fyetoh@yahoo.com); [fantongy@gmail.com](mailto:fantongy@gmail.com)

A combined study of major ions,  $\delta^{18}\text{O}$ ,  $\delta\text{D}$ ,  $^{13}\text{C}$ ,  $^{87}\text{Sr}/^{86}\text{Sr}$  isotopes, X-ray diffraction, scanning electron microscopy, and electron probe microanalyses on springs and spring mineral precipitates along the Cameroon Volcanic Line (CVL) was undertaken to understand water chemistry, and infer the type and origin of the precipitates. The waters are of evaporated Na+K-Cl and non-evaporated Ca+Mg-HCO<sub>3</sub> types, with the more mineralized (electrical conductivity-EC of 13130  $\mu\text{S}/\text{cm}$ ) Lobe spring inferred to result from interaction of circulating 49°C waters with magmatic volatiles of the active Mt. Cameroon. Water mineralization in the other springs follows the order: Sabga A > Sabga B > Bambui B > Bambui A > Nyos Cave. But for the Nyos Cave spring, all other springs contain fluoride (up to 0.5 - 35.6 mg/l above WHO potable water upper limit). The Sabga spring contains arsenic (up to 1.3 mg/l above the WHO limits). The springs show low fractionation temperatures in the range of 19 – 43 °C. The Lobe and Sabga A springs are precipitating dolomite ( $\text{CaMg}(\text{CO}_3)_2$ ), while the Nyos Cave, Bambui A, Bambui B and Sabga B springs precipitate trona ( $(\text{Na}_3\text{H}(\text{CO}_3)_2 \cdot \text{H}_2\text{O})$ ). Our data suggest a marine provenance for the carbonates, and point to a volcanic input for the Lobe, Nyos, Sabga A, and Bambui A springs. The latter springs are therefore proposed as proxies for monitoring volcanic activity for hazard mitigation along the CVL.

1 **Major ions,  $\delta^{18}\text{O}$ ,  $\delta^{13}\text{C}$  and  $^{87}\text{Sr}/^{86}\text{Sr}$  compositions of water and precipitates from springs**  
2 **along the Cameroon Volcanic Line (Cameroon, West Africa): Implications for provenance**  
3 **and volcanic hazards**

4  
5 Wilson Yetoh FANTONG<sup>1</sup> $\Psi$ , Brice Tchakam KAMTCHUENG<sup>1</sup>, Yasuo ISHIZAKI<sup>2</sup>, Ernest Chi  
6 FRU<sup>3</sup>, Emilia Bi FANTONG<sup>4</sup>, Mengnjo Jude WIRMVEM<sup>1</sup>, Festus Tongwa AKA<sup>1</sup>, Bertil  
7 NLEND<sup>1</sup>, Didier HARMAN<sup>4</sup>, Akira UEDA<sup>5</sup>, Minoru KUSAKABE<sup>5</sup>, Gregory TANYILEKE<sup>1</sup>,  
8 Takeshi OHBA<sup>6</sup>

9 <sup>1</sup> Hydrological Research Center/ IRGM, Box 4110, Yaounde-Cameroon

10 <sup>2</sup> Graduate School of Science and Engineering and Research, Environmental and Energy  
11 Sciences, Earth and Environmental Systems

12 <sup>3</sup> School of Earth and Ocean Sciences, Cardiff University, Cardiff, Park Place, Wales-United  
13 Kingdom

14 <sup>4</sup> Ministry of Secondary Education, Cameroon

15 <sup>5</sup>Laboratory of Environmental Biology and Chemistry, University of Toyama, Gofuku 3190,  
16 Toyama 930-8555 Japan

17 <sup>6</sup>Department of Chemistry, School of Science, Tokai University, Hiratsuka, 259-1211, Japan

18  $\Psi$  Corresponding author: [fyetoh@yahoo.com](mailto:fyetoh@yahoo.com); [fantongy@gmail.com](mailto:fantongy@gmail.com)

19 **Abstract**

20 A combined study of major ions,  $\delta^{18}\text{O}$ ,  $\delta\text{D}$ ,  $^{13}\text{C}$ ,  $^{87}\text{Sr}/^{86}\text{Sr}$  isotopes, X-ray diffraction, scanning  
21 electron microscopy, and electron probe microanalyses on springs and spring mineral  
22 precipitates along the Cameroon Volcanic Line (CVL) was undertaken to understand water  
23 chemistry, and infer the type and origin of the precipitates. The waters are of evaporated Na+K-  
24 Cl and non-evaporated Ca+Mg-HCO<sub>3</sub> types, with the more mineralized (electrical conductivity-  
25 EC of 13130  $\mu\text{S}/\text{cm}$ ) Lobe spring inferred to result from interaction of circulating 49°C waters  
26 with magmatic volatiles of the active Mt. Cameroon. Water mineralization in the other springs  
27 follows the order: Sabga A > Sabga B > Bambui B > Bambui A > Nyos Cave. But for the Nyos  
28 Cave spring, all other springs contain fluoride (up to 0.5 - 35.6 mg/l above WHO potable water  
29 upper limit). The Sabga spring contains arsenic (up to 1.3 mg/l above the WHO limits). The  
30 springs show low fractionation temperatures in the range of 19 – 43 °C. The Lobe and Sabga A  
31 springs are precipitating dolomite (CaMg(CO<sub>3</sub>)<sub>2</sub>), while the Nyos Cave, Bambui A, Bambui B

32 and Sabga B springs precipitate trona ( $(\text{Na}_3\text{H}(\text{CO}_3)_2 \cdot \text{H}_2\text{O})$ ). Our data suggest a marine provenance  
33 for the carbonates, and point to a volcanic input for the Lobe, Nyos, Sabga A, and Bambui A  
34 springs. The latter springs are therefore proposed as proxies for monitoring volcanic activity for  
35 hazard mitigation along the CVL.

36 Key words: *Bubbling springs. Precipitates. Composition. Provenance. Volcanic activity.*  
37 *Hazards mitigation.*

38

39

## 40 **Introduction**

41 Mineral-depositing springs are natural systems that offer a good opportunity to study various  
42 mechanisms by which waters establish equilibrium with conditions at the Earth's surface  
43 (Amundson and Kelly, 1987; Omelon et al., 2006). For example, carbonate-precipitating waters  
44 provide an opportunity to evaluate a dynamic carbonate system and the major controls associated  
45 with calcite precipitation (Barnes, 1965; Jacobson and Usdowski, 1975), including; isotope  
46 fractionation associated with natural calcite precipitation from spring waters (McCrea, 1950;  
47 Friedman, 1970; Usdowski et al., 1979; Dandurand et al., 1982; Amundson and Kelly, 1987;  
48 Usdowski and Hoefs, 1990; Hamilton et al., 1991; Liu et al., 2003), as well as the types,  
49 morphologies, textures, and processes involved in the formation of various carbonate phases  
50 (Tucker and Bathurst, 1990; Bradley and Eugster, 1969; Ford and Pedley, 1996; Forti, 2005).

51

52 Many orifices of gas-water-carbonate interacting systems occur along the Cameroon Volcanic  
53 Line (CVL-Fig. 1). Based on carbonate enrichment studies on volcanic debris and springs in part  
54 of the continental sector of the CVL (Le Marechal, 1976; Verla et al., 2014); chemical and  
55 isotopic characteristics of fluids along the CVL (Tanyileke, 1994); the geochemistry of gases in  
56 springs around Mt. Cameroon and Lake Nyos (Kusakabe et al., 1989; Sano et al., 1990; Aka,  
57 1991); the sedimentology and geochemistry of the Bongongo and Ngol travertines along the  
58 CVL (Bisse et al., 2018), the following hypotheses have been proposed: (1) the bubbling mineral  
59 springs along the CVL contain abundant  $\text{CO}_2$ . (2) The  $\text{CO}_2$  in the bubbling springs is dominantly  
60 of magmatic origin. (3) Helium and carbon isotope ratios of gases from a few of the springs

61 along the CVL revealed a signature similar to hotspot type magma. (4) The precipitating  
62 minerals are travertines.

63 Although these studies provide initial data to understand the geochemical dynamics within the  
64 CVL gas-water-carbonate systems, gaps required to better understand the system include; a) a  
65 total absence of comprehensive information on the classification and genetic processes of the  
66 precipitating carbonates, which is exploited by the indigenes for preparation of traditional soup,  
67 b) high concentration ( $> 100$  mg/l) of geogenic fluoride has been reported (e.g., Kut et al., 2016;  
68 and references there-in) in thermal waters along the Ethiopian rift. Such concentrations of  
69 fluoride in water that is used for domestic purposes and livestock rearing can cause tremendous  
70 health effects (e.g., Fantong et al., 2010). Livestock rearing on the slopes of the CVL heavily  
71 consumes water from the springs (Fig. 2), so there is still a need to re-assess their chemical  
72 characteristics with focus on potential harmful elements like fluoride and arsenic, and c) the  
73 carbonate-water fractionation temperature remains unknown.

74 Against this backdrop, the objectives of this study are to 1) characterize the water chemistry with  
75 focus on health implications, 2) estimate the carbonate-water fractionation temperature, and 3)  
76 identify, describe and classify the carbonates that are precipitating from the springs.

77

## 78 **Study area**

79 Figure 1 shows, the sample sites along the CVL, a prominent 1600 km long Y-shaped chain of  
80 Tertiary to Recent, generally alkaline volcanoes that overlap an array of dextral faults called the  
81 Central Africa Shear Zone (CASZ) (Ngako et al., 2006) on the African continent, comparable  
82 only to the East Africa Rift System. The CVL follows a trend of crustal weakness that stretches  
83 from the Atlantic Island of Annobon, through the Gulf of Guinea, to the interior of the African  
84 continent (Fitton, 1980; Déruelle et al., 1987, Halliday et al., 1988;). It is unique amongst  
85 intraplate volcanic provinces in that it straddles the continental margin and includes both oceanic  
86 and continental intraplate volcanism. The oceanic sector constitutes a mildly alkaline volcanic  
87 series, which evolves towards phonolite, while the continental sector evolves towards rhyolite  
88 (e.g., Fitton, 1980). Isotopic studies of lavas (Halliday et al., 1988) divide the CVL into three  
89 sectors: an oceanic zone, ocean-continent boundary zone and a continental zone.

90 The study area overlaps two (coastal and tropical western highlands) of the five climatic zones in  
91 Cameroon, with mean annual rainfall of 5000 and 3000 mm, mean annual atmospheric

92 temperatures of 26°C and 21°C, humidity of 85% and 80%, and evaporation of 600 mm and 700  
93 mm, respectively (Sighomnou, 2004). Hydrologically, three (coastal, Sanaga, and Niger) of the  
94 five river basins in Cameroon drain the study area in a dendritic manner. According to Le  
95 Marechal (1968) and Tanyileke (1994), riverine and in aquifer waters encounter heat and mantle-  
96 derived CO<sub>2</sub> gas that emanate through the CASZ, causing heating and bubbling of the spring  
97 systems along the CVL. At each spring site the gas phase manifests as either bubbles or ‘rotten  
98 egg’ smell, while the precipitates occur as white films, white grains in volcanic ash, stalactite and  
99 stalactmite in caves, and mounds around orifices as shown in Fig. 3. At the sites of Sabga A in  
100 Fig. 3, animals consume the water as a source of salt, while humans exploit the precipitates for  
101 food recipes.

102

### 103 **Method of study**

104 Water and precipitate samples were collected from selected bubbling soda spring sites along the  
105 CVL (Fig. 3) in October 2015. Each water sample was collected in 3 acid-washed 250 ml  
106 polyethylene bottles after rinsing them thrice with the sample. At each sampling site, an  
107 unfiltered, unacidified and tightly corked sample was collected in one bottle for subsequent  
108 analyses for stable environmental isotopes of hydrogen ( $\delta^2\text{H}$ ) and oxygen ( $\delta^{18}\text{O}$ ). The second  
109 bottle contained un-acidified but filtered sample for anion analyses, and the third filtered and  
110 acidified sample for cations and trace elements analyses. Prior to sample collection, in-situ  
111 physicochemical measurements were recorded for pH (TOA-DKK HM-30P meter), electrical  
112 conductivity (TOA-DKK CM-31P EC meter), reduction-oxidation potential (TOA-DKK ORP  
113 meter), and water temperature. Geographical parameters (latitude, longitude and altitude) of each  
114 sample site were recorded in the field using a hand-held Garmin GPS. Alkalinity was measured  
115 using a ‘‘Hach’’ field titration kit, after addition of 0.16 N H<sub>2</sub>SO<sub>4</sub> to the sample to reach the  
116 endpoint titration (pH 4.5). Samples were filtered through 0.2  $\mu\text{m}$  filters prior to major ions and  
117 dissolved silica determination. Three kilograms chunks of massive carbonate was chipped off  
118 with a hammer at sites with consolidated precipitate, and 300 g scoped from sites with  
119 unconsolidated precipitate. Each precipitate was put in a clean plastic container, sealed and  
120 labelled.

121 Water samples and precipitates were transported to the University of Toyama, in Japan for  
122 chemical analyses.

123 The various chemical analyses that were done in various institutes in Japan are tabulated in Table  
124 1.

125

## 126 **Results and Discussions**

### 127 *Variation of water chemistry*

128 Chemical compositions and isotopic ratios of water samples and carbonate phases are presented  
129 in Tables 2 and 3. Measured in-situ parameters show values in the range of 54 - 13130  $\mu\text{S}/\text{cm}$  for  
130 EC, 4.3 - 7.5 for pH, and 19.3 - 47.4°C for water temperature.

131 The chemistry of the observed water resources determined with the use of the Piper's diagram  
132 (Piper, 1944) (Fig. 4a), shows that water from the Lobe soda springs and its nearby hand dug  
133 wells, located in the ocean-continent-boundary (OCB) and close to the ocean (Fig. 4a), have a  
134 dominant Na+K-Cl signature. On the other hand, water from the soda springs in Sabga, Bambui,  
135 and Nyos have dominantly Ca+Mg-HCO<sub>3</sub> signature. The observed disparity in water facies may  
136 be due to the proximity of the Lobe springs to the ocean, which impacts the sodium chloride  
137 characteristics as accorded in Le Marechal (1976). Whilst in the other springs, an interaction  
138 between primary and secondary minerals in rocks and water could be the dominant explanation  
139 as also explained by other researchers (Kamctung et al., 2014; Fantong et al., 2015). The Stiff  
140 diagrams for the water chemistry (Fig. 4b), also depict similar water facies like the Piper's  
141 diagram, but they further suggest varying degree of mineralization of the water sources. In the  
142 OCB, the larger sizes of the stiff diagram for the Lobe soda springs indicate more mineralization  
143 than for water from the wells. Likewise in the samples from the continental sector (CS) the water  
144 in the Sabga soda springs are most mineralized, followed by those in Bambui and the least  
145 mineralized is that from the Nyos soda spring. The observed variation in degree of mineralisation  
146 could in part be indicating variation in residence time, where the older springs are enriched in  
147 elements from aquifer minerals than in younger springs (e.g., Fantong et al., 2010a; Kamctung  
148 et al., 2015) that are renewed through a local and short recharge-discharge flow paths.

149

### 150 *Recharge mechanisms and evaporation of the sampled waters*

151 Isotopic ratios of hydrogen and oxygen, which are used in this study to infer recharge and  
152 evaporation mechanisms in the waters are also shown in Table 2 and graphically presented in Fig.  
153 5. The  $\delta\text{D}$  values ranged from -41.8 in Sabga A soda spring to -26 ‰ in water from well 5.

154 Oxygen isotope ( $\delta^{18}\text{O}$ ) values range from -6.3 ‰ in Sabga A spring to -3.1 ‰ in water from well  
155 3. Due to the paucity of isotope data on local rainfall, the Global Meteoric Water Line (GMWL)  
156 of Craig (1961), which is defined by the line  $\delta\text{D} = 8\delta^{18}\text{O} + 10$  is also presented as a reference.  
157 Distribution of sample water in the  $\delta\text{D}$ - $\delta^{18}\text{O}$  graph suggests that water in the Bambui and Sabga  
158 soda springs are subject to little or no evaporation, while the Lobe soda springs suggest slight  
159 evaporation, but water from the wells and Nyos soda springs show remarkable evaporation  
160 tendencies. Such a pattern depicts that the Bambui and Sabga soda springs are subject to the  
161 mechanism of preferential flow pass, which is caused by rapid recharge (e.g., Tsujimura et al.,  
162 2007; Asai et al., 2009), that is favored by the highly altered and jointed lavas as opposed to the  
163 Lobe and Nyos cave soda springs, and the wells. Except for the Lobe soda springs, the other  
164 springs are sources of drinking water for animals (cattle and goats), and a source of minerals  
165 (carbonate) for local manufacture of soup for consumption by the nearby population, thus it is  
166 important to assess at a preliminary scale the medical hydrogeochemical characteristics of the  
167 springs.

#### 168 ***Health implications of the water chemistry***

169 Given that the gas bubbling springs are located in the area of livestock rearing and human  
170 activities, their chemistry is here preliminarily evaluated to assess potential health implications.  
171 With respect to fluoride, Figure 6a shows that except for the Nyos cave soda spring, all the other  
172 soda springs contain fluoride at concentrations that are above the WHO optimal limit (1.5 mg/l  
173 e.g., Kut et al., 2016). This indicates that the animals and the population that exploit these  
174 springs are potentially exposed to fluoride poisoning as reported by Fantong et al. (2010b) in the  
175 Far Northern Region of Cameroon. The potential geogenic and volcanic provenance (Davies,  
176 2013), and actual epidemic effects of such high concentrations of fluoride are not within the  
177 scope of this study, and need further investigation.

178 With respect to arsenic (As), Figure 6b shows that the Sabga soda springs contain As at  
179 concentrations as high as 1.33 ppm that are above the WHO upper limit (0.03 ppm in drinking  
180 water). Based on the field observations that water from the Sabga soda springs is heavily  
181 consumed by cattle, and carbonate there-from is exploited for consumption by the population, it  
182 is also a challenge for medical geochemists to carry out a comprehensive investigation into the  
183 incidence, origin, mobilization and epidemiological effects of arsenic in these areas.

184

185 ***Impact of volcanic volatile or magmatic input on chemistry of the spring water***

186 The dissolved state of elements and saturation state of compounds observed in the springs are to  
187 an extent determined by their saturation indices and stoichiometry (e.g., Faure, 1991).

188

189 ***Saturation indices and activity diagrams***

190 The saturation index (SI) of a given mineral in an aqueous system is defined as (Lloyd and  
191 Heathcoat, 1985; and Deutch, 1997):

192 
$$SI = \log \left( \frac{IAP}{K_{sp}} \right) \quad (1)$$

193 where IAP is the ion activity product and  $K_{sp}$  is the solubility product of the mineral in the  
194 system. A  $SI > 0$  points to supersaturation, and a tendency for the mineral to precipitate from the  
195 water. Saturation can be produced by factors like incongruent dissolution, common ion effect,  
196 evaporation, and rapid increase in temperature and  $CO_2$  exsolution (Appelo and Postma, 2005).  
197 A  $SI < 0$  points toward undersaturation, and implies that water dissolves the minerals from  
198 surrounding rocks. Negative SI value might also reflect that the character of water is either from  
199 a formation with insufficient concentrations of the mineral for precipitation to occur (Garrels and  
200 Mackenzie, 1967).

201 The thermodynamic data used in this computation are those contained in the database of  
202 'Phreeqc for Windows'. A plot of the calculated SI (with respect to quartz, anhydrite, aragonite,  
203 calcite and dolomite) versus TDS (Fig.7) groups the water samples into three subgroups:  
204 subgroup 1, which consists of water from the shallow wells is undersaturated with respect to all  
205 the selected phases and has the lowest TDS values that ranged from 63-83 mg/l. The  
206 undersaturation of subgroup 1 suggests that no mineral precipitates in the wells as observed on  
207 the field. Subgroup 2, which consists of Nyos cave soda spring, Bambui soda spring B and Sabga  
208 soda spring B, show supersaturation with respect to quartz, dolomite. On the field, this subgroup  
209 is found to be dominantly precipitating trona (a Na-rich carbonate) and dolomite to a lesser  
210 extent. Subgroup 3 that consists of the Lobe and Sabga A soda springs, are supersaturated with  
211 respect to dolomite, quartz and calcite, and it is actually precipitating more of dolomite, and  
212 trona to a lesser extent.

213 The stability of secondary minerals (Na and Ca montmorillonites, kaolinite, gibbsite) and  
214 amorphous quartz in the springs and wells were evaluated by plotting  $\log (a_{Na}/a_H)$  vs  $\log (a_{H_4SiO_4})$

215 (the albite system) (Fig. 8a) and  $\log (a_{\text{Ca}2}/a_{\text{H}})$  versus  $\log (a_{\text{H}_4\text{SiO}_4})$  (the anorthite system) (Fig.  
216 8b). These diagrams were drawn with the assumption that aluminum was preserved in the  
217 weathering product (Appelo and Postma,1993), because the amount of alumina will remain  
218 constant in fresh rocks and its altered equivalent. The constant amount in alumina ( $\text{Al}_2\text{O}_3$ ) is  
219 because an apparent increase in its weight % is actually always caused by a reduction in the  
220 weight of the fresh rock to some smaller amount (Faure, 1991). End member compositions were  
221 also assumed using equilibrium relationship for standard temperature ( $25^\circ\text{C}$ ) and pressure (1  
222 atmosphere), which approximately reflect the springs and groundwater conditions. Activities of  
223 the species were computed using the analytical concentrations and activity coefficient  
224 determined by Phreeqc for Windows version 2.1 under the above conditions (Appelo and  
225 Postma, 1993). According to the figures, groundwater from the wells span the stability field of  
226 kaolinite, while all the soda springs with exception of the Nyos soda spring are in equilibrium  
227 within the Na and Ca -montmorillonite stability fields. This concurs with the incidence of clay  
228 minerals in the study area (Fantong et al., 2015). Moreover, the presence of kaolinite and  
229 montmorillonite in the study area occur as groundmass in the XRD (X-Ray Defraction) peaks of  
230 Figures 9b,10b, 11b, 12b, and 14b. A combination of information from the saturation indices and  
231 stability diagrams is supported by the presence of precipitating carbonate phases in the soda  
232 springs as shown in Fig. 1.

233

### 234 *Typology of carbonate phases*

235 The typology of the carbonate phases that precipitate from the observed soda springs is done by  
236 describing the morphology by using SEM images, and identifying the carbonate phase by using  
237 XRD diagrams and EPMA elemental mapping.

238

### 239 **Carbonate from the Nyos cave soda spring**

240 The SEM image in Fig. 9a shows that the carbonate is an association of cluster of powdery  
241 amorphous groundmass upon which sub-euhedral crystals developed. This carbonate is identified  
242 with XRD peaks (Fig.9b) as a trona (low- syn trisodium hydrogen dehydrate carbonate). To  
243 accentuate the trona phase, an elemental EPMA mapping (Fig.9 c, d, e and f) shows the  
244 dominance of sodium, traces of calcium and total absence of magnesium.

245

246 **Carbonate from Sabga A soda spring**

247 The SEM image of Fig. 10a shows that the carbonate is nail-shaped stalactite crystals protruding  
248 from a cluster of powdery amorphous groundmass. This carbonate is identified with XRD peaks  
249 (Fig.10b) as a dolomite (calcium-magnesium bicarbonate). Dolomite precipitate in this spring is  
250 supported by an elemental EPMA mapping (Fig. 10 c, d, e and f), which shows a dominance and  
251 remarkable presence of both calcium and magnesium, with traces of sodium.

252

253 **Carbonate from Sabga B soda spring**

254 The SEM image of Fig. 11a shows that the carbonate is made up of radiating tabular columns of  
255 crystals whose faces are edged by bacteria. This carbonate is identified with XRD peaks (Fig.  
256 11b) as a trona (low-syn trisodium hydrogen dehydrate carbonate). The presence of this trona  
257 precipitating in this spring is justified by an elemental EPMA mapping (Fig. 11c, d, e and f),  
258 which shows a dominance of sodium and an almost absence of calcium and magnesium.

259

260 **Carbonate from Bambui B soda spring**

261 The SEM image of Fig. 12a shows that the morphology of the carbonate is an intersecting  
262 mosaic of tabular crystals whose faces are edged by bacteria. This carbonate is identified with  
263 XRD peaks (Fig. 12b) as a trona similar to that of Sabga B. The presence of this trona  
264 precipitating in this spring is supported by an elemental EPMA mapping (Fig. 12 c, d, e and f),  
265 which shows a dominance of sodium and low content of calcium and magnesium. The  
266 disseminated distribution of fluorine, which almost coincide with the distribution of faint calcite  
267 suggest the presence of fluorite (CaF<sub>2</sub>), which could be dissolving to enrich the water phase with  
268 fluoride as seen in Fig. 13e.

269

270 **Carbonate from Lobe D soda spring**

271 The SEM image of Fig. 14a shows that the carbonate is a coliform flower-shape radiating  
272 crystals, which is colonized by bacteria. This carbonate is identified with XRD peaks (Fig. 14b)  
273 as a dolomite. The occurrence of dolomite as the precipitate in this spring is supported by an  
274 elemental EPMA mapping (Fig. 14c, d, e and f), which shows high content of both calcium and  
275 magnesium, and low content of sodium.

276 Summarily, the carbonate phases that are precipitating from the studied soda springs along the  
277 CVL are dominantly dolomite and trona. The pristine geochemical attributes and characteristics  
278 of the carbonate are at a later phase altered (Demeny, 2016) by diatoms and bacteria as shown in  
279 Figure 11a and 12a. The incidence of bacteria in such a hydrogeochemical system leaves  
280 biogeochemists with another opportunity to assess the incidence and role of bacteria in the soda  
281 spring systems.

282

### 283 **Origin of the fluids and carbonates**

284 In a bid to identify the formation (sources and paleo temperature) processes that led to the  
285 formation of the observed carbonates, we used  $^{13}\text{C}$  isotopes,  $^{87}\text{Sr}/^{86}\text{Sr}$ , carbonate-water  
286 fractionation temperatures, and  $\text{Cl}^-$  versus  $\text{F}^-$  plot as geochemical tracers.

287

### 288 *Carbonate-water fractionation temperature*

289 Although oxygen-isotope thermometry based on isotopic fractionation of oxygen between  
290 carbonates and water dates back to the Mid-1900s, the carbonate-water oxygen isotopic  
291 fractionation equations are still being discussed. The use of isotope thermometry is based on  
292 several criteria: (i) the temperature dependence of the isotopic fractionation between the  
293 investigated compounds (in our case dolomite/trona and water) and (ii) the isotopic compositions  
294 of the compounds are known, (iii) the isotopic equilibrium between the compounds can be  
295 proven or at least reasonably assumed, and (iv) no subsequent isotopic alteration occurred after  
296 the deposition of carbonates. These considerations are valid for inorganic carbonate formation, as  
297 biogenic carbonate is severely affected by the organisms' metabolism, resulting in a species-  
298 dependent ‘‘vital effect’’ (Demeny et al., 2010 and references therein)

299 The temperatures at which the carbonate phases precipitate from the springs were calculated by  
300 using the empirical equation for the temperature dependence of calcite-water oxygen isotope  
301 fractionation from 10 to 70 °C as shown in equations 2 and 3 that were reported by Demeny et al.  
302 (2010).

$$303 \quad 1000 \cdot \ln \alpha = 17599/T - 29.64 \quad [\text{for travertines with a temperature range of } 30 \text{ to } 70^\circ\text{C}] \quad (2)$$

$$304 \quad 1000 \cdot \ln \alpha = 17500/T - 29.89 \quad [\text{for cave deposits for the range } 10 \text{ to } 25^\circ\text{C}] \quad (3)$$

305 The variable T are in °C.

306 The values obtained suggest that carbonates precipitate from soda springs along the CVL at  
307 temperature that varied from 18.5 - 43°C. The lowest fractionation temperatures (18.5 - 18.6°C)  
308 occurred in the Sabga soda springs, while the highest (35 - 43°C), occurred in the Lobe soda  
309 springs (Table 3). A plot (Fig. 15), shows that with the exception of the dolomite in the ‘Sabga  
310 A soda spring’, the tronas fractionated at lower temperature (~18.5 - 20 °C) than the dolomites,  
311 which fractionated at temperature ranging from 35.2 - 43°C. Based on Figure 15, the oxygen  
312 isotopes in carbonates precipitating along the Cameroon Volcanic Line yielded an empirical  
313 fractionation– temperature equations of:

$$314 \quad 1000.\ln\alpha = -0.2153T + 35.3 \quad (4)$$

315

### 316 *Stable isotopes of <sup>13</sup>C, <sup>87</sup>Sr/<sup>86</sup>Sr, and <sup>18</sup>O*

317 The observed carbonates (dolomite and trona) facies in the samples showed broad ranges in  
318 <sup>87</sup>Sr/<sup>86</sup>Sr, <sup>13</sup>C and δ<sup>18</sup>O. The <sup>87</sup>Sr/<sup>86</sup>Sr ratio varied from 0.706 - 0.713, the <sup>13</sup>C varied from -3.09 to  
319 5.22 VPDB and δ<sup>18</sup>O from -8.4 to -1.4 VPDB as shown in Table 3. Their δ<sup>13</sup>C values of observed  
320 dolomites are close to the range of values reported for carbonates precipitating from seawater (0  
321 -4 VPDB; Veizer et al., 1999; Shah et al., 2012). Indication of marine origin of the dolomites  
322 corroborates with field observation, because the dolomite precipitates from the Lobe soda spring  
323 located in the OCB of the study area. However, the carbonates (trona) identified in our study  
324 area showed relatively depleted δ<sup>13</sup>C signatures, which may indicate a possible external source of  
325 carbon during trona precipitation (Fig. 16) or a temperature dependent fractionation effect (Shah  
326 et al., 2012). The depleted δ<sup>18</sup>O in dolomite from the 49°C Lobe soda springs, may be due to its  
327 higher temperatures (thermogenic type) (Bisse et al., 2018), given that precipitation of dolomite  
328 from hot springs leads to relatively depleted δ<sup>18</sup>O ratios (Land, 1983).

329 With exception of the Lobe soda springs, where <sup>87</sup>Sr/<sup>86</sup>Sr value did not vary between the  
330 carbonate and water phases, in the other soda springs (Bambui soda springs A and B, Sabga soda  
331 springs A and B, and Nyos cave soda spring), the <sup>87</sup>Sr/<sup>86</sup>Sr ratio shows a decoupling tendency  
332 where the water phases contain relatively higher values than the carbonate phases (Fig. 17a). The  
333 relatively higher <sup>87</sup>Sr/<sup>86</sup>Sr ratio in the Lobe soda springs may indicate interaction of dolomitizing  
334 fluids with radiogenic lithologies (Shah et al., 2012), which commonly occur along the CVL  
335 (e.g., Aka et al., 2000; 2001). Moreover, the <sup>87</sup>Sr/<sup>86</sup>Sr versus <sup>18</sup>O cross plot (Fig. 17b), shows that  
336 the dolomites are richer in <sup>87</sup>Sr/<sup>86</sup>Sr ratio than the tronas. However, the signatures in the dolomite

337 of the Sabga soda spring “A” together with those in the tronas are closer to those of the marine  
338 signatures (McArthur et al., 2001). Such marine signatures in tronas (Na-rich carbonate) within  
339 the continental sector of the Cameroon Volcanic Line, may suggest the presence of paleo-  
340 continental sabkha environments, where various sodium carbonates have been recorded in  
341 tropical regions (Whitten and Brooks, 1972). This suggestion, however, requires further  
342 investigation.

343

#### 344 **Implications for monitoring and hazard mitigation**

345 Volcanogenic sources of fluorine (e.g., Symonds et al., 1987; Symonds et al., 1988; Bellomo et  
346 al., 2003) and chlorine (e.g., Keene and Graedel 1995) containing gasses have been reported in  
347 active and passive volcanic areas, and recently in the Nyiragongo volcano in Congo (Liotta et al.,  
348 2017). As used by the later, we also used a cross plot of chloride versus fluoride (Fig. 18) to infer  
349 volcanogenic contribution in the observed springs along the CVL. The figure suggests  
350 volcanogenic inputs into the Lobe, Nyos, Sabga A, and Bambui A springs. The implication of a  
351 volcanic input to these fluids suggests that they can be used to monitor volcanic activity and thus  
352 mitigate hazards, especially in the vicinity of the Lobe spring located close to the currently active  
353 Mt. Cameroon. Moreover, the dominant fluids in the Lobe, Nyos, Sabga A, and Bambui A  
354 springs are magmatic CO<sub>2</sub> and H<sub>2</sub>O (Sano 1990). Water dissolves slightly more in silicic melts  
355 than in basaltic melts, whereas CO<sub>2</sub> dissolves more in basaltic than in silicic melts. Kusakabe  
356 (2017) reports that the solubility of CO<sub>2</sub> and H<sub>2</sub>O in basaltic melts at 1200°C is a function of the  
357 total pressure of the volatiles, whose composition in the melt changes as the decompression  
358 proceeds. For example, at low pressure the mole fraction of H<sub>2</sub>O equals 0.2 and that of CO<sub>2</sub> is  
359 0.8, implying that basaltic melt becomes rich in CO<sub>2</sub> as the magma ascends and the confining  
360 pressure reduces, resulting to degassing. If degassing takes place in an open system, CO<sub>2</sub>-rich  
361 fluid leaves the magma. This solubility-controlled behavior of CO<sub>2</sub> in basaltic magma may  
362 explain a CO<sub>2</sub>-rich nature of fluids separated from the magma. The ultimate source of CO<sub>2</sub> in the  
363 Nyos, Lobe, Sabga A, and Bambui A springs may therefore be derived from the decarbonation of  
364 crystallized metasomatic fluids in the subcontinental lithosphere (Aka, 2015; Asaah et al., 2015).  
365 The low (-2 to -3 ‰) <sup>13</sup>C values of carbonates in the Nyos and Sabga soda spring may also  
366 indicate magmatic origin of the CO<sub>2</sub> that contributes in precipitating the carbonates. Thus, the

367 permanent supply of such CO<sub>2</sub> in the springs provides good sites for monitoring volcanic activity  
368 for hazard mitigation.

369

### 370 **Conclusions**

371 The chemistry of water in the bubbling soda springs observed along the Cameroon Volcanic Line  
372 shows an evaporated Na+K-Cl and non-evaporated Ca+Mg-HCO<sub>3</sub> facies in the ocean continental  
373 boundary sector (OCB) and continental sector (CS), respectively. In the OCB, the Lobe soda  
374 springs shows more mineralization than water from nearby hand dug wells. This may indicate  
375 that spring water (T=49°C) is circulating deeper than the well water. In the continental sector  
376 (CS) the water in the Sabga soda springs are the most mineralized, followed by those in Bambui  
377 soda spring and the least mineralized is the Nyos soda spring. With exception of the soda springs  
378 in the Nyos area, all other studied soda springs contain fluoride from geogenic fluorine at  
379 concentrations above the WHO upper limit, whilst concentrations of arsenic (> 0.3 mg/l) that  
380 also call for health concern occur in the Sabga soda springs. The observed soda springs are either  
381 saturated or super-saturated with respect to quartz, and carbonate phases, which are actually  
382 precipitating as dolomite and trona. The carbonate-water fractionation temperature varies from  
383 18.5 - 43°C. X-ray diffraction spectra and chemical mapping by electron probe microanalyzer  
384 unraveled that the precipitating carbonates occur as dolomite in the Lobe and Sabga A soda  
385 springs, and as trona in the Nyos, Bambui and Sabga B soda springs. Scanning electron  
386 microscope (SEM), reveals various morphologies of the carbonates, including amorphous to  
387 tabular euhedral tronas, and nail shaped to bacteria-colonized coliform dolomites. Geochemical  
388 tracers of <sup>13</sup>C, <sup>87</sup>Sr/<sup>86</sup>Sr, and <sup>18</sup>O indicate a dominantly marine provenance of the carbonate.  
389 Chloride versus fluoride cross plot suggest a contribution from volcanic volatiles in the Lobe,  
390 Nyos, Sabga A, and Bambui A springs. This contribution of a volcanic input to these fluids  
391 suggests that they can be used to monitor volcanic activity and thus mitigate hazards, especially  
392 in the vicinity of the Lobe spring that is located close to the currently active Mt. Cameroon.

393

### 394 **Acknowledgements**

395 We thank the Institute of Geological and Mining Research (IRGM), Yaoundé, for financial and  
396 logistical support during sampling. Thanks to the funders (JICA and JST) of SATREPS-IRGM  
397 project that provided field and laboratory equipment that were used to generate the data during

398 this study. We thank all the members of the Department of Environmental Biology and  
399 Chemistry, University of Toyama, Japan, for their enriching comments during the preparation of  
400 this manuscript. We are also grateful to Prof. Suh Emmanuel and Prof. Loic Peiffer for their  
401 review comments that enriched the content of the manuscript.

402

403

404

405

406

407

408

409

410

## 411 **References**

412

413 Aka, F.T., 1991. Volcano Monitoring by Geochemical Analyses of Volcanic Gases. Thesis, The  
414 University of Leeds, LS2 9JT. 94 pp.

415

416

417 Aka, F.T., 2000. Noble gas systematics and K–Ar Chronology: implications on the geotectonic  
418 evolution of the Cameroon Volcanic Line, West Africa, PhD thesis, Univ. Okayama, Japan.  
419 175 pp.

420 Aka, F. T. (2015) Depth of melt segregation below the Nyos maar-diatreme volcano (Cameroon,  
421 West Africa): Major trace element evidence and their bearing on the origin of CO<sub>2</sub> in Lake  
422 Nyos. Volcanic Lakes (Rouwet, D., Christenson, B., Tassi, F. and Vandemeulebrouck, J.,  
423 eds.), Springer-Heidelberg.

424

425

426 Aka, F.T., Kusakabe, M.K., Nagao, K., Tanyileke, G., 2001. Noble gas isotopic compositions  
427 and water/gas chemistry of soda springs from the islands of Bioko, Saõ Tome' and  
428 Annobon, along the Cameroon Volcanic Line, West Africa. Appl. Geochem.16, 323–338.

429

430 Amundson, R., Kelly, E., 1987. The chemistry and mineralogy of a CO<sub>2</sub>-rich travertine  
431 depositing spring in the California Coast Range. Geochim. Cosmochim. Acta 51, 2883–2890.

432

433 Appelo, C.A.J., Postma, D., 2005. Geochemistry, groundwater, and pollution. 2nd edn. Balkema  
434 Publishers, Rotterdam, 649 pp

435 Asai, K., Satake, H., and Tsujimura, M., 2009. Isotopic approach to understanding the

436 groundwater flow system within the andesitic strato-volcano in a temperate humid  
437 region: case study of Ontake volcano, Central Japan. *Hydrol. Processes*. 23, 559-571.  
438

439 Asaah, A. N. E., Yokoyama, T., Aka, F. T., Usui, T., Kuritani, T., Wirmvem, M. J., Iwamori, H.,  
440 Fozing, E. M., Tamen, J., Mofor, G. J., Ohba, T., Tanyileke, G. and Hell, J. V. (2015)  
441 Geochemistry of lavas from maar-bearing volcanoes in the Oku Volcanic Group of the  
442 Cameroon Volcanic Line. *Chem. Geol.* 406, 55–69.  
443

444 Barnes, I., 1965. Geochemistry of Birch Creek, Inyo County, California: a travertine depositing  
445 creek in an arid climate. *Geochim. Cosmochim. Acta* 29, 85–112.  
446

447

448 Bellomo, S., D’Alessandro, W., and Longo, M., 2003. Volcanogenic fluorine in rainwater around  
449 active degassing volcanoes: Mt.Etna and Stromboli Island, Italy. *Sci. Total Environ.* 301,  
450 175–185.  
451

452 Bisse, S. B., Ekomané, E., Eyong, J.T., Ollivier, V., Douville, E., Nganne, M.J.M., Bokanda,  
453 E.E., Bitom, L.D., 2018. Sedimentological and geochemical study of the Bongongo and  
454 Ngol travertines located at the Cameroon Volcanic Line. *Journal of African Earth Sciences*.  
455 DOI.org/10.1016/j.jafrearsci.2018.03.028  
456

457 Craig, H., 1961. Isotopic variations in meteoric waters. *Science* 133:1702–1703  
458

459 Dandurand, J.L., Gout, R., Hoefs, J., Menschel, G., Schott, J., Usdowski, E., 1982. Kinetically  
460 controlled variations of major components and carbon and oxygen isotopes in a calcite  
461 precipitating spring. *Chem. Geol.* 36, 299–315.  
462

463 Davies, T.C., 2013. Geochemical variables as plausible aetiological cofactors in the incidence of  
464 some common environmental diseases in Africa. *Journ. African Earth Sciences.* 79, 24-49  
465

466

467 Demeny, A., Kele, S., and Siklosy, Z., 2010. Empirical equations for the temperature  
468 dependence of calcite-water oxygen isotope fractionation from 10 to 70°C. *Rapid Commun.*  
469 *Mass Spectro.* 24, 3521-3526

470 Demeny, A., Nemeth, P., Czuppon, G., Leel-Ossy, S., Szabo, M., Judik, K., Nemeth, T., Steiber,  
471 J., 2016. Formation of amorphous calcium carbonate in caves and its implications for  
472 speleothem research. *Scientific Report.* 6, 39602  
473

474 Deruelle, B., Nni, J., and Kambou, R., 1987. Mount Cameroon: An active volcano of the  
475 Cameroon Volcanic Line. *J. African Earth Sciences.* 6, 197-214  
476

477 Deutsch, W.J., 1997. Groundwater geochemistry: fundamentals and application to  
478 contamination. CRC, Boca Raton  
479

480 Bradley, W.H., and Eugster, H.P., 1969. Geochemistry and paleolimnology of the trona deposits  
481 and associated authigenic minerals of green river formation of Wyoming. Geological Survey  
482 Professional Paper 496-B, US Government Printing office, Washington, 66 pp  
483

484 Fantong, W.Y., Satake, H., Ayonghe, S.N., Suh, C.E., Adelana, S.M.A., Fantong, E.B.S.,  
485 Banseka, H.S., Gwanfogbe, C.D., Woincham, L.N., Uehara, Y., Zhang, J., 2010b.  
486 Geochemical provenance and spatial distribution of fluoride in groundwater of Mayo  
487 Tsanaga River Basin, Far north Region, Cameroon: implications for incidence of fluorosis  
488 and optimal consumption dose. *Environ Geochem Health*. Vol. 32: 147-163  
489

490 Fantong, W.Y., Kamtchueng, B.T., Yamaguchi, K., Ueda, A., Issa, Ntchantcho, R., Wirmvem,  
491 M.J., Kusakabe, M., Ohba, T., Zhang, J., Aka, F.T., Tanyileke, G.Z., Hell, J.V., 2015.  
492 Characteristics of Chemical weathering and water-rock interaction in Lake Nyos dam  
493 (Cameroon): Implications for vulnerability to failure and re-enforcement. *Journal of African  
494 Earth Sciences*: 101:42-55  
495

496 Fantong, W.Y., Satake, H., Aka, F.T., Ayonghe, S.N., Kazuyoshi, A., Mandal, A.K., Ako, A.A.,  
497 2010a. Hydrochemical and isotopic evidence of recharge, apparent age, and flow direction  
498 of groundwater in Mayo Tsanaga River Basin, Cameroon: Bearings on contamination.  
499 *Journal of Environ Earth Sci*. Vol. 60: 107-120  
500

501 Faure, G., 1991. Principles and Applications of Inorganic Geochemistry. *Macmillan Publishing  
502 Company*, New York, 626 p.  
503  
504

505 Fitton, J.D., 1980. The Benue Trough and the Cameroon Line – A Migrating Rift System in  
506 West Africa. *Earth Planet. Sci. Lett.* 51, 132-138  
507

508 Ford, T.D., Pedley, H.M. 1996. A Review of Tufa and Travertine Deposits of the World. *Earth  
509 Science Reviews* 41, 117-175.  
510

511 Forti, P., 2005. Genetic processes of cave minerals in volcanic environments: an overview.  
512 *Journal of Cave and Karst Studies*. Vol 67:1, 3-13.  
513  
514

515 Friedman, I., 1970. Some investigations of the deposition of travertine from Hot Springs – I. The  
516 isotopic chemistry of a travertine-depositing spring. *Geochim. Cosmochim. Acta* 34, 1303–  
517 1315.

518  
519

520 Garrels, R.M., Mackenzie, F.T., 1967. Origin of the chemical composition of some springs and  
521 lakes. In: RF Gould (ed.). *Equilibrium concepts in natural water systems*. Washington, DC:  
522 American Chemical Society, pp 222-242.

523

524 Halliday, A.N., Dicken, A.P., Fallice, A.E., and Fitton, J.T., 1988. Mantle dynamics. A Nd, Sr,  
525 Pb, and O isotope study of the Cameroon Volcanic Line. *J. Petrol.* 29, 181-211

526  
527

528 Hamilton, S.M., Michel, F.A., Jefferson, C.W., 1991. CO<sub>2</sub>-rich ground waters of the Flat River  
529 Valley, N.W.T. In: Prowse, T., Ommanney, C. (Eds.), *Northern Hydrology Selected  
530 Perspectives, Proceedings of the Northern Hydrology Symposium, 10–12 July 1990,*  
531 *Saskatoon, Saskatchewan, NHRI Paper #6*, pp. 105–199.

532

533 Jacobson, R.L., Usdowski, E., 1975. Geochemical controls on a calcite precipitating spring.  
534 *Contrib. Mineral. Petrol.* 51, 65–74.

535  
536

537 Kamtchueng, B. T., Fantong, W.Y., Wirmvem, M.J., Tiodjio, R.E., Takounjou, A.F., Asai, K.,  
538 Serges L. Djomou, S.L.B., Kusakabe, M., Ohba, T., Tanyileke, G., Hell, J.V., Ueda A.,  
539 2015. A multi-tracer approach for assessing the origin, apparent age and recharge  
540 mechanism of shallow groundwater in the Lake Nyos catchment, Northwest, Cameroon.  
541 *Journal of Hydrology*, 523:790–803.

542

543 Kamtchueng, B.T., Fantong, W.Y., Ueda, A., Tiodjio, E.R., Anazawa, K., Wirmvem, J.,  
544 Mvondo, J.O., Nkamdjou, L., Kusakabe, M., Ohba, T., Tanyileke, G.Z., Joseph, V. H.,  
545 2014. Assessment of shallow groundwater in Lake Nyos catchment (Cameroon, Central-  
546 Africa): implications for hydrogeochemical controls and uses. *Environmental Earth  
547 Sciences*, 72:3663–3678.

548 Kusakabe, M., 2017. Lakes Nyos and Monoun gas disasters (Cameroon)—Limnic eruptions  
549 caused by excessive accumulation of magmatic CO<sub>2</sub> in crater lakes. *GEOchem. Monogr.*  
550 *Ser. 1*, 1–50, doi:10.5047/gems.2017.00101.0001.

551

552 Kusakabe, M., Ohsumi, T., and Arakami, S., 1989. The Lake Nyos gas disaster: chemical and  
553 isotopic evidence in waters and dissolved gases in three Cameroonian Lakes, Nyos,  
554 Monoun and Wum. In: Le Guern, F., and Sigvaldason, G., (Editors), The Lake Nyos Event  
555 and Natural Carbon dioxide Degassing, 1. J. Volcanol. Geothermal Res., 39, 167-185.  
556

557 Kut, K.M.K., Sarsevat, A., Srivastava, A., Pitmann, C.U., Moham, D., 2016. A review of  
558 Fluoride in African Groundwater and Local Remediation Methods. Groundwater for  
559 Sustainable Development 2, 190-175  
560

561 Land, L.S., 1983. The application of stable isotopes to studies of the origin of dolomite and to  
562 problems of diagenesis of clastic sediments, in: Arthur M.A., Anderson T.F. (eds), Stable  
563 isotopes in Sedimentary Geology, Soc. Econ. Paleont. Miner. Short Course No. 10, 4.1-  
564 4.22.  
565

566 Le Marechal, A., 1976. Geologie et Geochemie des sources thermominerales du Cameroun.  
567 ORSTOM, Paris  
568

569

570 Liotta, M., Shamavu, P., Scaglione, S., D'Alessandra, W., Bobrowski, N., Giuffrida, G.B.,  
571 Tedesco, D., Calabrese, S., 2017. Mobility of plume-derived volcanogenic elements in  
572 meteoric water at Nyiragongo volcano (Congo) inferred from the chemical composition of  
573 single rainfall events. *Geochimica et Cosmochimica Acta.* 217, 254-272  
574

575 Liu, Z., Zhang, M., Li, Q., You, S., 2003. Hydrochemical and isotope characteristics of spring  
576 water and travertine in the Baishuitai area (SW China) and their meaning for  
577 paleoenvironmental reconstruction. *Environ. Geol.* 44, 698-704.  
578

579 Lloyd, J.W., Heathcoat, J.A., 1985. Natural inorganic hydrochemistry in relation to groundwater:  
580 an introduction. Oxford University Press, New York, p 296  
581

582

583 McArthur, J.M., Howarth, R.J., Bailey, T.R., 2001. Strontium isotope stratigraphy: LOWESS  
584 Version 3. Best-fit line to the marine Sr-isotope curve for 0 to 509 Ma and accompanying  
585 look-up table for deriving numerical age, *J. Geol.* **109**, 155-169.  
586

587 McCrea, 1950. On the Isotope Chemistry of Carbonates and a Paleotemperature Scale. The  
588 Journal of Chemical Physics. 18, 6.  
589  
590

591 Ngako, V., Njonfang, E., Aka, F. T., Affaton, P., & Nnange, J. M., 2006. The north–south  
592 Paleozoic to Quaternary trend of alkaline magmatism from Niger-Nigeria to Cameroon:  
593 complex interaction between hotspots and Precambrian faults. *Journal of African Earth*  
594 *Sciences*, 45, 241–256. doi:10.1016/j.jafrearsci.2006.03.003.  
595

596 Omelon CR, Pollard WH, Anderson DT (2006) A geochemical evaluation of perennial spring  
597 activity and associated mineral precipitates at Expedition Fjord, Axel Heiberg Island,  
598 Canadian High Arctic. *Applied geochemistry* 21,1-15  
599

600

601 Piper, A.M., 1944. A graphic procedure in the geochemical interpretation of water analyses. *Am*  
602 *Geophys Union Trans* 25:914–923  
603

604 Sano, Y., Kusakabe, M., Hirabayashi, J., Nojiri, Y., Shinohara, H., Njini, T., Tanyileke, G.Z.,  
605 1990. Helium and Carbon Fluxes in Lake Nyos, Cameroon: Constraints on next gas burst.  
606 *Earth and Planetary Science Letters*. 99, 303-314  
607

608

609 Shah, M.M., Nader, F.H., Garcia, D., Swennen, R., Ellam, R., 2012. Hydrothermal dolomites in  
610 the Early Albian (Cretaceous) platform carbonates: (NW Spain): Nature and origin of  
611 dolomite and dolomitizing fluids. *Oil & Gas Science and Technology-Rev. IFP Energies*  
612 *nouvelles* 67:1, 88-122  
613

614 Sighomnou, D., 2004. Analyse et Redefinition des Regimes Climatiques et Hydrologiques du  
615 Cameroun: Perspectives d'évolution des Ressources en Eau. Ph.D Thesis, University of  
616 Yaounde 1. 292 pp.  
617

618

619 Symonds, R. B., Rose, W. I., Reed, M. H., Lichte, F. E., and Finnegan, D. L., 1987.  
620 Volatilization, transport and sublimation of metallic and non-metallic elements in high  
621 temperature gases at Merapi Volcano, Indonesia. *Geochim. Cosmochim.Acta* 51, 2083–  
622 2101.  
623

624 Symonds, R.B., Rose, W.I., Reed, M.H., 1988. Contribution of Cl<sup>-</sup> and F<sup>-</sup> bearing gases to the  
625 atmosphere by volcanoes, *Nature*, 334, 415-418.  
626

627 Tanyileke, G.Z., 1994. Fluid Geochemistry of CO<sub>2</sub> – Rich Lakes and Soda Springs Along the  
628 Cameroon Volcanic Line. Dissertation, Okayama University, Japan.  
629

- 630 Tsujimura, M., Abe, Y., Tanaka, T., Shimada, J., Higuchi, S., Yamanaka, T., Davaa, G.,  
631 Oyunbaatar, D., 2007. Stable isotopic and geochemical characteristics of groundwater in  
632 Kherlin River Basin: a semiarid region in Eastern Mongolia. *J Hydrol* 333:47–57  
633
- 634 Tucker, M. E., and Bathurst, R.G.C., 1990. Carbonate Diagenesis. Reprint series volume 1 of the  
635 International Association of Sedimentologists. Blackwell Scientific Publications. 312 pages  
636  
637
- 638 Usdowski, E., Hoefs, J., Menschel, G., 1979. Relationship between  $^{13}\text{C}$  and  $^{18}\text{O}$  fractionation and  
639 changes in major element composition in a recent calcite-depositing spring – a model of  
640 chemical variations with inorganic  $\text{CaCO}_3$  precipitation. *Earth Planet. Sci. Lett.* 42, 267–  
641 276.  
642
- 643 Usdowski, E., Hoefs, J., 1990. Kinetic  $^{13}\text{C}/^{12}\text{C}$  and  $^{18}\text{O}/^{16}\text{O}$  effects upon dissolution and  
644 outgassing of  $\text{CO}_2$  in the system  $\text{CO}_2\text{--H}_2\text{O}$ . *Chem. Geol.* 80, 109–118.  
645
- 646 Veizer, J., Ala, D., Azmy, K., Bruckschen, P., Buhl, D., Bruhn, F., Carden, G.A.F., Diener, A.,  
647 Ebner, S., Godderis, Y., Jasper, T., Korte, C., Pawellek, F., Podlaha, O., Strauss, H., 1999.  
648  $^{87}\text{Sr}/^{86}\text{Sr}$ ,  $\delta^{13}\text{C}$  and  $\delta^{18}\text{O}$  evolution of Phanerozoic seawater, *Chem. Geol.* **161**, 59-88.  
649  
650
- 651 Verla, R.B., Mboudou, G.M.M., Njoh, O., Ngoran, G.N., Afahnwie, A.N., 2014. Carbonate  
652 Enrichment in Volcanic Debris and Its Relationship with Carbonate Dissolution Signatures  
653 of Springs in the Sabga-Bamessing, North West, Cameroon. *International Journal of*  
654 *Geosciences*, 2014, 5, 107-121  
655
- 656 Whitten, D.G.A., and Brooks, J.R.V., 1972. *The Penguin Dictionary of Geology*. Penguin book  
657 limited, England-Great Britain. 493 pages  
658  
659

### 660 **Figures captions**

661 Fig. 1. Locations of sampled carbonate depositing soda springs along the Cameroon Volcanic  
662 Line (CVL). CS stands for the continental sector of the CVL, and OCB stands for the oceanic  
663 continental boundary of the CVL. The locations of Lake Monoun (L. Monoun), Lake Nyos (L.  
664 Nyos), and Mount Cameroon (Mt. Cameroon) are also shown. The black dots correspond to  
665 samples' locations

666

667 Fig.2. Herds of cattle consuming water from the carbonate depositing springs that have been  
668 harnessed

669

670 Fig. 3. Samples (deposited carbonates and water) collection sites from observed springs

671 Fig. 4. Water chemistry presented as Piper's diagram (a), and Stiff diagrams (b) for the observed  
672 springs

673 Fig. 5. Plot of  $\delta H$  and  $\delta^{18}O$  in water from observed springs. The Sabga and Bambui springs  
674 showed no evaporation effect, while the Lobe springs, the Nyos spring and water in shallow  
675 wells around Lobe spring were subjected to evaporation relative to the meteoric water lines.  
676 Zone 1 represents the soda springs and zone 2 represents shallow groundwater in the Lobe spring  
677 neighborhood. LMWL: Local meteoric water line. GMWL: Global meteoric water line

678 Fig. 6. With respect to fluoride concentrations (a), all the observed soda springs with exception  
679 of that in Nyos, contain fluoride above the WHO upper limit of 1.5 mg/l. With respect to Arsenic  
680 (As) concentrations (b), the springs in the continental sector contain As above the WHO upper  
681 limit

682 Fig. 7. The plots of saturation indices (SI; with respect to quartz, anhydrite, aragonite, calcite and  
683 dolomite) versus total dissolved solid (TDS) for investigated water samples (wells and springs),  
684 show three subgroups (1: undersaturated wells. 2: trona precipitating springs. 3: dolomite  
685 precipitating springs).

686 Fig. 8. Stability diagrams for some minerals in the systems  $Na_2-Al_2O_3-SiO_2-H_2O$  (a) and  $CaO-$   
687  $Al_2O_3-SiO_2-H_2O$  (b) at 25°C

688

689 Fig. 9. The scanning electron microscope image (a), X-ray diffraction peaks (b), and electron  
690 probe microanalyzer mapping (c,d, e,f) of carbonate precipitate from Nyos cave spring

691 Fig. 10. The scanning electron microscope image (a), X-ray diffraction peaks (b), and electron  
692 probe microanalyzer mapping (c,d, e,f) of carbonate precipitate from the Sabga A spring

693 Fig. 11. The scanning electron microscope image (a), X-ray diffraction peaks (b), and electron  
694 probe microanalyzer mapping (c,d, e,f) of carbonate precipitate from the Sabga B spring

695 Fig.12. The scanning electron microscope image (a), X-ray diffraction peaks (b), and electron  
696 probe microanalyzer mapping (c,d, e,f) of carbonate precipitate from Bambui B spring

697 Fig. 13. Electron probe microanalyzer mapping of Na, Ca, Mg, and F of carbonate precipitate  
698 from Bambui B spring, showing enrichment of fluorine in the matrix of the carbonate

699 Fig. 14. The scanning electron microscope image (a), X-ray diffraction peaks (b), and electron  
700 probe microanalyzer mapping (c,d, e,f) of carbonate precipitate from Lobe D spring

701 Fig. 15. Carbonates-water oxygen isotopic fractionation temperature in observed soda springs  
702 along the CVL. Dolomites fractionated at relatively higher temperatures (35-43°C) than tronas  
703 (circum 20°C).

704  
705 Fig. 16. Plots of  $^{13}\text{C}$  and  $\delta^{18}\text{O}$  (PDB), showed observed tronas to be relatively depleted in  $^{13}\text{C}$   
706 and enriched in  $^{18}\text{O}$  (PDB).

707  
708 Fig. 17. Except for the Lobe springs that showed highest  $^{87}\text{Sr}/^{86}\text{Sr}$  ratio, in all the other observed  
709 springs the carbonate phases are relatively enriched in  $^{87}\text{Sr}/^{86}\text{Sr}$  ratio than the water phase (a),  
710 and  $^{87}\text{Sr}/^{86}\text{Sr}$  are relatively depleted in tronas than in dolomites (b)

711  
712 Fig. 18. Chloride versus fluoride cross plots showing volcanogenic contributions into the Lobe,  
713 Bambui and Nyos springs

714

715

### 716 **Table captions**

717

718 Table 1. Laboratory analytical methods of the carbonates and water phases in observed springs

719

720 Table 2. Chemical composition of water from the observed springs and shallow wells. ND: not  
721 detected. NM: not measured

722

723 Table 3. Fractionation temperature and isotopic compositions of carbonates precipitating from  
724 the observed springs

725

726

727

728

Table 3.

Sample name	$\delta^{18}\text{O}$ (SMOW) carbonate	$\delta^{18}\text{O}$ (SMOW) water	$1000\ln\alpha$ ( $\delta^{18}\text{O}$ calcite-water)	Fractionation temperature ( $^{\circ}\text{C}$ )	Observed temperature ( $^{\circ}\text{C}$ )	$^{13}\text{C}$ carbonate (VPDB)	$^{18}\text{O}$ carbonate (VPDB)	$^{87}\text{Sr}/^{86}\text{Sr}$ in carbonate	Carbonate type
LobeD ssp	22.17	-4.65	26.82	43	49	1.74	-8.44	0.713	Dolomite
Lobe Assp	22.68	-4.70	27.38	35.2	47.4	5.22	-7.1	0.713	Dolomite
Bambui B ssp	24.92	-6.30	31.22	20	22.2	-1.84		0.707	Trona
Bambui A ssp	25.2	-6.7	31.90	19.8	21.8			0.707	Trona
Sabga B ssp	25.00	-6.30	31.30	18.6	19.3	-1.98	-1.4	0.707	Trona
Sabga A ssp	24.23	-6.01	31.09	18.5	20	-3.09	-5.6	0.708	Dolomite
Nyos C ssp	24.92	-3.40	28.32			-2.1	-5.9	0.706	Trona

SMOW : Standard Mean Ocean Water. VPDB : Vienna Pee Dee Belemnite.  $^{\circ}\text{C}$  : Degree Celsius. Ssp :Soda springs. Chemical formula for dolomite is  $\text{CaMg}(\text{CO}_3)_2$  and for trona is  $\text{Na}_3\text{H}(\text{CO}_3)_2 \cdot \text{H}_2\text{O}$

Table 1

<b>Table 1:</b> Summary of laboratory analytical procedures during the studies				
<b>Mineral phase</b>	<b>Parameter analyzed/determined</b>	<b>Equipment used</b>	<b>Analytical precision/data reliability and conditions</b>	<b>Institution</b>
Carbonate	Crystal habit	Scanning Electron Microscope, TM-1000 miniscope	Vacc : 15.0kV Accelerating voltage : 15000V Emission current : 102.6mA Sample coating : Gold	University of Toyama, Japan
	Carbonate type	X-Ray Diffraction (XRD). Bruker model D8 Discover-TUS, serial No 27062	Voltage : 30kv Current : 15mA Scan speed 4000°/minute Measurement angle : 3-60°	University of Toyama, Japan
	Elemental composition	JEOL, JXA-8230T Electron Probe Micro Analyzer (EMPA)	Voltage : 15kv Current : 1.001-9e-0008A Time (ms) : 2.00	University of Toyama, Japan
	<sup>87</sup> Sr/ <sup>86</sup> Sr	Thermal Ionization Mass Spectrometer (TIMS)	2σ = ±2E-5	Research Institute for Humanity and Nature- Kyoto
	<sup>13</sup> C and <sup>18</sup> O	Isotope Ratio Mass Spectrometer (IRMS), after decomposing carbonate with 100% phosphoric acid	±0.1‰	University of Toyama, Japan

		at 25°C (McCrea, 1950)		
Water	Major cations and anions	Alkalinity titration for $\text{HCO}_3^-$ , and Ion chromatography for the other ions. More details are explained in Fantong et al. 2008; 2010; and 2016	$\pm 10\%$	University of Toyama, Japan
	Stable Environmental Isotopes ( $^2\text{H}$ and $^{18}\text{O}$ )	Micromass model prism Isotope Ratio Mass Spectrometer, as explained in Coleman et al. 1982 for $^2\text{H}$ , and Epstein and Mayeda 1953 for $^{18}\text{O}$	$\pm 1.5\text{‰}$ for $\delta\text{D}$ and $\pm 0.1\text{‰}$ for $\delta^{18}\text{O}$	University of Toyama, Japan
	Trace elements including arsenic	ICP-MS	SD = $\pm 0.5$	University of Toyama, Japan

1 **Major ions,  $\delta^{18}\text{O}$ ,  $\delta^{13}\text{C}$  and  $^{87}\text{Sr}/^{86}\text{Sr}$  compositions of water and precipitates from springs**  
2 **along the Cameroon Volcanic Line (Cameroon, West Africa): Implications for provenance**  
3 **and volcanic hazards**

4  
5 Wilson Yetoh FANTONG<sup>1</sup> $\Psi$ , Brice Tchakam KAMTCHUENG<sup>1</sup>, Yasuo ISHIZAKI<sup>2</sup>, Ernest Chi  
6 FRU<sup>3</sup>, Emilia Bi FANTONG<sup>4</sup>, Mengnjo Jude WIRMVEM<sup>1</sup>, Festus Tongwa AKA<sup>1</sup>, Bertil  
7 NLEND<sup>1</sup>, Didier HARMAN<sup>4</sup>, Akira UEDA<sup>5</sup>, Minoru KUSAKABE<sup>5</sup>, Gregory TANYILEKE<sup>1</sup>,  
8 Takeshi OHBA<sup>6</sup>

9 <sup>1</sup> Hydrological Research Center/ IRGM, Box 4110, Yaounde-Cameroon

10 <sup>2</sup> Graduate School of Science and Engineering and Research, Environmental and Energy  
11 Sciences, Earth and Environmental Systems

12 <sup>3</sup> School of Earth and Ocean Sciences, Cardiff University, Cardiff, [Park Place](#), Wales-United  
13 Kingdom

14 <sup>4</sup> Ministry of Secondary Education, Cameroon

15 <sup>5</sup>Laboratory of Environmental Biology and Chemistry, University of Toyama, Gofuku 3190,  
16 Toyama 930-8555 Japan

17 <sup>6</sup>Department of Chemistry, School of Science, Tokai University, Hiratsuka, 259-1211, Japan

18  $\Psi$  Corresponding author: [fyetoh@yahoo.com](mailto:fyetoh@yahoo.com); [fantongy@gmail.com](mailto:fantongy@gmail.com)

19 **Abstract**

20 A combined study of major ions,  $\delta^{18}\text{O}$ ,  $\delta\text{D}$ ,  $^{13}\text{C}$ ,  $^{87}\text{Sr}/^{86}\text{Sr}$  isotopes, X-ray diffraction, scanning  
21 electron [microscopy](#), and electron probe microanalyses on springs and spring mineral  
22 precipitates along the Cameroon Volcanic Line (CVL) was undertaken to understand water  
23 chemistry, and infer the type and origin of the precipitates. The waters are of evaporated Na+K-  
24 Cl and non-evaporated Ca+Mg-HCO<sub>3</sub> types, with the more mineralized (electrical conductivity-  
25 EC of 13130  $\mu\text{S}/\text{cm}$ ) Lobe spring inferred to result from interaction of circulating 49°C waters  
26 with magmatic volatiles of the active Mt. Cameroon. Water mineralization in the other springs  
27 follows the order: Sabga A > Sabga B > Bambui B > Bambui A > Nyos Cave. But for the Nyos  
28 Cave spring, all other springs contain fluoride (up to 0.5 - 35.6 mg/l above WHO potable water  
29 upper limit). The Sabga spring **contains** arsenic (up to 1.3 mg/l above the WHO limits). The  
30 springs show low [fractionation temperatures in the range of 19 – 43 °C](#). The Lobe and Sabga A  
31 springs are precipitating dolomite ( $\text{CaMg}(\text{CO}_3)_2$ ), while the Nyos Cave, Bambui A, Bambui B

32 and Sabga B springs precipitate trona ( $(\text{Na}_3\text{H}(\text{CO}_3)_2 \cdot \text{H}_2\text{O})$ ). Our data suggest a marine provenance  
33 for the carbonates, and point to a volcanic input for the Lobe, Nyos, Sabga A, and Bambui A  
34 springs. The latter springs are therefore proposed as proxies for monitoring volcanic activity for  
35 hazard mitigation along the CVL.

36 Key words: *Bubbling springs. Precipitates. Composition. Provenance. Volcanic activity.*  
37 *Hazards mitigation.*

38

39

## 40 **Introduction**

41 Mineral-depositing springs are natural systems that offer a good opportunity to study various  
42 mechanisms by which waters establish equilibrium with conditions at the Earth's surface  
43 (Amundson and Kelly, 1987; Omelon et al., 2006). For example, carbonate-precipitating waters  
44 provide an opportunity to evaluate a dynamic carbonate system and the major controls associated  
45 with calcite precipitation (Barnes, 1965; Jacobson and Usdowski, 1975), including; isotope  
46 fractionation associated with natural calcite precipitation from spring waters (McCrea, 1950;  
47 Friedman, 1970; Usdowski et al., 1979; Dandurand et al., 1982; Amundson and Kelly, 1987;  
48 Usdowski and Hoefs, 1990; Hamilton et al., 1991; Liu et al., 2003), as well as the types,  
49 morphologies, textures, and processes involved in the formation of various carbonate phases  
50 (Tucker and Bathurst, 1990; Bradley and Eugster, 1969; Ford and Pedley, 1996; Forti, 2005).

51

52 Many orifices of gas-water-carbonate interacting systems occur along the Cameroon Volcanic  
53 Line (CVL-Fig. 1). Based on carbonate enrichment studies on volcanic debris and springs in part  
54 of the continental sector of the CVL (Le Marechal, 1976; Verla et al., 2014); chemical and  
55 isotopic characteristics of fluids along the CVL (Tanyileke, 1994); the geochemistry of gases in  
56 springs around Mt. Cameroon and Lake Nyos (Kusakabe et al., 1989; Sano et al., 1990; Aka,  
57 1991); the sedimentology and geochemistry of the Bongongo and Ngol travertines along the  
58 CVL (Bisse et al., 2018), the following hypotheses have been proposed: (1) the bubbling mineral  
59 springs along the CVL contain abundant  $\text{CO}_2$ . (2) The  $\text{CO}_2$  in the bubbling springs is dominantly  
60 of magmatic origin. (3) Helium and carbon isotope ratios of gases from a few of the springs

61 along the CVL revealed a signature similar to hotspot type magma. (4) The precipitating  
62 minerals are travertines.

63 Although these studies provide initial data to understand the geochemical dynamics within the  
64 CVL gas-water-carbonate systems, gaps required to better understand the system include; a) a  
65 total absence of comprehensive information on the classification and genetic processes of the  
66 precipitating carbonates, which is exploited by the indigenes for preparation of traditional soup,  
67 b) high concentration ( > 100 mg/l) of geogenic fluoride has been reported (e.g., Kut et al., 2016;  
68 and references there-in) in thermal waters along the Ethiopian rift. Such concentrations of  
69 fluoride in water that is used for domestic purposes and livestock rearing can cause tremendous  
70 health effects (e.g., Fantong et al., 2010). Livestock rearing on the slopes of the CVL heavily  
71 consumes water from the springs (Fig. 2), so there is still a need to re-assess their chemical  
72 characteristics with focus on potential harmful elements like fluoride and arsenic, and c) the  
73 carbonate-water fractionation temperature remains unknown.

74 Against this backdrop, the objectives of this study are to 1) characterize the water chemistry with  
75 focus on health implications, 2) estimate the carbonate-water fractionation temperature, and 3)  
76 identify, describe and classify the carbonates that are precipitating from the springs.

77

## 78 **Study area**

79 Figure 1 shows, the sample sites along the CVL, a prominent 1600 km long Y-shaped chain of  
80 Tertiary to Recent, generally alkaline volcanoes that overlap an array of dextral faults called the  
81 Central Africa Shear Zone (CASZ) (Ngako et al., 2006) on the African continent, comparable  
82 only to the East Africa Rift System. The CVL follows a trend of crustal weakness that stretches  
83 from the Atlantic Island of Annobon, through the Gulf of Guinea, to the interior of the African  
84 continent (Fitton, 1980; Déruelle et al., 1987, Halliday et al., 1988;). It is unique amongst  
85 intraplate volcanic provinces in that it straddles the continental margin and includes both oceanic  
86 and continental intraplate volcanism. The oceanic sector constitutes a mildly alkaline volcanic  
87 series, which evolves towards phonolite, while the continental sector evolves towards rhyolite  
88 (e.g., Fitton, 1980). Isotopic studies of lavas (Halliday et al., 1988) divide the CVL into three  
89 sectors: an oceanic zone, ocean-continent boundary zone and a continental zone.

90 The study area overlaps two (coastal and tropical western highlands) of the five climatic zones in  
91 Cameroon, with mean annual rainfall of 5000 and 3000 mm, mean annual atmospheric

92 temperatures of 26°C and 21°C, humidity of 85% and 80%, and evaporation of 600 mm and 700  
93 mm, **respectively** (Sighomnou, 2004). Hydrologically, three (coastal, Sanaga, and Niger) of the  
94 five river basins in Cameroon drain the study area in a dendritic manner. According to Le  
95 Marechal (1968) and Tanyileke (1994), **riverine and in aquifer waters** encounter heat and mantle-  
96 derived CO<sub>2</sub> gas that emanate through the CASZ, **causing heating** and bubbling of the spring  
97 systems along the CVL. At each spring site the gas phase manifests as either bubbles or ‘rotten  
98 egg’ smell, while the precipitates occur as white films, white grains in volcanic ash, stalactite and  
99 stalactmite in caves, and mounds around orifices as shown in **Fig. 3**. At the sites of Sabga A in  
100 **Fig. 3**, animals consume the water as a source of salt, while humans exploit the precipitates **for**  
101 **food recipes**.

102

### 103 **Method of study**

104 Water and precipitate samples were collected from selected bubbling soda spring sites along the  
105 CVL (**Fig. 3**) in October 2015. Each water sample was collected in 3 acid-washed 250 ml  
106 polyethylene bottles after rinsing them thrice with the sample. At each sampling site, an  
107 unfiltered, unacidified and tightly **corked** sample was collected in one bottle for subsequent  
108 analyses for stable environmental isotopes **of hydrogen ( $\delta^2\text{H}$ ) and oxygen ( $\delta^{18}\text{O}$ )**. The second  
109 bottle contained un-acidified but filtered sample for anion analyses, and the third filtered and  
110 acidified sample for cations and trace elements analyses. Prior to sample collection, in-situ  
111 physicochemical measurements were **recorded** for pH (TOA-DKK HM-30P meter), electrical  
112 conductivity (TOA-DKK CM-31P EC meter), **reduction-oxidation** potential (TOA-DKK ORP  
113 meter), and water temperature. Geographical parameters (latitude, longitude and altitude) of each  
114 sample site were recorded **in** the field using a hand-held Garmin GPS. Alkalinity was measured  
115 using a ‘‘Hach’’ field titration kit, after addition of 0.16 N H<sub>2</sub>SO<sub>4</sub> to the sample to reach the  
116 endpoint titration (pH 4.5). Samples were filtered through 0.2  $\mu\text{m}$  filters prior to major ions and  
117 dissolved silica determination. Three kilograms chunks of massive carbonate was chipped off  
118 with a hammer at sites with consolidated precipitate, and 300 g scoped from sites with  
119 unconsolidated precipitate. Each precipitate was put in a clean plastic container, sealed and  
120 labelled.

121 Water samples and precipitates were transported to the University of Toyama, in Japan for  
122 chemical analyses.

123 The various chemical analyses that were done in various institutes in Japan are tabulated in Table  
124 1.

125

## 126 **Results and Discussions**

### 127 *Variation of water chemistry*

128 Chemical compositions and isotopic ratios of water samples and carbonate phases are presented  
129 in Tables 2 and 3. Measured in-situ parameters show values [in the range of](#) 54 - 13130  $\mu\text{S}/\text{cm}$  for  
130 EC, 4.3 - 7.5 for pH, and 19.3 - 47.4°C for water temperature.

131 The chemistry of the observed water resources determined with the use of the Piper's diagram  
132 (Piper, 1944) (Fig. 4a), shows that water from the Lobe soda springs and its nearby hand dug  
133 wells, located in the ocean-continent-boundary (OCB) and close to the ocean (Fig. 4a), have a  
134 dominant Na+K-Cl signature. On the other hand, water from the soda springs in Sabga, Bambui,  
135 and Nyos have dominantly Ca+Mg-HCO<sub>3</sub> signature. The observed disparity in water facies may  
136 be due to the proximity of the Lobe springs to the ocean, which **impacts** the sodium chloride  
137 characteristics as accorded in Le Marechal (1976). Whilst in the other springs, an interaction  
138 between primary and secondary minerals in rocks and water could be the dominant explanation  
139 as also explained by other researchers (Kamctung et al., 2014; Fantong et al., 2015). The Stiff  
140 diagrams for the water chemistry (Fig. 4b), also depict similar water facies like the Piper's  
141 diagram, but they further suggest varying degree of mineralization of the water sources. In the  
142 OCB, the larger sizes of the stiff diagram for the Lobe soda springs indicate more mineralization  
143 than for water from the wells. Likewise in the samples from the continental sector (CS) the water  
144 in the Sabga soda springs are most mineralized, followed by those in Bambui and the least  
145 mineralized is that from the Nyos soda spring. The observed variation in degree of mineralisation  
146 could in part be indicating variation in residence time, where the older springs are enriched in  
147 elements from aquifer minerals than in younger springs (e.g., Fantong et al., 2010a; Kamctung  
148 et al., 2015) that are renewed through a local and short recharge-discharge flow paths.

149

### 150 *Recharge mechanisms and evaporation of the sampled waters*

151 Isotopic ratios of hydrogen and oxygen, which are used in this study to infer recharge and  
152 evaporation mechanisms in the waters are also shown in Table 2 and graphically presented in Fig.  
153 5. The  $\delta\text{D}$  values ranged from -41.8 in Sabga A soda spring to -26 ‰ in water from well 5.

154 Oxygen isotope ( $\delta^{18}\text{O}$ ) values range from -6.3 ‰ in Sabga A spring to -3.1 ‰ in water from well  
155 3. Due to the paucity of isotope data on local rainfall, the Global Meteoric Water Line (GMWL)  
156 of Craig (1961), which is defined by the line  $\delta\text{D} = 8\delta^{18}\text{O} + 10$  is also presented as a reference.  
157 Distribution of sample water in the  $\delta\text{D}$ - $\delta^{18}\text{O}$  graph suggests that water in the Bambui and Sabga  
158 soda springs are subject to little or no evaporation, while the Lobe soda springs suggest slight  
159 evaporation, but water from the wells and Nyos soda springs show remarkable evaporation  
160 tendencies. Such a pattern depicts that the Bambui and Sabga soda springs are subject to the  
161 mechanism of preferential flow pass, which is caused by rapid recharge (e.g., Tsujimura et al.,  
162 2007; Asai et al., 2009), that is favored by the highly altered and jointed lavas as opposed to the  
163 Lobe and Nyos cave soda springs, and the wells. Except for the Lobe soda springs, the other  
164 springs are sources of drinking water for animals (cattle and goats), and a source of minerals  
165 (carbonate) for local manufacture of soup for consumption by the nearby population, thus it is  
166 important to assess at a preliminary scale the medical hydrogeochemical characteristics of the  
167 springs.

#### 168 *Health implications of the water chemistry*

169 Given that the gas bubbling springs are located in the area of livestock rearing and human  
170 activities, their chemistry is here preliminarily evaluated to assess potential health implications.  
171 With respect to fluoride, Figure 6a shows that except for the Nyos cave soda spring, all the other  
172 soda springs contain fluoride at concentrations that are above the WHO optimal limit (1.5 mg/l  
173 e.g., Kut et al., 2016). This indicates that the animals and the population that exploit these  
174 springs are potentially exposed to fluoride poisoning as reported by Fantong et al. (2010b) in the  
175 Far Northern Region of Cameroon. **The potential geogenic and volcanic provenance (Davies,  
176 2013), and actual epidemic effects of such high concentrations of fluoride are not within the  
177 scope of this study, and need further investigation.**

178 With respect to arsenic (As), Figure 6b shows that the Sabga soda springs contain As at  
179 concentrations as high as 1.33 ppm that are above the WHO upper limit (0.03 ppm in drinking  
180 water). Based on the field observations that water from the Sabga soda springs is heavily  
181 consumed by cattle, and carbonate there-from is exploited for consumption by the population, it  
182 is also a challenge for medical geochemists to carry out a comprehensive investigation into the  
183 incidence, origin, mobilization and epidemiological effects of arsenic in these areas.

184

185 ***Impact of volcanic volatile or magmatic input on chemistry of the spring water***

186 The dissolved state of elements and saturation state of compounds observed in the springs are to  
187 **an extent determined by their saturation indices and stoichiometry (e.g., Faure, 1991).**

188

189 ***Saturation indices and activity diagrams***

190 The saturation index (SI) of a given mineral in an aqueous system is defined as (Lloyd and  
191 **Heathcoat, 1985; and Deutch, 1997):**

192 
$$SI = \log \left( \frac{IAP}{K_{sp}} \right) \quad (1)$$

193 where IAP is the ion activity product and  $K_{sp}$  is the solubility product of the mineral in the  
194 system. A  $SI > 0$  points to supersaturation, and a tendency for the mineral to precipitate from the  
195 water. Saturation can be produced by factors like incongruent dissolution, common ion effect,  
196 evaporation, and rapid increase in temperature and  $CO_2$  exsolution (Appelo and Postma, 2005).  
197 A  $SI < 0$  points toward undersaturation, and implies that water dissolves the minerals from  
198 surrounding rocks. Negative SI value might also reflect that the character of water is either from  
199 a formation with insufficient concentrations of the mineral for precipitation to occur (Garrels and  
200 **Mackenzie, 1967).**

201 The thermodynamic data used in this computation are those contained in the database of  
202 'Phreeqc for Windows'. A plot of the calculated SI (with respect to quartz, anhydrite, aragonite,  
203 calcite and dolomite) versus TDS (Fig.7) groups the water samples into three subgroups:  
204 subgroup 1, which consists of water from the shallow wells is undersaturated with respect to all  
205 the selected phases and has the lowest TDS values that ranged from 63-83 mg/l. The  
206 undersaturation of subgroup 1 suggests that no mineral precipitates in the wells as observed on  
207 the field. Subgroup 2, which consists of Nyos cave soda spring, Bambui soda spring B and Sabga  
208 soda spring B, show supersaturation with respect to quartz, dolomite. On the field, this subgroup  
209 is found to be dominantly precipitating trona (a Na-rich carbonate) and dolomite to a lesser  
210 extent. Subgroup 3 that consists of the Lobe and Sabga A soda springs, are supersaturated with  
211 respect to dolomite, quartz and calcite, and it is actually precipitating more of dolomite, and  
212 trona to a lesser extent.

213 The stability of secondary minerals (Na and Ca montmorillonites, kaolinite, gibbsite) and  
214 amorphous quartz in the springs and wells were evaluated by plotting  $\log (a_{Na}/a_H)$  vs  $\log (a_{H_4SiO_4})$

215 (the albite system) (Fig. 8a) and  $\log (a_{Ca2}/a_{2H})$  versus  $\log (a_{H4SiO4})$  (the anorthite system) (Fig.  
216 8b). These diagrams were drawn with the assumption that aluminum was preserved in the  
217 weathering product (Appelo and Postma,1993), because the amount of alumina will remain  
218 constant in fresh rocks and its altered equivalent. The constant amount in alumina ( $Al_2O_3$ ) is  
219 because an apparent increase in its weight % is actually always caused by a reduction in the  
220 weight of the fresh rock to some smaller amount (Faure, 1991). End member compositions were  
221 also assumed using equilibrium relationship for standard temperature (25°C) and pressure (1  
222 atmosphere), which approximately reflect the springs and groundwater conditions. Activities of  
223 the species were computed using the analytical concentrations and activity coefficient  
224 determined by Phreeqc for Windows version 2.1 under the above conditions (Appelo and  
225 Postma, 1993). According to the figures, groundwater from the wells span the stability field of  
226 kaolinite, while all the soda springs with exception of the Nyos soda spring are in equilibrium  
227 within the Na and Ca -montmorillonite stability fields. This concurs with the incidence of clay  
228 minerals in the study area (Fantong et al., 2015). Moreover, the presence of kaolinite and  
229 montmorillonite in the study area occur as groundmass in the XRD (X-Ray Defraction) peaks of  
230 Figures 9b,10b, 11b, 12b, and 14b. A combination of information from the saturation indices and  
231 stability diagrams is supported by the presence of precipitating carbonate phases in the soda  
232 springs as shown in Fig. 1.

233

### 234 *Typology of carbonate phases*

235 The typology of the carbonate phases that precipitate from the observed soda springs is done by  
236 describing the morphology by using SEM images, and identifying the carbonate phase by using  
237 XRD diagrams and EPMA elemental mapping.

238

### 239 **Carbonate from the Nyos cave soda spring**

240 The SEM image in Fig. 9a shows that the carbonate is an association of cluster of powdery  
241 amorphous groundmass upon which sub-euhedral crystals developed. This carbonate is identified  
242 with XRD peaks (Fig.9b) as a trona (low- syn trisodium hydrogen dehydrate carbonate). To  
243 accentuate the trona phase, an elemental EPMA mapping (Fig.9 c, d, e and f) shows the  
244 dominance of sodium, traces of calcium and total absence of magnesium.

245

246 **Carbonate from Sabga A soda spring**

247 The SEM image of Fig. 10a shows that the carbonate is nail-shaped stalactite crystals protruding  
248 from a cluster of powdery amorphous groundmass. This carbonate is identified with XRD peaks  
249 (Fig.10b) as a dolomite (calcium-magnesium bicarbonate). Dolomite precipitate in this spring is  
250 supported by an elemental EPMA mapping (Fig. 10 c, d, e and f), which shows a dominance and  
251 remarkable presence of both calcium and magnesium, with traces of sodium.

252

253 **Carbonate from Sabga B soda spring**

254 The SEM image of Fig. 11a shows that the carbonate is made up of radiating tabular columns of  
255 crystals whose faces are edged by bacteria. This carbonate is identified with XRD peaks (Fig.  
256 11b) as a trona (low-syn trisodium hydrogen dehydrate carbonate). The presence of this trona  
257 precipitating in this spring is justified by an elemental EPMA mapping (Fig. 11c, d, e and f),  
258 which shows a dominance of sodium and an almost absence of calcium and magnesium.

259

260 **Carbonate from Bambui B soda spring**

261 The SEM image of Fig. 12a shows that the morphology of the carbonate is an intersecting  
262 mosaic of tabular crystals whose faces are edged by bacteria. This carbonate is identified with  
263 XRD peaks (Fig. 12b) as a trona similar to that of Sabga B. The presence of this trona  
264 precipitating in this spring is supported by an elemental EPMA mapping (Fig. 12 c, d, e and f),  
265 which shows a dominance of sodium and low content of calcium and magnesium. The  
266 disseminated distribution of fluorine, which almost coincide with the distribution of faint calcite  
267 suggest the presence of fluorite (CaF<sub>2</sub>), which could be dissolving to enrich the water phase with  
268 fluoride as seen in Fig. 13e.

269

270 **Carbonate from Lobe D soda spring**

271 The SEM image of Fig. 14a shows that the carbonate is a coliform flower-shape radiating  
272 crystals, which is colonized by bacteria. This carbonate is identified with XRD peaks (Fig. 14b)  
273 as a dolomite. The occurrence of dolomite as the precipitate in this spring is supported by an  
274 elemental EPMA mapping (Fig. 14c, d, e and f), which shows high content of both calcium and  
275 magnesium, and low content of sodium.

276 Summarily, the carbonate phases that are precipitating from the studied soda springs along the  
277 CVL are dominantly dolomite and trona. The pristine geochemical attributes and characteristics  
278 of the carbonate are at a later phase altered (Demeny, 2016) by diatoms and bacteria as shown in  
279 Figure 11a and 12a. The incidence of bacteria in such a hydrogeochemical system leaves  
280 biogeochemists with another opportunity to assess the incidence and role of bacteria in the soda  
281 spring systems.

282

### 283 **Origin of the fluids and carbonates**

284 In a bid to identify the formation (sources and paleo temperature) processes that led to the  
285 formation of the observed carbonates, we used  $^{13}\text{C}$  isotopes,  $^{87}\text{Sr}/^{86}\text{Sr}$ , carbonate-water  
286 fractionation temperatures, and  $\text{Cl}^-$  versus  $\text{F}^-$  plot as geochemical tracers.

287

### 288 *Carbonate-water fractionation temperature*

289 Although oxygen-isotope thermometry based on isotopic fractionation of oxygen between  
290 carbonates and water dates back to the **Mid-1900s**, the carbonate-water oxygen isotopic  
291 fractionation equations are still being discussed. The use of isotope thermometry is based on  
292 several criteria: (i) the temperature dependence of the isotopic fractionation between the  
293 investigated compounds (in our case dolomite/trona and water) and (ii) the isotopic compositions  
294 of the compounds are known, (iii) the isotopic equilibrium between the compounds can be  
295 proven or at least reasonably assumed, and (iv) no subsequent isotopic alteration occurred after  
296 the deposition of carbonates. These considerations are valid for inorganic carbonate formation, as  
297 biogenic carbonate is severely affected by the organisms' metabolism, resulting in a species-  
298 dependent ‘‘vital effect’’ (Demeny et al., 2010 and references therein)

299 The temperatures at which the carbonate phases precipitate from the springs were calculated by  
300 using the empirical equation for the temperature dependence of calcite-water oxygen isotope  
301 fractionation from 10 to 70 °C as shown in equations 2 and 3 that were reported by Demeny et al.  
302 (2010).

$$303 \quad 1000 \cdot \ln \alpha = 17599/T - 29.64 \quad [\text{for travertines with a temperature range of } 30 \text{ to } 70^\circ\text{C}] \quad (2)$$

$$304 \quad 1000 \cdot \ln \alpha = 17500/T - 29.89 \quad [\text{for cave deposits for the range } 10 \text{ to } 25^\circ\text{C}] \quad (3)$$

305 **The variable T are in °C.**

306 The values obtained suggest that carbonates precipitate from soda springs along the CVL at  
307 temperature that varied from 18.5 - 43°C. The lowest fractionation temperatures (18.5 - 18.6°C)  
308 occurred in the Sabga soda springs, while the highest (35 - 43°C), occurred in the Lobe soda  
309 springs (Table 3). A plot (Fig. 15), shows that with the exception of the dolomite in the 'Sabga  
310 A soda spring', the tronas fractionated at lower temperature (~18.5 - 20 °C) than the dolomites,  
311 which fractionated at temperature ranging from 35.2 - 43°C. Based on Figure 15, the oxygen  
312 isotopes in carbonates precipitating along the Cameroon Volcanic Line yielded an empirical  
313 fractionation– temperature equations of:

$$314 \quad 1000.\ln\alpha = -0.2153T + 35.3 \quad (4)$$

315

### 316 *Stable isotopes of $^{13}\text{C}$ , $^{87}\text{Sr}/^{86}\text{Sr}$ , and $^{18}\text{O}$*

317 The observed carbonates (dolomite and trona) facies in the samples showed broad ranges in  
318  $^{87}\text{Sr}/^{86}\text{Sr}$ ,  $^{13}\text{C}$  and  $\delta^{18}\text{O}$ . The  $^{87}\text{Sr}/^{86}\text{Sr}$  ratio varied from 0.706 - 0.713, the  $^{13}\text{C}$  varied from -3.09 to  
319 5.22 VPDB and  $\delta^{18}\text{O}$  from -8.4 to -1.4 VPDB as shown in Table 3. Their  $\delta^{13}\text{C}$  values of observed  
320 dolomites are close to the range of values reported for carbonates precipitating from seawater (0  
321 -4 VPDB; Veizer et al., 1999; Shah et al., 2012). Indication of marine origin of the dolomites  
322 corroborates with field observation, because the dolomite precipitates from the Lobe soda spring  
323 located in the **OCB** of the study area. However, the carbonates (trona) identified in our study  
324 area showed relatively depleted  $\delta^{13}\text{C}$  signatures, which may indicate a possible external source of  
325 carbon during trona precipitation (Fig. 16) or a temperature dependent fractionation effect (Shah  
326 et al., 2012). The depleted  $\delta^{18}\text{O}$  in dolomite from the 49°C Lobe soda springs, may be due to its  
327 higher temperatures (thermogenic type) (Bisse et al., 2018), given that precipitation of dolomite  
328 from hot springs leads to relatively depleted  $\delta^{18}\text{O}$  ratios (Land, 1983).

329 With exception of the Lobe soda springs, where  $^{87}\text{Sr}/^{86}\text{Sr}$  value did not vary between the  
330 carbonate and water phases, in the other soda springs (Bambui soda springs A and B, Sabga soda  
331 springs A and B, and Nyos cave soda spring), the  $^{87}\text{Sr}/^{86}\text{Sr}$  ratio shows a decoupling tendency  
332 where the water phases contain relatively higher values than the carbonate phases (Fig. 17a). The  
333 relatively higher  $^{87}\text{Sr}/^{86}\text{Sr}$  ratio in the Lobe soda springs may indicate interaction of dolomitizing  
334 fluids with radiogenic lithologies (Shah et al., 2012), which commonly occur along the CVL  
335 (e.g., Aka et al., 2000; 2001). Moreover, the  $^{87}\text{Sr}/^{86}\text{Sr}$  versus  $^{18}\text{O}$  cross plot (Fig. 17b), shows that  
336 the dolomites are richer in  $^{87}\text{Sr}/^{86}\text{Sr}$  ratio than the tronas. However, the signatures in the dolomite

337 of the Sabga soda spring “A” together with those in the tronas are closer to those of the marine  
338 signatures (McArthur et al., 2001). Such marine signatures in tronas (Na-rich carbonate) within  
339 the continental sector of the Cameroon Volcanic Line, may suggest the presence of paleo-  
340 continental sabkha environments, where various sodium carbonates have been recorded in  
341 tropical regions (Whitten and Brooks, 1972). This suggestion, however, requires further  
342 investigation.

343

#### 344 **Implications for monitoring and hazard mitigation**

345 Volcanogenic sources of fluorine (e.g., Symonds et al., 1987; Symonds et al., 1988; Bellomo et  
346 al., 2003) and chlorine (e.g., Keene and Graedel 1995) containing gasses have been reported in  
347 active and passive volcanic areas, and recently in the Nyiragongo volcano in Congo (Liotta et al.,  
348 2017). As used by the later, we also used a cross plot of chloride versus fluoride (Fig. 18) to infer  
349 volcanogenic contribution in the observed springs along the CVL. The figure suggests  
350 volcanogenic inputs into the Lobe, Nyos, Sabga A, and Bambui A springs. The implication of a  
351 volcanic input to these fluids suggests that they can be used to monitor volcanic activity and thus  
352 mitigate hazards, especially in the vicinity of the Lobe spring located close to the currently active  
353 Mt. Cameroon. Moreover, the dominant fluids in the Lobe, Nyos, Sabga A, and Bambui A  
354 springs are magmatic CO<sub>2</sub> and H<sub>2</sub>O (Sano 1990). Water dissolves slightly more in silicic melts  
355 than in basaltic melts, whereas CO<sub>2</sub> dissolves more in basaltic than in silicic melts. Kusakabe  
356 (2017) reports that the solubility of CO<sub>2</sub> and H<sub>2</sub>O in basaltic melts at 1200°C is a function of the  
357 total pressure of the volatiles, whose composition in the melt changes as the decompression  
358 proceeds. For example, at low pressure the mole fraction of H<sub>2</sub>O equals 0.2 and that of CO<sub>2</sub> is  
359 0.8, implying that basaltic melt becomes rich in CO<sub>2</sub> as the magma ascends and the confining  
360 pressure reduces, resulting to degassing. If degassing takes place in an open system, CO<sub>2</sub>-rich  
361 fluid leaves the magma. This solubility-controlled behavior of CO<sub>2</sub> in basaltic magma may  
362 explain a CO<sub>2</sub>-rich nature of fluids separated from the magma. The ultimate source of CO<sub>2</sub> in the  
363 Nyos, Lobe, Sabga A, and Bambui A springs may therefore be derived from the decarbonation of  
364 crystallized metasomatic fluids in the subcontinental lithosphere (Aka, 2015; Asaah et al., 2015).  
365 The **low** (-2 to -3 ‰) <sup>13</sup>C values of carbonates in the Nyos and Sabga soda spring may also  
366 indicate magmatic origin of the **CO<sub>2</sub>** that contributes in precipitating the carbonates. Thus, the

367 permanent supply of such CO<sub>2</sub> in the springs provides good sites for monitoring volcanic activity  
368 for hazard mitigation.

369

### 370 **Conclusions**

371 The chemistry of water in the bubbling soda springs observed along the Cameroon Volcanic Line  
372 shows an evaporated Na+K-Cl and non-evaporated Ca+Mg-HCO<sub>3</sub> facies in the ocean continental  
373 boundary sector (OCB) and continental sector (CS), respectively. In the OCB, the Lobe soda  
374 springs shows more mineralization than water from nearby hand dug wells. This may indicate  
375 that spring water (T=49°C) is circulating deeper than the well water. In the continental sector  
376 (CS) the water in the Sabga soda springs are the most mineralized, followed by those in Bambui  
377 soda spring and the least mineralized is the Nyos soda spring. With exception of the soda springs  
378 in the Nyos area, all other studied soda springs contain fluoride from geogenic fluorine at  
379 concentrations above the WHO upper limit, whilst concentrations of arsenic (> 0.3 mg/l) that  
380 also call for health concern occur in the Sabga soda springs. The observed soda springs are either  
381 saturated or super-saturated with respect to quartz, and carbonate phases, which are actually  
382 precipitating as dolomite and trona. The carbonate-water fractionation temperature varies from  
383 18.5 - 43°C. X-ray diffraction spectra and chemical mapping by electron probe microanalyzer  
384 unraveled that the precipitating carbonates occur as dolomite in the Lobe and Sabga A soda  
385 springs, and as trona in the Nyos, Bambui and Sabga B soda springs. Scanning electron  
386 microscope (SEM), reveals various morphologies of the carbonates, including amorphous to  
387 tabular euhedral tronas, and nail shaped to bacteria-colonized coliform dolomites. Geochemical  
388 tracers of <sup>13</sup>C, <sup>87</sup>Sr/<sup>86</sup>Sr, and <sup>18</sup>O indicate a dominantly marine provenance of the carbonate.  
389 Chloride versus fluoride cross plot suggest a contribution from volcanic volatiles in the Lobe,  
390 Nyos, Sabga A, and Bambui A springs. This contribution of a volcanic input to these fluids  
391 suggests that they can be used to monitor volcanic activity and thus mitigate hazards, especially  
392 in the vicinity of the Lobe spring that is located close to the currently active Mt. Cameroon.

393

### 394 **Acknowledgements**

395 We thank the Institute of Geological and Mining Research (IRGM), Yaoundé, for financial and  
396 logistical support during sampling. Thanks to the funders (JICA and JST) of SATREPS-IRGM  
397 project that provided field and laboratory equipment that were used to generate the data during

398 this study. We thank all the members of the Department of Environmental Biology and  
399 Chemistry, University of Toyama, Japan, for their enriching comments during the preparation of  
400 this manuscript. We are also grateful to Prof. Suh Emmanuel and Prof. Loic Peiffer for their  
401 review comments that enriched the content of the manuscript.

402

403

404

405

406

407

408

409

410

## 411 **References**

412

413 Aka, F.T., 1991. Volcano Monitoring by Geochemical Analyses of Volcanic Gases. Thesis, The  
414 University of Leeds, LS2 9JT. 94 pp.

415

416

417 Aka, F.T., 2000. Noble gas systematics and K–Ar Chronology: implications on the geotectonic  
418 evolution of the Cameroon Volcanic Line, West Africa, PhD thesis, Univ. Okayama, Japan.  
419 175 pp.

420 Aka, F. T. (2015) Depth of melt segregation below the Nyos maar-diatreme volcano (Cameroon,  
421 West Africa): Major trace element evidence and their bearing on the origin of CO<sub>2</sub> in Lake  
422 Nyos. Volcanic Lakes (Rouwet, D., Christenson, B., Tassi, F. and Vandemeulebrouck, J.,  
423 eds.), Springer-Heidelberg.

424

425

426 Aka, F.T., Kusakabe, M.K., Nagao, K., Tanyileke, G., 2001. Noble gas isotopic compositions  
427 and water/gas chemistry of soda springs from the islands of Bioko, Saõ Tome' and  
428 Annobon, along the Cameroon Volcanic Line, West Africa. Appl. Geochem.16, 323–338.

429

430 Amundson, R., Kelly, E., 1987. The chemistry and mineralogy of a CO<sub>2</sub>-rich travertine  
431 depositing spring in the California Coast Range. Geochim. Cosmochim. Acta 51, 2883–2890.

432

433 Appelo, C.A.J., Postma, D., 2005. Geochemistry, groundwater, and pollution. 2nd edn. Balkema  
434 Publishers, Rotterdam, 649 pp

435 Asai, K., Satake, H., and Tsujimura, M., 2009. Isotopic approach to understanding the

436 groundwater flow system within the andesitic strato-volcano in a temperate humid  
437 region: case study of Ontake volcano, Central Japan. *Hydrol. Processes*. 23, 559-571.  
438

439 Asaah, A. N. E., Yokoyama, T., Aka, F. T., Usui, T., Kuritani, T., Wirmvem, M. J., Iwamori, H.,  
440 Fozing, E. M., Tamen, J., Mofor, G. J., Ohba, T., Tanyileke, G. and Hell, J. V. (2015)  
441 Geochemistry of lavas from maar-bearing volcanoes in the Oku Volcanic Group of the  
442 Cameroon Volcanic Line. *Chem. Geol.* 406, 55–69.  
443

444 Barnes, I., 1965. Geochemistry of Birch Creek, Inyo County, California: a travertine depositing  
445 creek in an arid climate. *Geochim. Cosmochim. Acta* 29, 85–112.  
446

447

448 Bellomo, S., D’Alessandro, W., and Longo, M., 2003. Volcanogenic fluorine in rainwater around  
449 active degassing volcanoes: Mt.Etna and Stromboli Island, Italy. *Sci. Total Environ.* 301,  
450 175–185.  
451

452 Bisse, S. B., Ekomané, E., Eyong, J.T., Ollivier, V., Douville, E., Nganne, M.J.M., Bokanda,  
453 E.E., Bitom, L.D., 2018. Sedimentological and geochemical study of the Bongongo and  
454 Ngol travertines located at the Cameroon Volcanic Line. *Journal of African Earth Sciences*.  
455 DOI.org/10.1016/j.jafrearsci.2018.03.028  
456

457 Craig, H., 1961. Isotopic variations in meteoric waters. *Science* 133:1702–1703  
458

459 Dandurand, J.L., Gout, R., Hoefs, J., Menschel, G., Schott, J., Usdowski, E., 1982. Kinetically  
460 controlled variations of major components and carbon and oxygen isotopes in a calcite  
461 precipitating spring. *Chem. Geol.* 36, 299–315.  
462

463 Davies, T.C., 2013. Geochemical variables as plausible aetiological cofactors in the incidence of  
464 some common environmental diseases in Africa. *Journ. African Earth Sciences.* 79, 24-49  
465

466

467 Demeny, A., Kele, S., and Siklosy, Z., 2010. Empirical equations for the temperature  
468 dependence of calcite-water oxygen isotope fractionation from 10 to 70°C. *Rapid Commun.*  
469 *Mass Spectro.* 24, 3521-3526

470 Demeny, A., Nemeth, P., Czuppon, G., Leel-Ossy, S., Szabo, M., Judik, K., Nemeth, T., Steiber,  
471 J., 2016. Formation of amorphous calcium carbonate in caves and its implications for  
472 speleothem research. *Scientific Report.* 6, 39602  
473

474 Deruelle, B., Nni, J., and Kambou, R., 1987. Mount Cameroon: An active volcano of the  
475 Cameroon Volcanic Line. *J. African Earth Sciences.* 6, 197-214  
476

477 Deutsch, W.J., 1997. Groundwater geochemistry: fundamentals and application to  
478 contamination. CRC, Boca Raton  
479

480 Bradley, W.H., and Eugster, H.P., 1969. Geochemistry and paleolimnology of the trona deposits  
481 and associated authigenic minerals of green river formation of Wyoming. Geological Survey  
482 Professional Paper 496-B, US Government Printing office, Washington, 66 pp  
483

484 Fantong, W.Y., Satake, H., Ayonghe, S.N., Suh, C.E., Adelana, S.M.A., Fantong, E.B.S.,  
485 Banseka, H.S., Gwanfogbe, C.D., Woincham, L.N., Uehara, Y., Zhang, J., 2010b.  
486 Geochemical provenance and spatial distribution of fluoride in groundwater of Mayo  
487 Tsanaga River Basin, Far north Region, Cameroon: implications for incidence of fluorosis  
488 and optimal consumption dose. *Environ Geochem Health*. Vol. 32: 147-163  
489

490 Fantong, W.Y., Kamtchueng, B.T., Yamaguchi, K., Ueda, A., Issa, Ntchantcho, R., Wirmvem,  
491 M.J., Kusakabe, M., Ohba, T., Zhang, J., Aka, F.T., Tanyileke, G.Z., Hell, J.V., 2015.  
492 Characteristics of Chemical weathering and water-rock interaction in Lake Nyos dam  
493 (Cameroon): Implications for vulnerability to failure and re-enforcement. *Journal of African  
494 Earth Sciences*: 101:42-55  
495

496 Fantong, W.Y., Satake, H., Aka, F.T., Ayonghe, S.N., Kazuyoshi, A., Mandal, A.K., Ako, A.A.,  
497 2010a. Hydrochemical and isotopic evidence of recharge, apparent age, and flow direction  
498 of groundwater in Mayo Tsanaga River Basin, Cameroon: Bearings on contamination.  
499 *Journal of Environ Earth Sci*. Vol. 60: 107-120  
500

501 Faure, G., 1991. Principles and Applications of Inorganic Geochemistry. *Macmillan Publishing  
502 Company*, New York, 626 p.  
503  
504

505 Fitton, J.D., 1980. The Benue Trough and the Cameroon Line – A Migrating Rift System in  
506 West Africa. *Earth Planet. Sci. Lett.* 51, 132-138  
507

508 Ford, T.D., Pedley, H.M. 1996. A Review of Tufa and Travertine Deposits of the World. *Earth  
509 Science Reviews* 41, 117-175.  
510

511 Forti, P., 2005. Genetic processes of cave minerals in volcanic environments: an overview.  
512 *Journal of Cave and Karst Studies*. Vol 67:1, 3-13.  
513  
514

515 Friedman, I., 1970. Some investigations of the deposition of travertine from Hot Springs – I. The  
516 isotopic chemistry of a travertine-depositing spring. *Geochim. Cosmochim. Acta* 34, 1303–  
517 1315.

518  
519

520 Garrels, R.M., Mackenzie, F.T., 1967. Origin of the chemical composition of some springs and  
521 lakes. In: RF Gould (ed.). *Equilibrium concepts in natural water systems*. Washington, DC:  
522 American Chemical Society, pp 222-242.

523

524 Halliday, A.N., Dicken, A.P., Fallice, A.E., and Fitton, J.T., 1988. Mantle dynamics. A Nd, Sr,  
525 Pb, and O isotope study of the Cameroon Volcanic Line. *J. Petrol.* 29, 181-211

526  
527

528 Hamilton, S.M., Michel, F.A., Jefferson, C.W., 1991. CO<sub>2</sub>-rich ground waters of the Flat River  
529 Valley, N.W.T. In: Prowse, T., Ommanney, C. (Eds.), *Northern Hydrology Selected  
530 Perspectives, Proceedings of the Northern Hydrology Symposium, 10–12 July 1990,*  
531 *Saskatoon, Saskatchewan, NHRI Paper #6*, pp. 105–199.

532

533 Jacobson, R.L., Usdowski, E., 1975. Geochemical controls on a calcite precipitating spring.  
534 *Contrib. Mineral. Petrol.* 51, 65–74.

535  
536

537 Kamtchueng, B. T., Fantong, W.Y., Wirmvem, M.J., Tiodjio, R.E., Takounjou, A.F., Asai, K.,  
538 Serges L. Djomou, S.L.B., Kusakabe, M., Ohba, T., Tanyileke, G., Hell, J.V., Ueda A.,  
539 2015. A multi-tracer approach for assessing the origin, apparent age and recharge  
540 mechanism of shallow groundwater in the Lake Nyos catchment, Northwest, Cameroon.  
541 *Journal of Hydrology*, 523:790–803.

542

543 Kamtchueng, B.T., Fantong, W.Y., Ueda, A., Tiodjio, E.R., Anazawa, K., Wirmvem, J.,  
544 Mvondo, J.O., Nkamdjou, L., Kusakabe, M., Ohba, T., Tanyileke, G.Z., Joseph, V. H.,  
545 2014. Assessment of shallow groundwater in Lake Nyos catchment (Cameroon, Central-  
546 Africa): implications for hydrogeochemical controls and uses. *Environmental Earth  
547 Sciences*, 72:3663–3678.

548 Kusakabe, M., 2017. Lakes Nyos and Monoun gas disasters (Cameroon)—Limnic eruptions  
549 caused by excessive accumulation of magmatic CO<sub>2</sub> in crater lakes. *GEOchem. Monogr.*  
550 *Ser. 1*, 1–50, doi:10.5047/gems.2017.00101.0001.

551

552 Kusakabe, M., Ohsumi, T., and Arakami, S., 1989. The Lake Nyos gas disaster: chemical and  
553 isotopic evidence in waters and dissolved gases in three Cameroonian Lakes, Nyos,  
554 Monoun and Wum. In: Le Guern, F., and Sigvaldason, G., (Editors), The Lake Nyos Event  
555 and Natural Carbon dioxide Degassing, 1. J. Volcanol. Geothermal Res., 39, 167-185.  
556

557 Kut, K.M.K., Sarsevat, A., Srivastava, A., Pitmann, C.U., Moham, D., 2016. A review of  
558 Fluoride in African Groundwater and Local Remediation Methods. Groundwater for  
559 Sustainable Development 2, 190-175  
560

561 Land, L.S., 1983. The application of stable isotopes to studies of the origin of dolomite and to  
562 problems of diagenesis of clastic sediments, in: Arthur M.A., Anderson T.F. (eds), Stable  
563 isotopes in Sedimentary Geology, Soc. Econ. Paleont. Miner. Short Course No. 10, 4.1-  
564 4.22.  
565

566 Le Marechal, A., 1976. Geologie et Geochemie des sources thermominerales du Cameroun.  
567 ORSTOM, Paris  
568

569

570 Liotta, M., Shamavu, P., Scaglione, S., D'Alessandra, W., Bobrowski, N., Giuffrida, G.B.,  
571 Tedesco, D., Calabrese, S., 2017. Mobility of plume-derived volcanogenic elements in  
572 meteoric water at Nyiragongo volcano (Congo) inferred from the chemical composition of  
573 single rainfall events. *Geochimica et Cosmochimica Acta.* 217, 254-272  
574

575 Liu, Z., Zhang, M., Li, Q., You, S., 2003. Hydrochemical and isotope characteristics of spring  
576 water and travertine in the Baishuitai area (SW China) and their meaning for  
577 paleoenvironmental reconstruction. *Environ. Geol.* 44, 698-704.  
578

579 Lloyd, J.W., Heathcoat, J.A., 1985. Natural inorganic hydrochemistry in relation to groundwater:  
580 an introduction. Oxford University Press, New York, p 296  
581

582

583 McArthur, J.M., Howarth, R.J., Bailey, T.R., 2001. Strontium isotope stratigraphy: LOWESS  
584 Version 3. Best-fit line to the marine Sr-isotope curve for 0 to 509 Ma and accompanying  
585 look-up table for deriving numerical age, *J. Geol.* **109**, 155-169.  
586

587 McCrea, 1950. On the Isotope Chemistry of Carbonates and a Paleotemperature Scale. The  
588 Journal of Chemical Physics. 18, 6.  
589  
590

591 Ngako, V., Njonfang, E., Aka, F. T., Affaton, P., & Nnange, J. M., 2006. The north–south  
592 Paleozoic to Quaternary trend of alkaline magmatism from Niger-Nigeria to Cameroon:  
593 complex interaction between hotspots and Precambrian faults. *Journal of African Earth*  
594 *Sciences*, 45, 241–256. doi:10.1016/j.jafrearsci.2006.03.003.  
595

596 Omelon CR, Pollard WH, Anderson DT (2006) A geochemical evaluation of perennial spring  
597 activity and associated mineral precipitates at Expedition Fjord, Axel Heiberg Island,  
598 Canadian High Arctic. *Applied geochemistry* 21,1-15  
599

600

601 Piper, A.M., 1944. A graphic procedure in the geochemical interpretation of water analyses. *Am*  
602 *Geophys Union Trans* 25:914–923  
603

604 Sano, Y., Kusakabe, M., Hirabayashi, J., Nojiri, Y., Shinohara, H., Njini, T., Tanyileke, G.Z.,  
605 1990. Helium and Carbon Fluxes in Lake Nyos, Cameroon: Constraints on next gas burst.  
606 *Earth and Planetary Science Letters*. 99, 303-314  
607

608

609 Shah, M.M., Nader, F.H., Garcia, D., Swennen, R., Ellam, R., 2012. Hydrothermal dolomites in  
610 the Early Albian (Cretaceous) platform carbonates: (NW Spain): Nature and origin of  
611 dolomite and dolomitizing fluids. *Oil & Gas Science and Technology-Rev. IFP Energies*  
612 *nouvelles* 67:1, 88-122  
613

614 Sighomnou, D., 2004. Analyse et Redefinition des Regimes Climatiques et Hydrologiques du  
615 Cameroun: Perspectives d'évolution des Ressources en Eau. Ph.D Thesis, University of  
616 Yaounde 1. 292 pp.  
617

618

619 Symonds, R. B., Rose, W. I., Reed, M. H., Lichte, F. E., and Finnegan, D. L., 1987.  
620 Volatilization, transport and sublimation of metallic and non-metallic elements in high  
621 temperature gases at Merapi Volcano, Indonesia. *Geochim. Cosmochim.Acta* 51, 2083–  
622 2101.  
623

624 Symonds, R.B., Rose, W.I., Reed, M.H., 1988. Contribution of Cl<sup>-</sup> and F<sup>-</sup> bearing gases to the  
625 atmosphere by volcanoes, *Nature*, 334, 415-418.  
626

627 Tanyileke, G.Z., 1994. Fluid Geochemistry of CO<sub>2</sub> – Rich Lakes and Soda Springs Along the  
628 Cameroon Volcanic Line. Dissertation, Okayama University, Japan.  
629

- 630 Tsujimura, M., Abe, Y., Tanaka, T., Shimada, J., Higuchi, S., Yamanaka, T., Davaa, G.,  
631 Oyunbaatar, D., 2007. Stable isotopic and geochemical characteristics of groundwater in  
632 Kherlin River Basin: a semiarid region in Eastern Mongolia. *J Hydrol* 333:47–57  
633
- 634 Tucker, M. E., and Bathurst, R.G.C., 1990. Carbonate Diagenesis. Reprint series volume 1 of the  
635 International Association of Sedimentologists. Blackwell Scientific Publications. 312 pages  
636  
637
- 638 Usdowski, E., Hoefs, J., Menschel, G., 1979. Relationship between  $^{13}\text{C}$  and  $^{18}\text{O}$  fractionation and  
639 changes in major element composition in a recent calcite-depositing spring – a model of  
640 chemical variations with inorganic  $\text{CaCO}_3$  precipitation. *Earth Planet. Sci. Lett.* 42, 267–  
641 276.  
642
- 643 Usdowski, E., Hoefs, J., 1990. Kinetic  $^{13}\text{C}/^{12}\text{C}$  and  $^{18}\text{O}/^{16}\text{O}$  effects upon dissolution and  
644 outgassing of  $\text{CO}_2$  in the system  $\text{CO}_2\text{--H}_2\text{O}$ . *Chem. Geol.* 80, 109–118.  
645
- 646 Veizer, J., Ala, D., Azmy, K., Bruckschen, P., Buhl, D., Bruhn, F., Carden, G.A.F., Diener, A.,  
647 Ebner, S., Godderis, Y., Jasper, T., Korte, C., Pawellek, F., Podlaha, O., Strauss, H., 1999.  
648  $^{87}\text{Sr}/^{86}\text{Sr}$ ,  $\delta^{13}\text{C}$  and  $\delta^{18}\text{O}$  evolution of Phanerozoic seawater, *Chem. Geol.* **161**, 59-88.  
649  
650
- 651 Verla, R.B., Mboudou, G.M.M., Njoh, O., Ngoran, G.N., Afahnwie, A.N., 2014. Carbonate  
652 Enrichment in Volcanic Debris and Its Relationship with Carbonate Dissolution Signatures  
653 of Springs in the Sabga-Bamessing, North West, Cameroon. *International Journal of*  
654 *Geosciences*, 2014, 5, 107-121  
655
- 656 Whitten, D.G.A., and Brooks, J.R.V., 1972. *The Penguin Dictionary of Geology*. Penguin book  
657 limited, England-Great Britain. 493 pages  
658  
659

### 660 **Figures captions**

661 Fig. 1. Locations of sampled carbonate depositing soda springs along the Cameroon Volcanic  
662 Line (CVL). CS stands for the continental sector of the CVL, and OCB stands for the oceanic  
663 continental boundary of the CVL. The locations of Lake Monoun (L. Monoun), Lake Nyos (L.  
664 Nyos), and Mount Cameroon (Mt. Cameroon) are also shown. The black dots correspond to  
665 samples' locations

666

667 Fig.2. Herds of cattle consuming water from the carbonate depositing springs that have been  
668 harnessed

669

670 Fig. 3. Samples (deposited carbonates and water) collection sites from observed springs

671 Fig. 4. Water chemistry presented as Piper's diagram (a), and Stiff diagrams (b) for the observed  
672 springs

673 Fig. 5. Plot of  $\delta\text{H}$  and  $\delta^{18}\text{O}$  in water from observed springs. The Sabga and Bambui springs  
674 showed no evaporation effect, while the Lobe springs, the Nyos spring and water in shallow  
675 wells around Lobe spring were subjected to evaporation relative to the meteoric water lines.  
676 Zone 1 represents the soda springs and zone 2 represents shallow groundwater in the Lobe spring  
677 neighborhood. LMWL: Local meteoric water line. GMWL: Global meteoric water line

678 Fig. 6. With respect to fluoride concentrations (a), all the observed soda springs with exception  
679 of that in Nyos, contain fluoride above the WHO upper limit of 1.5 mg/l. With respect to Arsenic  
680 (As) concentrations (b), the springs in the continental sector contain As above the WHO upper  
681 limit

682 Fig. 7. The plots of saturation indices (SI; with respect to quartz, anhydrite, aragonite, calcite and  
683 dolomite) versus total dissolved solid (TDS) for investigated water samples (wells and springs),  
684 show three subgroups (1: undersaturated wells. 2: trona precipitating springs. 3: dolomite  
685 precipitating springs).

686 Fig. 8. Stability diagrams for some minerals in the systems  $\text{Na}_2\text{-Al}_2\text{O}_3\text{-SiO}_2\text{-H}_2\text{O}$  (a) and  $\text{CaO-}$   
687  $\text{Al}_2\text{O}_3\text{-SiO}_2\text{-H}_2\text{O}$  (b) at 25°C

688

689 Fig. 9. The scanning electron microscope image (a), X-ray diffraction peaks (b), and electron  
690 probe microanalyzer mapping (c,d, e,f) of carbonate precipitate from Nyos cave spring

691 Fig. 10. The scanning electron microscope image (a), X-ray diffraction peaks (b), and electron  
692 probe microanalyzer mapping (c,d, e,f) of carbonate precipitate from the Sabga A spring

693 Fig. 11. The scanning electron microscope image (a), X-ray diffraction peaks (b), and electron  
694 probe microanalyzer mapping (c,d, e,f) of carbonate precipitate from the Sabga B spring

695 Fig.12. The scanning electron microscope image (a), X-ray diffraction peaks (b), and electron  
696 probe microanalyzer mapping (c,d, e,f) of carbonate precipitate from Bambui B spring

697 Fig. 13. Electron probe microanalyzer mapping of Na, Ca, Mg, and F of carbonate precipitate  
698 from Bambui B spring, showing enrichment of fluorine in the matrix of the carbonate

699 Fig. 14. The scanning electron microscope image (a), X-ray diffraction peaks (b), and electron  
700 probe microanalyzer mapping (c,d, e,f) of carbonate precipitate from Lobe D spring

701 Fig. 15. Carbonates-water oxygen isotopic fractionation temperature in observed soda springs  
702 along the CVL. Dolomites fractionated at relatively higher temperatures (35-43°C) than tronas  
703 (circum 20°C).

704  
705 Fig. 16. Plots of  $^{13}\text{C}$  and  $\delta^{18}\text{O}$  (PDB), showed observed tronas to be relatively depleted in  $^{13}\text{C}$   
706 and enriched in  $^{18}\text{O}$  (PDB).

707  
708 Fig. 17. Except for the Lobe springs that showed highest  $^{87}\text{Sr}/^{86}\text{Sr}$  ratio, in all the other observed  
709 springs the carbonate phases are relatively enriched in  $^{87}\text{Sr}/^{86}\text{Sr}$  ratio than the water phase (a),  
710 and  $^{87}\text{Sr}/^{86}\text{Sr}$  are relatively depleted in tronas than in dolomites (b)

711  
712 Fig. 18. Chloride versus fluoride cross plots showing volcanogenic contributions into the Lobe,  
713 Bambui and Nyos springs

714

715

### 716 **Table captions**

717

718 Table 1. Laboratory analytical methods of the carbonates and water phases in observed springs

719

720 Table 2. Chemical composition of water from the observed springs and shallow wells. ND: not  
721 detected. NM: not measured

722

723 Table 3. Fractionation temperature and isotopic compositions of carbonates precipitating from  
724 the observed springs

725

726

727

728

**Abstract**

A combined study of major ions,  $\delta^{18}\text{O}$ ,  $\delta\text{D}$ ,  $^{13}\text{C}$ ,  $^{87}\text{Sr}/^{86}\text{Sr}$  isotopes, X-ray diffraction, scanning electron microscopy, and electron probe microanalyses on springs and spring mineral precipitates along the Cameroon Volcanic Line (CVL) was undertaken to understand water chemistry, and infer the type and origin of the precipitates. The waters are of evaporated Na+K-Cl and non-evaporated Ca+Mg-HCO<sub>3</sub> types, with the more mineralized (electrical conductivity-EC of 13130  $\mu\text{S}/\text{cm}$ ) Lobe spring inferred to result from interaction of circulating 49°C waters with magmatic volatiles of the active Mt. Cameroon. Water mineralization in the other springs follows the order: Sabga A > Sabga B > Bambui B > Bambui A > Nyos Cave. But for the Nyos Cave spring, all other springs contain fluoride (up to 0.5 - 35.6 mg/l above WHO potable water upper limit). The Sabga spring contains arsenic (up to 1.3 mg/l above the WHO limits). The springs show low fractionation temperatures in the range of 19 – 43 °C. The Lobe and Sabga A springs are precipitating dolomite ( $\text{CaMg}(\text{CO}_3)_2$ ), while the Nyos Cave, Bambui A, Bambui B and Sabga B springs precipitate trona ( $(\text{Na}_3\text{H}(\text{CO}_3)_2 \cdot \text{H}_2\text{O})$ ). Our data suggest a marine provenance for the carbonates, and point to a volcanic input for the Lobe, Nyos, Sabga A, and Bambui A springs. The latter springs are therefore proposed as proxies for monitoring volcanic activity for hazard mitigation along the CVL.

**Key words:** *Bubbling springs. Precipitates. Composition. Provenance. Volcanic activity. Hazards mitigation.*

1  
2  
3  
4  
5  
6  
7  
8  
9  
10  
11  
12  
13  
14  
15  
16  
17  
18  
19  
20  
21  
22  
23  
24  
25  
26  
27  
28  
29  
30  
31  
32  
33  
34  
35  
36  
37  
38  
39  
40  
41  
42  
43  
44  
45  
46  
47  
48  
49  
50  
51  
52  
53  
54  
55  
56  
57  
58  
59  
60  
61  
62  
63  
64  
65

*Bubbling springs. Precipitates. Composition. Provenance. Volcanic activity. Hazards mitigation.*

1  
2  
3  
4  
5  
6  
7  
8  
9  
10  
11  
12  
13  
14  
15  
16  
17  
18  
19  
20  
21  
22  
23  
24  
25  
26  
27  
28  
29  
30  
31  
32  
33  
34  
35  
36  
37  
38  
39  
40  
41  
42  
43  
44  
45  
46  
47  
48  
49  
50  
51  
52  
53  
54  
55  
56  
57  
58  
59  
60  
61  
62  
63  
64  
65

1 **Major ions,  $\delta^{18}\text{O}$ ,  $\delta^{13}\text{C}$  and  $^{87}\text{Sr}/^{86}\text{Sr}$  compositions of water and precipitates from springs**  
 2 **along the Cameroon Volcanic Line (Cameroon, West Africa): Implications for provenance**  
 3 **and volcanic hazards**

4  
 5 Wilson Yetoh FANTONG<sup>1Ψ</sup>, Brice Tchakam KAMTCHUENG<sup>1</sup>, Yasuo ISHIZAKI<sup>2</sup>, Ernest Chi  
 6 FRU<sup>3</sup>, Emilia Bi FANTONG<sup>4</sup>, Mengnjo Jude WIRMVEM<sup>1</sup>, Festus Tongwa AKA<sup>1</sup>, Bertil  
 7 NLEND<sup>1</sup>, Didier HARMAN<sup>4</sup>, Akira UEDA<sup>5</sup>, Minoru KUSAKABE<sup>5</sup>, Gregory TANYILEKE<sup>1</sup>,  
 8 Takeshi OHBA<sup>6</sup>

9 <sup>1</sup> Hydrological Research Center/ IRGM, Box 4110, Yaounde-Cameroon

10 <sup>2</sup> Graduate School of Science and Engineering and Research, Environmental and Energy  
 11 Sciences, Earth and Environmental Systems

12 <sup>3</sup> School of Earth and Ocean Sciences, Cardiff University, Cardiff, Park Place, Wales-United  
 13 Kingdom

14 <sup>4</sup> Ministry of Secondary Education, Cameroon

15 <sup>5</sup>Laboratory of Environmental Biology and Chemistry, University of Toyama, Gofuku 3190,  
 16 Toyama 930-8555 Japan

17 <sup>6</sup>Department of Chemistry, School of Science, Tokai University, Hiratsuka, 259-1211, Japan

18 Ψ Corresponding author: [fyetoh@yahoo.com](mailto:fyetoh@yahoo.com); [fantongy@gmail.com](mailto:fantongy@gmail.com)

19 **Abstract**

20 A combined study of major ions,  $\delta^{18}\text{O}$ ,  $\delta\text{D}$ ,  $^{13}\text{C}$ ,  $^{87}\text{Sr}/^{86}\text{Sr}$  isotopes, X-ray diffraction, scanning  
 21 electron microscopy, and electron probe microanalyses on springs and spring mineral  
 22 precipitates along the Cameroon Volcanic Line (CVL) was undertaken to understand water  
 23 chemistry, and infer the type and origin of the precipitates. The waters are of evaporated Na+K-  
 24 Cl and non-evaporated Ca+Mg-HCO<sub>3</sub> types, with the more mineralized (electrical conductivity-  
 25 EC of 13130  $\mu\text{S}/\text{cm}$ ) Lobe spring inferred to result from interaction of circulating 49°C waters  
 26 with magmatic volatiles of the active Mt. Cameroon. Water mineralization in the other springs  
 27 follows the order: Sabga A > Sabga B > Bambui B > Bambui A > Nyos Cave. But for the Nyos  
 28 Cave spring, all other springs contain fluoride (up to 0.5 - 35.6 mg/l above WHO potable water  
 29 upper limit). The Sabga spring contains arsenic (up to 1.3 mg/l above the WHO limits). The  
 30 springs show low fractionation temperatures in the range of 19 – 43 °C. The Lobe and Sabga A  
 31 springs are precipitating dolomite (CaMg(CO<sub>3</sub>)<sub>2</sub>), while the Nyos Cave, Bambui A, Bambui B

1  
2  
3  
4 32 and Sabga B springs precipitate trona ( $(\text{Na}_3\text{H}(\text{CO}_3)_2 \cdot \text{H}_2\text{O})$ ). Our data suggest a marine provenance  
5  
6 33 for the carbonates, and point to a volcanic input for the Lobe, Nyos, Sabga A, and Bambui A  
7  
8 34 springs. The latter springs are therefore proposed as proxies for monitoring volcanic activity for  
9  
10 35 hazard mitigation along the CVL.

11 36 Key words: *Bubbling springs. Precipitates. Composition. Provenance. Volcanic activity.*  
12  
13 37 *Hazards mitigation.*  
14

15 38  
16  
17 39  
18

## 20 40 **Introduction**

21  
22 41 Mineral-depositing springs are natural systems that offer a good opportunity to study various  
23  
24 42 mechanisms by which waters establish equilibrium with conditions at the Earth's surface  
25  
26 43 (Amundson and Kelly, 1987; Omelon et al., 2006). For example, carbonate-precipitating waters  
27  
28 44 provide an opportunity to evaluate a dynamic carbonate system and the major controls associated  
29  
30 45 with calcite precipitation (Barnes, 1965; Jacobson and Usdowski, 1975), including; isotope  
31  
32 46 fractionation associated with natural calcite precipitation from spring waters (McCrea, 1950;  
33  
34 47 Friedman, 1970; Usdowski et al., 1979; Dandurand et al., 1982; Amundson and Kelly, 1987;  
35  
36 48 Usdowski and Hoefs, 1990; Hamilton et al., 1991; Liu et al., 2003), as well as the types,  
37  
38 49 morphologies, textures, and processes involved in the formation of various carbonate phases  
39  
40 50 (Tucker and Bathurst, 1990; Bradley and Eugster, 1969; Ford and Pedley, 1996; Forti, 2005).  
41

42 51  
43 52 Many orifices of gas-water-carbonate interacting systems occur along the Cameroon Volcanic  
44  
45 53 Line (CVL-Fig. 1). Based on carbonate enrichment studies on volcanic debris and springs in part  
46  
47 54 of the continental sector of the CVL (Le Marechal, 1976; Verla et al., 2014); chemical and  
48  
49 55 isotopic characteristics of fluids along the CVL (Tanyileke, 1994); the geochemistry of gases in  
50  
51 56 springs around Mt. Cameroon and Lake Nyos (Kusakabe et al., 1989; Sano et al., 1990; Aka,  
52  
53 57 1991); the sedimentology and geochemistry of the Bongongo and Ngol travertines along the  
54  
55 58 CVL (Bisse et al., 2018), the following hypotheses have been proposed: (1) the bubbling mineral  
56  
57 59 springs along the CVL contain abundant  $\text{CO}_2$ . (2) The  $\text{CO}_2$  in the bubbling springs is dominantly  
58  
59 60 of magmatic origin. (3) Helium and carbon isotope ratios of gases from a few of the springs  
60  
61  
62  
63  
64  
65

1  
2  
3  
4 61 along the CVL revealed a signature similar to hotspot type magma. (4) The precipitating  
5  
6 62 minerals are travertines.  
7

8  
9 63 Although these studies provide initial data to understand the geochemical dynamics within the  
10  
11 64 CVL gas-water-carbonate systems, gaps required to better understand the system include; a) a  
12  
13 65 total absence of comprehensive information on the classification and genetic processes of the  
14  
15 66 precipitating carbonates, which is exploited by the indigenes for preparation of traditional soup,  
16  
17 67 b) high concentration ( > 100 mg/l) of geogenic fluoride has been reported (e.g., Kut et al., 2016;  
18  
19 68 and references there-in) in thermal waters along the Ethiopian rift. Such concentrations of  
20  
21 69 fluoride in water that is used for domestic purposes and livestock rearing can cause tremendous  
22  
23 70 health effects (e.g., Fantong et al., 2010). Livestock rearing on the slopes of the CVL heavily  
24  
25 71 consumes water from the springs (Fig. 2), so there is still a need to re-assess their chemical  
26  
27 72 characteristics with focus on potential harmful elements like fluoride and arsenic, and c) the  
28  
29 73 carbonate-water fractionation temperature remains unknown.

30  
31 74 Against this backdrop, the objectives of this study are to 1) characterize the water chemistry with  
32  
33 75 focus on health implications, 2) estimate the carbonate-water fractionation temperature, and 3)  
34  
35 76 identify, describe and classify the carbonates that are precipitating from the springs.  
36  
37 77

## 38 78 **Study area**

39  
40 79 Figure 1 shows, the sample sites along the CVL, a prominent 1600 km long Y-shaped chain of  
41  
42 80 Tertiary to Recent, generally alkaline volcanoes that overlap an array of dextral faults called the  
43  
44 81 Central Africa Shear Zone (CASZ) (Ngako et al., 2006) on the African continent, comparable  
45  
46 82 only to the East Africa Rift System. The CVL follows a trend of crustal weakness that stretches  
47  
48 83 from the Atlantic Island of Annobon, through the Gulf of Guinea, to the interior of the African  
49  
50 84 continent (Fitton, 1980; Déruelle et al., 1987, Halliday et al., 1988;). It is unique amongst  
51  
52 85 intraplate volcanic provinces in that it straddles the continental margin and includes both oceanic  
53  
54 86 and continental intraplate volcanism. The oceanic sector constitutes a mildly alkaline volcanic  
55  
56 87 series, which evolves towards phonolite, while the continental sector evolves towards rhyolite  
57  
58 88 (e.g., Fitton, 1980). Isotopic studies of lavas (Halliday et al., 1988) divide the CVL into three  
59  
60 89 sectors: an oceanic zone, ocean-continent boundary zone and a continental zone.

61  
62 90 The study area overlaps two (coastal and tropical western highlands) of the five climatic zones in  
63  
64 91 Cameroon, with mean annual rainfall of 5000 and 3000 mm, mean annual atmospheric  
65

1  
2  
3  
4 92 temperatures of 26°C and 21°C, humidity of 85% and 80%, and evaporation of 600 mm and 700  
5  
6 93 mm, respectively (Sighomnou, 2004). Hydrologically, three (coastal, Sanaga, and Niger) of the  
7  
8 94 five river basins in Cameroon drain the study area in a dendritic manner. According to Le  
9  
10 95 Marechal (1968) and Tanyileke (1994), riverine and in aquifer waters encounter heat and mantle-  
11  
12 96 derived CO<sub>2</sub> gas that emanate through the CASZ, causing heating and bubbling of the spring  
13  
14 97 systems along the CVL. At each spring site the gas phase manifests as either bubbles or ‘rotten  
15  
16 98 egg’ smell, while the precipitates occur as white films, white grains in volcanic ash, stalactite and  
17  
18 99 stalactmite in caves, and mounds around orifices as shown in Fig. 3. At the sites of Sabga A in  
19  
20 100 Fig. 3, animals consume the water as a source of salt, while humans exploit the precipitates for  
21  
22 101 food recipes.

### 23 102 24 103 **Method of study**

25  
26 104 Water and precipitate samples were collected from selected bubbling soda spring sites along the  
27  
28 105 CVL (Fig. 3) in October 2015. Each water sample was collected in 3 acid-washed 250 ml  
29  
30 106 polyethylene bottles after rinsing them thrice with the sample. At each sampling site, an  
31  
32 107 unfiltered, unacidified and tightly corked sample was collected in one bottle for subsequent  
33  
34 108 analyses for stable environmental isotopes of hydrogen ( $\delta^2\text{H}$ ) and oxygen ( $\delta^{18}\text{O}$ ). The second  
35  
36 109 bottle contained un-acidified but filtered sample for anion analyses, and the third filtered and  
37  
38 110 acidified sample for cations and trace elements analyses. Prior to sample collection, in-situ  
39  
40 111 physicochemical measurements were recorded for pH (TOA-DKK HM-30P meter), electrical  
41  
42 112 conductivity (TOA-DKK CM-31P EC meter), reduction-oxidation potential (TOA-DKK ORP  
43  
44 113 meter), and water temperature. Geographical parameters (latitude, longitude and altitude) of each  
45  
46 114 sample site were recorded in the field using a hand-held Garmin GPS. Alkalinity was measured  
47  
48 115 using a ‘‘Hach’’ field titration kit, after addition of 0.16 N H<sub>2</sub>SO<sub>4</sub> to the sample to reach the  
49  
50 116 endpoint titration (pH 4.5). Samples were filtered through 0.2  $\mu\text{m}$  filters prior to major ions and  
51  
52 117 dissolved silica determination. Three kilograms chunks of massive carbonate was chipped off  
53  
54 118 with a hammer at sites with consolidated precipitate, and 300 g scoped from sites with  
55  
56 119 unconsolidated precipitate. Each precipitate was put in a clean plastic container, sealed and  
57  
58 120 labelled.  
59 121 Water samples and precipitates were transported to the University of Toyama, in Japan for  
60  
61 122 chemical analyses.  
62  
63  
64  
65

1  
2  
3  
4 123 The various chemical analyses that were done in various institutes in Japan are tabulated in Table  
5  
6 124 1.

## 7 8 125 9 10 126 **Results and Discussions**

### 11 127 *Variation of water chemistry*

12 128 Chemical compositions and isotopic ratios of water samples and carbonate phases are presented  
13  
14 129 in Tables 2 and 3. Measured in-situ parameters show values in the range of 54 - 13130  $\mu\text{S}/\text{cm}$  for  
15  
16 130 EC, 4.3 - 7.5 for pH, and 19.3 - 47.4°C for water temperature.

17 131 The chemistry of the observed water resources determined with the use of the Piper's diagram  
18  
19 132 (Piper, 1944) (Fig. 4a), shows that water from the Lobe soda springs and its nearby hand dug  
20  
21 133 wells, located in the ocean-continent-boundary (OCB) and close to the ocean (Fig. 4a), have a  
22  
23 134 dominant Na+K-Cl signature. On the other hand, water from the soda springs in Sabga, Bambui,  
24  
25 135 and Nyos have dominantly Ca+Mg-HCO<sub>3</sub> signature. The observed disparity in water facies may  
26  
27 136 be due to the proximity of the Lobe springs to the ocean, which impacts the sodium chloride  
28  
29 137 characteristics as accorded in Le Marechal (1976). Whilst in the other springs, an interaction  
30  
31 138 between primary and secondary minerals in rocks and water could be the dominant explanation  
32  
33 139 as also explained by other researchers (Kamctung et al., 2014; Fantong et al., 2015). The Stiff  
34  
35 140 diagrams for the water chemistry (Fig. 4b), also depict similar water facies like the Piper's  
36  
37 141 diagram, but they further suggest varying degree of mineralization of the water sources. In the  
38  
39 142 OCB, the larger sizes of the stiff diagram for the Lobe soda springs indicate more mineralization  
40  
41 143 than for water from the wells. Likewise in the samples from the continental sector (CS) the water  
42  
43 144 in the Sabga soda springs are most mineralized, followed by those in Bambui and the least  
44  
45 145 mineralized is that from the Nyos soda spring. The observed variation in degree of mineralisation  
46  
47 146 could in part be indicating variation in residence time, where the older springs are enriched in  
48  
49 147 elements from aquifer minerals than in younger springs (e.g., Fantong et al., 2010a; Kamctung  
50  
51 148 et al., 2015) that are renewed through a local and short recharge-discharge flow paths.

### 52 149 53 54 150 *Recharge mechanisms and evaporation of the sampled waters*

55 151 Isotopic ratios of hydrogen and oxygen, which are used in this study to infer recharge and  
56  
57 152 evaporation mechanisms in the waters are also shown in Table 2 and graphically presented in Fig.  
58  
59 153 5. The  $\delta\text{D}$  values ranged from -41.8 in Sabga A soda spring to -26 ‰ in water from well 5.

1  
2  
3  
4  
5  
6  
7  
8  
9  
10  
11  
12  
13  
14  
15  
16  
17  
18  
19  
20  
21  
22  
23  
24  
25  
26  
27  
28  
29  
30  
31  
32  
33  
34  
35  
36  
37  
38  
39  
40  
41  
42  
43  
44  
45  
46  
47  
48  
49  
50  
51  
52  
53  
54  
55  
56  
57  
58  
59  
60  
61  
62  
63  
64  
65

Oxygen isotope ( $\delta^{18}\text{O}$ ) values range from -6.3 ‰ in Sabga A spring to -3.1 ‰ in water from well 3. Due to the paucity of isotope data on local rainfall, the Global Meteoric Water Line (GMWL) of Craig (1961), which is defined by the line  $\delta\text{D} = 8\delta^{18}\text{O} + 10$  is also presented as a reference. Distribution of sample water in the  $\delta\text{D}$ - $\delta^{18}\text{O}$  graph suggests that water in the Bambui and Sabga soda springs are subject to little or no evaporation, while the Lobe soda springs suggest slight evaporation, but water from the wells and Nyos soda springs show remarkable evaporation tendencies. Such a pattern depicts that the Bambui and Sabga soda springs are subject to the mechanism of preferential flow pass, which is caused by rapid recharge (e.g., Tsujimura et al., 2007; Asai et al., 2009), that is favored by the highly altered and jointed lavas as opposed to the Lobe and Nyos cave soda springs, and the wells. Except for the Lobe soda springs, the other springs are sources of drinking water for animals (cattle and goats), and a source of minerals (carbonate) for local manufacture of soup for consumption by the nearby population, thus it is important to assess at a preliminary scale the medical hydrogeochemical characteristics of the springs.

***Health implications of the water chemistry***

Given that the gas bubbling springs are located in the area of livestock rearing and human activities, their chemistry is here preliminarily evaluated to assess potential health implications. With respect to fluoride, Figure 6a shows that except for the Nyos cave soda spring, all the other soda springs contain fluoride at concentrations that are above the WHO optimal limit (1.5 mg/l e.g., Kut et al., 2016). This indicates that the animals and the population that exploit these springs are potentially exposed to fluoride poisoning as reported by Fantong et al. (2010b) in the Far Northern Region of Cameroon. The potential geogenic and volcanic provenance (Davies, 2013), and actual epidemic effects of such high concentrations of fluoride are not within the scope of this study, and need further investigation.

With respect to arsenic (As), Figure 6b shows that the Sabga soda springs contain As at concentrations as high as 1.33 ppm that are above the WHO upper limit (0.03 ppm in drinking water). Based on the field observations that water from the Sabga soda springs is heavily consumed by cattle, and carbonate there-from is exploited for consumption by the population, it is also a challenge for medical geochemists to carry out a comprehensive investigation into the incidence, origin, mobilization and epidemiological effects of arsenic in these areas.

1  
2  
3  
4 185 ***Impact of volcanic volatile or magmatic input on chemistry of the spring water***

5  
6 186 The dissolved state of elements and saturation state of compounds observed in the springs are to  
7  
8 187 an extent determined by their saturation indices and stoichiometry (e.g., Faure, 1991).  
9

10 188  
11  
12 189 ***Saturation indices and activity diagrams***

13 190 The saturation index (SI) of a given mineral in an aqueous system is defined as (Lloyd and  
14  
15 191 Heathcoat, 1985; and Deutch, 1997):

16  
17  
18 192 
$$SI = \log \left( \frac{IAP}{K_{sp}} \right) \quad (1)$$
  
19  
20

21 193 where IAP is the ion activity product and  $K_{sp}$  is the solubility product of the mineral in the  
22  
23 194 system. A  $SI > 0$  points to supersaturation, and a tendency for the mineral to precipitate from the  
24  
25 195 water. Saturation can be produced by factors like incongruent dissolution, common ion effect,  
26  
27 196 evaporation, and rapid increase in temperature and  $CO_2$  exsolution (Appelo and Postma, 2005).  
28  
29 197 A  $SI < 0$  points toward undersaturation, and implies that water dissolves the minerals from  
30  
31 198 surrounding rocks. Negative SI value might also reflect that the character of water is either from  
32  
33 199 a formation with insufficient concentrations of the mineral for precipitation to occur (Garrels and  
34  
35 200 Mackenzie, 1967).

36 201 The thermodynamic data used in this computation are those contained in the database of  
37  
38 202 'Phreeqc for Windows'. A plot of the calculated SI (with respect to quartz, anhydrite, aragonite,  
39  
40 203 calcite and dolomite) versus TDS (Fig.7) groups the water samples into three subgroups:  
41  
42 204 subgroup 1, which consists of water from the shallow wells is undersaturated with respect to all  
43  
44 205 the selected phases and has the lowest TDS values that ranged from 63-83 mg/l. The  
45  
46 206 undersaturation of subgroup 1 suggests that no mineral precipitates in the wells as observed on  
47  
48 207 the field. Subgroup 2, which consists of Nyos cave soda spring, Bambui soda spring B and Sabga  
49  
50 208 soda spring B, show supersaturation with respect to quartz, dolomite. On the field, this subgroup  
51  
52 209 is found to be dominantly precipitating trona (a Na-rich carbonate) and dolomite to a lesser  
53  
54 210 extent. Subgroup 3 that consists of the Lobe and Sabga A soda springs, are supersaturated with  
55  
56 211 respect to dolomite, quartz and calcite, and it is actually precipitating more of dolomite, and  
57  
58 212 trona to a lesser extent.

59 213 The stability of secondary minerals (Na and Ca montmorillonites, kaolinite, gibbsite) and  
60 214 amorphous quartz in the springs and wells were evaluated by plotting  $\log (a_{Na}/a_H)$  vs  $\log (a_{H_4SiO_4})$   
61  
62  
63  
64  
65

1  
2  
3  
4  
5  
6  
7  
8  
9  
10  
11  
12  
13  
14  
15  
16  
17  
18  
19  
20  
21  
22  
23  
24  
25  
26  
27  
28  
29  
30  
31  
32  
33  
34  
35  
36  
37  
38  
39  
40  
41  
42  
43  
44  
45  
46  
47  
48  
49  
50  
51  
52  
53  
54  
55  
56  
57  
58  
59  
60  
61  
62  
63  
64  
65

(the albite system) (Fig. 8a) and  $\log (a_{Ca2}/a_{2H})$  versus  $\log (a_{H4SiO4})$  (the anorthite system) (Fig. 8b). These diagrams were drawn with the assumption that aluminum was preserved in the weathering product (Appelo and Postma,1993), because the amount of alumina will remain constant in fresh rocks and its altered equivalent. The constant amount in alumina ( $Al_2O_3$ ) is because an apparent increase in its weight % is actually always caused by a reduction in the weight of the fresh rock to some smaller amount (Faure, 1991). End member compositions were also assumed using equilibrium relationship for standard temperature ( $25^\circ C$ ) and pressure (1 atmosphere), which approximately reflect the springs and groundwater conditions. Activities of the species were computed using the analytical concentrations and activity coefficient determined by Phreeqc for Windows version 2.1 under the above conditions (Appelo and Postma, 1993). According to the figures, groundwater from the wells span the stability field of kaolinite, while all the soda springs with exception of the Nyos soda spring are in equilibrium within the Na and Ca -montmorillonite stability fields. This concurs with the incidence of clay minerals in the study area (Fantong et al., 2015). Moreover, the presence of kaolinite and montmorillonite in the study area occur as groundmass in the XRD (X-Ray Defraction) peaks of Figures 9b,10b, 11b, 12b, and 14b. A combination of information from the saturation indices and stability diagrams is supported by the presence of precipitating carbonate phases in the soda springs as shown in Fig. 1.

***Typology of carbonate phases***

The typology of the carbonate phases that precipitate from the observed soda springs is done by describing the morphology by using SEM images, and identifying the carbonate phase by using XRD diagrams and EPMA elemental mapping.

**Carbonate from the Nyos cave soda spring**

The SEM image in Fig. 9a shows that the carbonate is an association of cluster of powdery amorphous groundmass upon which sub-euhedral crystals developed. This carbonate is identified with XRD peaks (Fig.9b) as a trona (low- syn trisodium hydrogen dehydrate carbonate). To accentuate the trona phase, an elemental EPMA mapping (Fig.9 c, d, e and f) shows the dominance of sodium, traces of calcium and total absence of magnesium.

1  
2  
3  
4  
5  
6  
7  
8  
9  
10  
11  
12  
13  
14  
15  
16  
17  
18  
19  
20  
21  
22  
23  
24  
25  
26  
27  
28  
29  
30  
31  
32  
33  
34  
35  
36  
37  
38  
39  
40  
41  
42  
43  
44  
45  
46  
47  
48  
49  
50  
51  
52  
53  
54  
55  
56  
57  
58  
59  
60  
61  
62  
63  
64  
65

246 **Carbonate from Sabga A soda spring**

247 The SEM image of Fig. 10a shows that the carbonate is nail-shaped stalactite crystals protruding  
248 from a cluster of powdery amorphous groundmass. This carbonate is identified with XRD peaks  
249 (Fig.10b) as a dolomite (calcium-magnesium bicarbonate). Dolomite precipitate in this spring is  
250 supported by an elemental EPMA mapping (Fig. 10 c, d, e and f), which shows a dominance and  
251 remarkable presence of both calcium and magnesium, with traces of sodium.

252  
253 **Carbonate from Sabga B soda spring**

254 The SEM image of Fig. 11a shows that the carbonate is made up of radiating tabular columns of  
255 crystals whose faces are edged by bacteria. This carbonate is identified with XRD peaks (Fig.  
256 11b) as a trona (low-syn trisodium hydrogen dehydrate carbonate). The presence of this trona  
257 precipitating in this spring is justified by an elemental EPMA mapping (Fig. 11c, d, e and f),  
258 which shows a dominance of sodium and an almost absence of calcium and magnesium.

259  
260 **Carbonate from Bambui B soda spring**

261 The SEM image of Fig. 12a shows that the morphology of the carbonate is an intersecting  
262 mosaic of tabular crystals whose faces are edged by bacteria. This carbonate is identified with  
263 XRD peaks (Fig. 12b) as a trona similar to that of Sabga B. The presence of this trona  
264 precipitating in this spring is supported by an elemental EPMA mapping (Fig. 12 c, d, e and f),  
265 which shows a dominance of sodium and low content of calcium and magnesium. The  
266 disseminated distribution of fluorine, which almost coincide with the distribution of faint calcite  
267 suggest the presence of fluorite (CaF<sub>2</sub>), which could be dissolving to enrich the water phase with  
268 fluoride as seen in Fig. 13e.

269  
270 **Carbonate from Lobe D soda spring**

271 The SEM image of Fig. 14a shows that the carbonate is a coliform flower-shape radiating  
272 crystals, which is colonized by bacteria. This carbonate is identified with XRD peaks (Fig. 14b)  
273 as a dolomite. The occurrence of dolomite as the precipitate in this spring is supported by an  
274 elemental EPMA mapping (Fig. 14c, d, e and f), which shows high content of both calcium and  
275 magnesium, and low content of sodium.

1  
2  
3  
4  
5  
6  
7  
8  
9  
10  
11  
12  
13  
14  
15  
16  
17  
18  
19  
20  
21  
22  
23  
24  
25  
26  
27  
28  
29  
30  
31  
32  
33  
34  
35  
36  
37  
38  
39  
40  
41  
42  
43  
44  
45  
46  
47  
48  
49  
50  
51  
52  
53  
54  
55  
56  
57  
58  
59  
60  
61  
62  
63  
64  
65

276 Summarily, the carbonate phases that are precipitating from the studied soda springs along the  
277 CVL are dominantly dolomite and trona. The pristine geochemical attributes and characteristics  
278 of the carbonate are at a later phase altered (Demeny, 2016) by diatoms and bacteria as shown in  
279 Figure 11a and 12a. The incidence of bacteria in such a hydrogeochemical system leaves  
280 biogeochemists with another opportunity to assess the incidence and role of bacteria in the soda  
281 spring systems.

282  
283 **Origin of the fluids and carbonates**

284 In a bid to identify the formation (sources and paleo temperature) processes that led to the  
285 formation of the observed carbonates, we used <sup>13</sup>C isotopes, <sup>87</sup>Sr/<sup>86</sup>Sr, carbonate-water  
286 fractionation temperatures, and Cl<sup>-</sup> versus F<sup>-</sup> plot as geochemical tracers.

287  
288 *Carbonate-water fractionation temperature*

289 Although oxygen-isotope thermometry based on isotopic fractionation of oxygen between  
290 carbonates and water dates back to the Mid-1900s, the carbonate-water oxygen isotopic  
291 fractionation equations are still being discussed. The use of isotope thermometry is based on  
292 several criteria: (i) the temperature dependence of the isotopic fractionation between the  
293 investigated compounds (in our case dolomite/trona and water) and (ii) the isotopic compositions  
294 of the compounds are known, (iii) the isotopic equilibrium between the compounds can be  
295 proven or at least reasonably assumed, and (iv) no subsequent isotopic alteration occurred after  
296 the deposition of carbonates. These considerations are valid for inorganic carbonate formation, as  
297 biogenic carbonate is severely affected by the organisms' metabolism, resulting in a species-  
298 dependent "vital effect" (Demeny et al., 2010 and references therein)

299 The temperatures at which the carbonate phases precipitate from the springs were calculated by  
300 using the empirical equation for the temperature dependence of calcite-water oxygen isotope  
301 fractionation from 10 to 70 °C as shown in equations 2 and 3 that were reported by Demeny et al.  
302 (2010).

303  $1000 \cdot \ln \alpha = 17599/T - 29.64$  [for travertines with a temperature range of 30 to 70°C] (2)

304  $1000 \cdot \ln \alpha = 17500/T - 29.89$  [for cave deposits for the range 10 to 25°C] (3)

305 The variable T are in °C.

1  
2  
3  
4 306 The values obtained suggest that carbonates precipitate from soda springs along the CVL at  
5  
6 307 temperature that varied from 18.5 - 43°C. The lowest fractionation temperatures (18.5 - 18.6°C)  
7  
8 308 occurred in the Sabga soda springs, while the highest (35 - 43°C), occurred in the Lobe soda  
9  
10 309 springs (Table 3). A plot (Fig. 15), shows that with the exception of the dolomite in the 'Sabga  
11  
12 310 A soda spring', the tronas fractionated at lower temperature (~18.5 - 20 °C) than the dolomites,  
13  
14 311 which fractionated at temperature ranging from 35.2 - 43°C. Based on Figure 15, the oxygen  
15  
16 312 isotopes in carbonates precipitating along the Cameroon Volcanic Line yielded an empirical  
17  
18 313 fractionation– temperature equations of:

$$19 \quad 314 \quad 1000.\ln\alpha = -0.2153T + 35.3 \quad (4)$$

### 22 316 *Stable isotopes of <sup>13</sup>C, <sup>87</sup>Sr/<sup>86</sup>Sr, and <sup>18</sup>O*

24 317 The observed carbonates (dolomite and trona) facies in the samples showed broad ranges in  
25  
26 318 <sup>87</sup>Sr/<sup>86</sup>Sr, <sup>13</sup>C and δ<sup>18</sup>O. The <sup>87</sup>Sr/<sup>86</sup>Sr ratio varied from 0.706 - 0.713, the <sup>13</sup>C varied from -3.09 to  
27  
28 319 5.22 VPDB and δ<sup>18</sup>O from -8.4 to -1.4 VPDB as shown in Table 3. Their δ<sup>13</sup>C values of observed  
29  
30 320 dolomites are close to the range of values reported for carbonates precipitating from seawater (0  
31  
32 321 -4 VPDB; Veizer et al., 1999; Shah et al., 2012). Indication of marine origin of the dolomites  
33  
34 322 corroborates with field observation, because the dolomite precipitates from the Lobe soda spring  
35  
36 323 located in the OCB of the study area. However, the carbonates (trona) identified in our study  
37  
38 324 area showed relatively depleted δ<sup>13</sup>C signatures, which may indicate a possible external source of  
39  
40 325 carbon during trona precipitation (Fig. 16) or a temperature dependent fractionation effect (Shah  
41  
42 326 et al., 2012). The depleted δ<sup>18</sup>O in dolomite from the 49°C Lobe soda springs, may be due to its  
43  
44 327 higher temperatures (thermogenic type) (Bisse et al., 2018), given that precipitation of dolomite  
45  
46 328 from hot springs leads to relatively depleted δ<sup>18</sup>O ratios (Land, 1983).

46 329 With exception of the Lobe soda springs, where <sup>87</sup>Sr/<sup>86</sup>Sr value did not vary between the  
47  
48 330 carbonate and water phases, in the other soda springs (Bambui soda springs A and B, Sabga soda  
49  
50 331 springs A and B, and Nyos cave soda spring), the <sup>87</sup>Sr/<sup>86</sup>Sr ratio shows a decoupling tendency  
51  
52 332 where the water phases contain relatively higher values than the carbonate phases (Fig. 17a). The  
53  
54 333 relatively higher <sup>87</sup>Sr/<sup>86</sup>Sr ratio in the Lobe soda springs may indicate interaction of dolomitizing  
55  
56 334 fluids with radiogenic lithologies (Shah et al., 2012), which commonly occur along the CVL  
57  
58 335 (e.g., Aka et al., 2000; 2001). Moreover, the <sup>87</sup>Sr/<sup>86</sup>Sr versus <sup>18</sup>O cross plot (Fig. 17b), shows that  
59  
60 336 the dolomites are richer in <sup>87</sup>Sr/<sup>86</sup>Sr ratio than the tronas. However, the signatures in the dolomite

1  
2  
3  
4  
5  
6  
7  
8  
9  
10  
11  
12  
13  
14  
15  
16  
17  
18  
19  
20  
21  
22  
23  
24  
25  
26  
27  
28  
29  
30  
31  
32  
33  
34  
35  
36  
37  
38  
39  
40  
41  
42  
43  
44  
45  
46  
47  
48  
49  
50  
51  
52  
53  
54  
55  
56  
57  
58  
59  
60  
61  
62  
63  
64  
65

337 of the Sabga soda spring “A” together with those in the tronas are closer to those of the marine  
338 signatures (McArthur et al., 2001). Such marine signatures in tronas (Na-rich carbonate) within  
339 the continental sector of the Cameroon Volcanic Line, may suggest the presence of paleo-  
340 continental sabkha environments, where various sodium carbonates have been recorded in  
341 tropical regions (Whitten and Brooks, 1972). This suggestion, however, requires further  
342 investigation.

### 343 344 **Implications for monitoring and hazard mitigation**

345 Volcanogenic sources of fluorine (e.g., Symonds et al., 1987; Symonds et al., 1988; Bellomo et  
346 al., 2003) and chlorine (e.g., Keene and Graedel 1995) containing gasses have been reported in  
347 active and passive volcanic areas, and recently in the Nyiragongo volcano in Congo (Liotta et al.,  
348 2017). As used by the later, we also used a cross plot of chloride versus fluoride (Fig. 18) to infer  
349 volcanogenic contribution in the observed springs along the CVL. The figure suggests  
350 volcanogenic inputs into the Lobe, Nyos, Sabga A, and Bambui A springs. The implication of a  
351 volcanic input to these fluids suggests that they can be used to monitor volcanic activity and thus  
352 mitigate hazards, especially in the vicinity of the Lobe spring located close to the currently active  
353 Mt. Cameroon. Moreover, the dominant fluids in the Lobe, Nyos, Sabga A, and Bambui A  
354 springs are magmatic CO<sub>2</sub> and H<sub>2</sub>O (Sano 1990). Water dissolves slightly more in silicic melts  
355 than in basaltic melts, whereas CO<sub>2</sub> dissolves more in basaltic than in silicic melts. Kusakabe  
356 (2017) reports that the solubility of CO<sub>2</sub> and H<sub>2</sub>O in basaltic melts at 1200°C is a function of the  
357 total pressure of the volatiles, whose composition in the melt changes as the decompression  
358 proceeds. For example, at low pressure the mole fraction of H<sub>2</sub>O equals 0.2 and that of CO<sub>2</sub> is  
359 0.8, implying that basaltic melt becomes rich in CO<sub>2</sub> as the magma ascends and the confining  
360 pressure reduces, resulting to degassing. If degassing takes place in an open system, CO<sub>2</sub>-rich  
361 fluid leaves the magma. This solubility-controlled behavior of CO<sub>2</sub> in basaltic magma may  
362 explain a CO<sub>2</sub>-rich nature of fluids separated from the magma. The ultimate source of CO<sub>2</sub> in the  
363 Nyos, Lobe, Sabga A, and Bambui A springs may therefore be derived from the decarbonation of  
364 crystallized metasomatic fluids in the subcontinental lithosphere (Aka, 2015; Asaah et al., 2015).  
365 The low (-2 to -3 ‰) <sup>13</sup>C values of carbonates in the Nyos and Sabga soda spring may also  
366 indicate magmatic origin of the CO<sub>2</sub> that contributes in precipitating the carbonates. Thus, the

1  
2  
3  
4  
5  
6  
7  
8  
9  
10  
11  
12  
13  
14  
15  
16  
17  
18  
19  
20  
21  
22  
23  
24  
25  
26  
27  
28  
29  
30  
31  
32  
33  
34  
35  
36  
37  
38  
39  
40  
41  
42  
43  
44  
45  
46  
47  
48  
49  
50  
51  
52  
53  
54  
55  
56  
57  
58  
59  
60  
61  
62  
63  
64  
65

367 permanent supply of such CO<sub>2</sub> in the springs provides good sites for monitoring volcanic activity  
368 for hazard mitigation.

### 370 **Conclusions**

371 The chemistry of water in the bubbling soda springs observed along the Cameroon Volcanic Line  
372 shows an evaporated Na+K-Cl and non-evaporated Ca+Mg-HCO<sub>3</sub> facies in the ocean continental  
373 boundary sector (OCB) and continental sector (CS), respectively. In the OCB, the Lobe soda  
374 springs shows more mineralization than water from nearby hand dug wells. This may indicate  
375 that spring water (T=49°C) is circulating deeper than the well water. In the continental sector  
376 (CS) the water in the Sabga soda springs are the most mineralized, followed by those in Bambui  
377 soda spring and the least mineralized is the Nyos soda spring. With exception of the soda springs  
378 in the Nyos area, all other studied soda springs contain fluoride from geogenic fluorine at  
379 concentrations above the WHO upper limit, whilst concentrations of arsenic (> 0.3 mg/l) that  
380 also call for health concern occur in the Sabga soda springs. The observed soda springs are either  
381 saturated or super-saturated with respect to quartz, and carbonate phases, which are actually  
382 precipitating as dolomite and trona. The carbonate-water fractionation temperature varies from  
383 18.5 - 43°C. X-ray diffraction spectra and chemical mapping by electron probe microanalyzer  
384 unraveled that the precipitating carbonates occur as dolomite in the Lobe and Sabga A soda  
385 springs, and as trona in the Nyos, Bambui and Sabga B soda springs. Scanning electron  
386 microscope (SEM), reveals various morphologies of the carbonates, including amorphous to  
387 tabular euhedral tronas, and nail shaped to bacteria-colonized coliform dolomites. Geochemical  
388 tracers of <sup>13</sup>C, <sup>87</sup>Sr/<sup>86</sup>Sr, and <sup>18</sup>O indicate a dominantly marine provenance of the carbonate.  
389 Chloride versus fluoride cross plot suggest a contribution from volcanic volatiles in the Lobe,  
390 Nyos, Sabga A, and Bambui A springs. This contribution of a volcanic input to these fluids  
391 suggests that they can be used to monitor volcanic activity and thus mitigate hazards, especially  
392 in the vicinity of the Lobe spring that is located close to the currently active Mt. Cameroon.

### 394 **Acknowledgements**

395 We thank the Institute of Geological and Mining Research (IRGM), Yaoundé, for financial and  
396 logistical support during sampling. Thanks to the funders (JICA and JST) of SATREPS-IRGM  
397 project that provided field and laboratory equipment that were used to generate the data during

1  
2  
3  
4  
5  
6  
7  
8  
9  
10  
11  
12  
13  
14  
15  
16  
17  
18  
19  
20  
21  
22  
23  
24  
25  
26  
27  
28  
29  
30  
31  
32  
33  
34  
35  
36  
37  
38  
39  
40  
41  
42  
43  
44  
45  
46  
47  
48  
49  
50  
51  
52  
53  
54  
55  
56  
57  
58  
59  
60  
61  
62  
63  
64  
65

this study. We thank all the members of the Department of Environmental Biology and Chemistry, University of Toyama, Japan, for their enriching comments during the preparation of this manuscript. We are also grateful to Prof. Suh Emmanuel and Prof. Loic Peiffer for their review comments that enriched the content of the manuscript.

**References**

Aka, F.T., 1991. Volcano Monitoring by Geochemical Analyses of Volcanic Gases. Thesis, The University of Leeds, LS2 9JT. 94 pp.

Aka, F.T., 2000. Noble gas systematics and K–Ar Chronology: implications on the geotectonic evolution of the Cameroon Volcanic Line, West Africa, PhD thesis, Univ. Okayama, Japan. 175 pp.

Aka, F. T. (2015) Depth of melt segregation below the Nyos maar-diatreme volcano (Cameroon, West Africa): Majortrace element evidence and their bearing on the origin of CO<sub>2</sub> in Lake Nyos. Volcanic Lakes (Rouwet, D., Christenson, B., Tassi, F. and Vandemeulebrouck, J., eds.), Springer-Heidelberg.

Aka, F.T., Kusakabe, M.K., Nagao, K., Tanyileke, G., 2001. Noble gas isotopic compositions and water/gas chemistry of soda springs from the islands of Bioko, Saõ Tome´ and Annobon, along the Cameroon Volcanic Line, West Africa. Appl. Geochem.16, 323–338.

Amundson, R., Kelly, E., 1987. The chemistry and mineralogy of a CO<sub>2</sub>-rich travertine depositing spring in the California Coast Range. Geochim. Cosmochim. Acta 51, 2883–2890.

Appelo, C.A.J., Postma, D., 2005. Geochemistry, groundwater, and pollution. 2nd edn. Balkema Publishers, Rotterdam, 649 pp

Asai, K., Satake, H., and Tsujimura, M., 2009. Isotopic approach to understanding the

1  
2  
3  
4  
5  
6  
7  
8  
9  
10  
11  
12  
13  
14  
15  
16  
17  
18  
19  
20  
21  
22  
23  
24  
25  
26  
27  
28  
29  
30  
31  
32  
33  
34  
35  
36  
37  
38  
39  
40  
41  
42  
43  
44  
45  
46  
47  
48  
49  
50  
51  
52  
53  
54  
55  
56  
57  
58  
59  
60  
61  
62  
63  
64  
65

436 groundwater flow system within the andesitic strato-volcano in a temperate humid  
437 region: case study of Ontake volcano, Central Japan. *Hydrol. Processes*. 23, 559-571.  
438

439 Asaah, A. N. E., Yokoyama, T., Aka, F. T., Usui, T., Kuritani, T., Wirmvem, M. J., Iwamori, H.,  
440 Fozing, E. M., Tamen, J., Mofor, G. J., Ohba, T., Tanyileke, G. and Hell, J. V. (2015)  
441 Geochemistry of lavas from maar-bearing volcanoes in the Oku Volcanic Group of the  
442 Cameroon Volcanic Line. *Chem. Geol.* 406, 55–69.  
443

444 Barnes, I., 1965. Geochemistry of Birch Creek, Inyo County, California: a travertine depositing  
445 creek in an arid climate. *Geochim. Cosmochim. Acta* 29, 85–112.  
446

447

448 Bellomo, S., D’Alessandro, W., and Longo, M., 2003. Volcanogenic fluorine in rainwater around  
449 active degassing volcanoes: Mt.Etna and Stromboli Island, Italy. *Sci. Total Environ.* 301,  
450 175–185.  
451

452 Bisse, S. B., Ekomané, E., Eyong, J.T., Ollivier, V., Douville, E., Nganne, M.J.M., Bokanda,  
453 E.E., Bitom, L.D., 2018. Sedimentological and geochemical study of the Bongongo and  
454 Ngol travertines located at the Cameroon Volcanic Line. *Journal of African Earth Sciences*.  
455 DOI.org/10.1016/j.jafrearsci.2018.03.028  
456

457 Craig, H., 1961. Isotopic variations in meteoric waters. *Science* 133:1702–1703  
458

459 Dandurand, J.L., Gout, R., Hoefs, J., Menschel, G., Schott, J., Usdowski, E., 1982. Kinetically  
460 controlled variations of major components and carbon and oxygen isotopes in a calcite  
461 precipitating spring. *Chem. Geol.* 36, 299–315.  
462

463 Davies, T.C., 2013. Geochemical variables as plausible aetiological cofactors in the incidence of  
464 some common environmental diseases in Africa. *Journ. African Earth Sciences.* 79, 24-49  
465

466

467 Demeny, A., Kele, S., and Siklosy, Z., 2010. Empirical equations for the temperature  
468 dependence of calcite-water oxygen isotope fractionation from 10 to 70°C. *Rapid Commun.*  
469 *Mass Spectro.* 24, 3521-3526  
470

471 Demeny, A., Nemeth, P., Czuppon, G., Leel-Ossy, S., Szabo, M., Judik, K., Nemeth, T., Steiber,  
472 J., 2016. Formation of amorphous calcium carbonate in caves and its implications for  
473 speleothem research. *Scientific Report.* 6, 39602  
474

475 Deruelle, B., Nni, J., and Kambou, R., 1987. Mount Cameroon: An active volcano of the  
476 Cameroon Volcanic Line. *J. African Earth Sciences.* 6, 197-214

1  
2  
3  
4  
5  
6  
7  
8  
9  
10  
11  
12  
13  
14  
15  
16  
17  
18  
19  
20  
21  
22  
23  
24  
25  
26  
27  
28  
29  
30  
31  
32  
33  
34  
35  
36  
37  
38  
39  
40  
41  
42  
43  
44  
45  
46  
47  
48  
49  
50  
51  
52  
53  
54  
55  
56  
57  
58  
59  
60  
61  
62  
63  
64  
65

477 Deutsch, W.J., 1997. Groundwater geochemistry: fundamentals and application to  
478 contamination. CRC, Boca Raton  
479

480 Bradley, W.H., and Eugster, H.P., 1969. Geochemistry and paleolimnology of the trona deposits  
481 and associated authigenic minerals of green river formation of Wyoming. Geological Survey  
482 Professional Paper 496-B, US Government Printing office, Washington, 66 pp  
483

484 Fantong, W.Y., Satake, H., Ayonghe, S.N., Suh, C.E., Adelana, S.M.A., Fantong, E.B.S.,  
485 Banseka, H.S., Gwanfogbe, C.D., Woincham, L.N., Uehara, Y., Zhang, J., 2010b.  
486 Geochemical provenance and spatial distribution of fluoride in groundwater of Mayo  
487 Tsanaga River Basin, Far north Region, Cameroon: implications for incidence of fluorosis  
488 and optimal consumption dose. Environ Geochem Health. Vol. 32: 147-163  
489

490 Fantong, W.Y., Kamtchueng, B.T., Yamaguchi, K., Ueda, A., Issa, Ntchantcho, R., Wirmvem,  
491 M.J., Kusakabe, M., Ohba, T., Zhang, J., Aka, F.T., Tanyileke, G.Z., Hell, J.V., 2015.  
492 Characteristics of Chemical weathering and water-rock interaction in Lake Nyos dam  
493 (Cameroon): Implications for vulnerability to failure and re-enforcement. Journal of African  
494 Earth Sciences: 101:42-55  
495

496 Fantong, W.Y., Satake, H., Aka, F.T., Ayonghe, S.N., Kazuyoshi, A., Mandal, A.K., Ako, A.A.,  
497 2010a. Hydrochemical and isotopic evidence of recharge, apparent age, and flow direction  
498 of groundwater in Mayo Tsanaga River Basin, Cameroon: Bearings on contamination.  
499 Journal of Environ Earth Sci. Vol. 60: 107-120  
500

501 Faure, G., 1991. Principles and Applications of Inorganic Geochemistry. *Macmillan Publishing*  
502 *Company*, New York, 626 p.  
503

504

505 Fitton, J.D., 1980. The Benue Trough and the Cameroon Line – A Migrating Rift System in  
506 West Africa. Earth Planet. Sci. Lett. 51, 132-138  
507

508 Ford, T.D., Pedley, H.M. 1996. A Review of Tufa and Travertine Deposits of the World. Earth  
509 Science Reviews 41, 117-175.  
510

511 Forti, P., 2005. Genetic processes of cave minerals in volcanic environments: an overview.  
512 Journal of Cave and Karst Studies. Vol 67:1, 3-13.  
513

- 1  
2  
3  
4 515 Friedman, I., 1970. Some investigations of the deposition of travertine from Hot Springs – I. The  
5 isotopic chemistry of a travertine-depositing spring. *Geochim. Cosmochim. Acta* 34, 1303–  
6 516 1315.  
7 517  
8 518  
9 519
- 10 520 Garrels, R.M., Mackenzie, F.T., 1967. Origin of the chemical composition of some springs and  
11 521 lakes. In: RF Gould (ed.). *Equilibrium concepts in natural water systems*. Washington, DC:  
12 522 American Chemical Society, pp 222-242.  
13  
14  
15  
16 523  
17  
18 524 Halliday, A.N., Dicken, A.P., Fallice, A.E., and Fitton, J.T., 1988. Mantle dynamics. A Nd, Sr,  
19 525 Pb, and O isotope study of the Cameroon Volcanic Line. *J. Petrol.* 29, 181-211  
20 526  
21 527  
22  
23 528 Hamilton, S.M., Michel, F.A., Jefferson, C.W., 1991. CO<sub>2</sub>-rich ground waters of the Flat River  
24 529 Valley, N.W.T. In: Prowse, T., Ommanney, C. (Eds.), *Northern Hydrology Selected  
25 530 Perspectives, Proceedings of the Northern Hydrology Symposium, 10–12 July 1990,*  
26 531 *Saskatoon, Saskatchewan, NHRI Paper #6*, pp. 105–199.  
27 532  
28  
29 533 Jacobson, R.L., Usdowski, E., 1975. Geochemical controls on a calcite precipitating spring.  
30 534 *Contrib. Mineral. Petrol.* 51, 65–74.  
31 535  
32 536  
33  
34 537 Kamtchueng, B. T., Fantong, W.Y., Wirmvem, M.J., Tiodjio, R.E., Takounjou, A.F., Asai, K.,  
35 538 Serges L. Djomou, S.L.B., Kusakabe, M., Ohba, T., Tanyileke, G., Hell, J.V., Ueda A.,  
36 539 2015. A multi-tracer approach for assessing the origin, apparent age and recharge  
37 540 mechanism of shallow groundwater in the Lake Nyos catchment, Northwest, Cameroon.  
38 541 *Journal of Hydrology*, 523:790–803.  
39 542  
40  
41 543 Kamtchueng, B.T., Fantong, W.Y., Ueda, A., Tiodjio, E.R., Anazawa, K., Wirmvem, J.,  
42 544 Mvondo, J.O., Nkamdjou, L., Kusakabe, M., Ohba, T., Tanyileke, G.Z., Joseph, V. H.,  
43 545 2014. Assessment of shallow groundwater in Lake Nyos catchment (Cameroon, Central-  
44 546 Africa): implications for hydrogeochemical controls and uses. *Environmental Earth  
45 547 Sciences*, 72:3663–3678.  
46 548 Kusakabe, M., 2017. Lakes Nyos and Monoun gas disasters (Cameroon)—Limnic eruptions  
47 549 caused by excessive accumulation of magmatic CO<sub>2</sub> in crater lakes. *GEOchem. Monogr.*  
48 550 Ser. 1, 1–50, doi:10.5047/gems.2017.00101.0001.  
49 551  
50  
51  
52  
53  
54  
55  
56  
57  
58  
59  
60  
61  
62  
63  
64  
65

1  
2  
3  
4 552 Kusakabe, M., Ohsumi, T., and Arakami, S., 1989. The Lake Nyos gas disaster: chemical and  
5 isotopic evidence in waters and dissolved gases in three Cameroonian Lakes, Nyos,  
6 553  
7 554 Monoun and Wum. In: Le Guern, F., and Sigvaldason, G., (Editors), The Lake Nyos Event  
8 and Natural Carbon dioxide Degassing, 1. J. Volcanol. Geothermal Res., 39, 167-185.  
9 555  
10 556  
11 557 Kut, K.M.K., Sarsevat, A., Srivastava, A., Pitmann, C.U., Moham, D., 2016. A review of  
12 Fluoride in African Groundwater and Local Remediation Methods. Groundwater for  
13 558  
14 559 Sustainable Development 2, 190-175  
15 560  
16 561 Land, L.S., 1983. The application of stable isotopes to studies of the origin of dolomite and to  
17 problems of diagenesis of clastic sediments, in: Arthur M.A., Anderson T.F. (eds), Stable  
18 562  
19 563 isotopes in Sedimentary Geology, Soc. Econ. Paleont. Miner. Short Course No. 10, 4.1-  
20 564  
21 564 4.22.  
22 565  
23 566 Le Marechal, A., 1976. Geologie et Geochemie des sources thermominerales du Cameroun.  
24 567  
25 567 ORSTOM, Paris  
26 568  
27 568  
28 569  
29 570 Liotta, M., Shamavu, P., Scaglione, S., D'Alessandra, W., Bobrowski, N., Giuffrida, G.B.,  
30 571  
31 571 Tedesco, D., Calabrese, S., 2017. Mobility of plume-derived volcanogenic elements in  
32 572  
33 572 meteoric water at Nyiragongo volcano (Congo) inferred from the chemical composition of  
34 573  
35 573 single rainfall events. *Geochimica et Cosmochimica Acta*. 217, 254-272  
36 574  
37 575 Liu, Z., Zhang, M., Li, Q., You, S., 2003. Hydrochemical and isotope characteristics of spring  
38 576  
39 576 water and travertine in the Baishuitai area (SW China) and their meaning for  
40 577  
41 577 paleoenvironmental reconstruction. *Environ. Geol.* 44, 698-704.  
42 578  
43 579 Lloyd, J.W., Heathcoat, J.A., 1985. Natural inorganic hydrochemistry in relation to groundwater:  
44 580  
45 580 an introduction. Oxford University Press, New York, p 296  
46 581  
47 582  
48 583 McArthur, J.M., Howarth, R.J., Bailey, T.R., 2001. Strontium isotope stratigraphy: LOWESS  
49 584  
50 584 Version 3. Best-fit line to the marine Sr-isotope curve for 0 to 509 Ma and accompanying  
51 585  
52 585 look-up table for deriving numerical age, *J. Geol.* **109**, 155-169.  
53 586  
54 587 McCrea, 1950. On the Isotope Chemistry of Carbonates and a Paleotemperature Scale. *The*  
55 588  
56 588 *Journal of Chemical Physics*. 18, 6.  
57 589  
58 590  
59  
60  
61  
62  
63  
64  
65

1  
2  
3  
4  
5  
6  
7  
8  
9  
10  
11  
12  
13  
14  
15  
16  
17  
18  
19  
20  
21  
22  
23  
24  
25  
26  
27  
28  
29  
30  
31  
32  
33  
34  
35  
36  
37  
38  
39  
40  
41  
42  
43  
44  
45  
46  
47  
48  
49  
50  
51  
52  
53  
54  
55  
56  
57  
58  
59  
60  
61  
62  
63  
64  
65

591 Ngako, V., Njonfang, E., Aka, F. T., Affaton, P., & Nnange, J. M., 2006. The north–south  
592 Paleozoic to Quaternary trend of alkaline magmatism from Niger-Nigeria to Cameroon:  
593 complex interaction between hotspots and Precambrian faults. *Journal of African Earth*  
594 *Sciences*, 45, 241–256. doi:10.1016/j.jafrearsci.2006.03.003.

595  
596 Omelon CR, Pollard WH, Anderson DT (2006) A geochemical evaluation of perennial spring  
597 activity and associated mineral precipitates at Expedition Fjord, Axel Heiberg Island,  
598 Canadian High Arctic. *Applied geochemistry* 21,1-15

599  
600  
601 Piper, A.M., 1944. A graphic procedure in the geochemical interpretation of water analyses. *Am*  
602 *Geophys Union Trans* 25:914–923

603  
604 Sano, Y., Kusakabe, M., Hirabayashi, J., Nojiri, Y., Shinohara, H., Njini, T., Tanyileke, G.Z.,  
605 1990. Helium and Carbon Fluxes in Lake Nyos, Cameroon: Constraints on next gas burst.  
606 *Earth and Planetary Science Letters*. 99, 303-314

607  
608  
609 Shah, M.M., Nader, F.H., Garcia, D., Swennen, R., Ellam, R., 2012. Hydrothermal dolomites in  
610 the Early Albian (Cretaceous) platform carbonates: (NW Spain): Nature and origin of  
611 dolomite and dolomitizing fluids. *Oil & Gas Science and Technology-Rev. IFP Energies*  
612 *nouvelles* 67:1, 88-122

613  
614 Sighomnou, D., 2004. Analyse et Redefinition des Regimes Climatiques et Hydrologiques du  
615 Cameroun: Perspectives d’evolution des Ressources en Eau. Ph.D Thesis, University of  
616 Yaounde 1. 292 pp.

617  
618  
619 Symonds, R. B., Rose, W. I., Reed, M. H., Lichte, F. E., and Finnegan, D. L., 1987.  
620 Volatilization, transport and sublimation of metallic and non-metallic elements in high  
621 temperature gases at Merapi Volcano, Indonesia. *Geochim. Cosmochim.Acta* 51, 2083–  
622 2101.

623  
624 Symonds, R.B., Rose, W.I., Reed, M.H., 1988. Contribution of Cl<sup>-</sup> and F<sup>-</sup> bearing gases to the  
625 atmosphere by volcanoes, *Nature*, 334, 415-418.

626  
627 Tanyileke, G.Z., 1994. Fluid Geochemistry of CO<sub>2</sub> – Rich Lakes and Soda Springs Along the  
628 Cameroon Volcanic Line. Dissertation, Okayama University, Japan.

629

1  
2  
3  
4 630 Tsujimura, M., Abe, Y., Tanaka, T., Shimada, J., Higuchi, S., Yamanaka, T., Davaa, G.,  
5 631 Oyunbaatar, D., 2007. Stable isotopic and geochemical characteristics of groundwater in  
6 632 Kherlin River Basin: a semiarid region in Eastern Mongolia. *J Hydrol* 333:47–57  
7  
8 633  
9  
10 634 Tucker, M. E., and Bathurst, R.G.C., 1990. Carbonate Diagenesis. Reprint series volume 1 of the  
11 635 International Association of Sedimentologists. Blackwell Scientific Publications. 312 pages  
12  
13 636  
14 637  
15 638 Usdowski, E., Hoefs, J., Menschel, G., 1979. Relationship between  $^{13}\text{C}$  and  $^{18}\text{O}$  fractionation and  
16 639 changes in major element composition in a recent calcite-depositing spring – a model of  
17 640 chemical variations with inorganic  $\text{CaCO}_3$  precipitation. *Earth Planet. Sci. Lett.* 42, 267–  
18 641 276.  
19  
20 642  
21 643 Usdowski, E., Hoefs, J., 1990. Kinetic  $^{13}\text{C}/^{12}\text{C}$  and  $^{18}\text{O}/^{16}\text{O}$  effects upon dissolution and  
22 644 outgassing of  $\text{CO}_2$  in the system  $\text{CO}_2\text{--H}_2\text{O}$ . *Chem. Geol.* 80, 109–118.  
23  
24 645  
25 646 Veizer, J., Ala, D., Azmy, K., Bruckschen, P., Buhl, D., Bruhn, F., Carden, G.A.F., Diener, A.,  
26 647 Ebner, S., Godderis, Y., Jasper, T., Korte, C., Pawellek, F., Podlaha, O., Strauss, H., 1999.  
27 648  $^{87}\text{Sr}/^{86}\text{Sr}$ ,  $\delta^{13}\text{C}$  and  $\delta^{18}\text{O}$  evolution of Phanerozoic seawater, *Chem. Geol.* **161**, 59-88.  
28  
29 649  
30 650  
31 651 Verla, R.B., Mboudou, G.M.M., Njoh, O., Ngoran, G.N., Afahnwie, A.N., 2014. Carbonate  
32 652 Enrichment in Volcanic Debris and Its Relationship with Carbonate Dissolution Signatures  
33 653 of Springs in the Sabga-Bamessing, North West, Cameroon. *International Journal of*  
34 654 *Geosciences*, 2014, 5, 107-121  
35  
36 655  
37 656 Whitten, D.G.A., and Brooks, J.R.V., 1972. *The Penguin Dictionary of Geology*. Penguin book  
38 657 limited, England-Great Britain. 493 pages  
39  
40 658  
41 659  
42 660

### Figures captions

43 661 Fig. 1. Locations of sampled carbonate depositing soda springs along the Cameroon Volcanic  
44 662 Line (CVL). CS stands for the continental sector of the CVL, and OCB stands for the oceanic  
45 663 continental boundary of the CVL. The locations of Lake Monoun (L. Monoun), Lake Nyos (L.  
46 664 Nyos), and Mount Cameroon (Mt. Cameroon) are also shown. The black dots correspond to  
47 665 samples' locations  
48  
49  
50  
51  
52  
53

54 666  
55 667 Fig.2. Herds of cattle consuming water from the carbonate depositing springs that have been  
56 668 harnessed  
57  
58  
59  
60  
61  
62  
63  
64  
65

1  
2  
3  
4  
5  
6  
7  
8  
9  
10  
11  
12  
13  
14  
15  
16  
17  
18  
19  
20  
21  
22  
23  
24  
25  
26  
27  
28  
29  
30  
31  
32  
33  
34  
35  
36  
37  
38  
39  
40  
41  
42  
43  
44  
45  
46  
47  
48  
49  
50  
51  
52  
53  
54  
55  
56  
57  
58  
59  
60  
61  
62  
63  
64  
65

669

670 Fig. 3. Samples (deposited carbonates and water) collection sites from observed springs

671 Fig. 4. Water chemistry presented as Piper's diagram (a), and Stiff diagrams (b) for the observed  
672 springs

673 Fig. 5. Plot of  $\delta H$  and  $\delta^{18}O$  in water from observed springs. The Sabga and Bambui springs  
674 showed no evaporation effect, while the Lobe springs, the Nyos spring and water in shallow  
675 wells around Lobe spring were subjected to evaporation relative to the meteoric water lines.  
676 Zone 1 represents the soda springs and zone 2 represents shallow groundwater in the Lobe spring  
677 neighborhood. LMWL: Local meteoric water line. GMWL: Global meteoric water line

678 Fig. 6. With respect to fluoride concentrations (a), all the observed soda springs with exception  
679 of that in Nyos, contain fluoride above the WHO upper limit of 1.5 mg/l. With respect to Arsenic  
680 (As) concentrations (b), the springs in the continental sector contain As above the WHO upper  
681 limit

682 Fig. 7. The plots of saturation indices (SI; with respect to quartz, anhydrite, aragonite, calcite and  
683 dolomite) versus total dissolved solid (TDS) for investigated water samples (wells and springs),  
684 show three subgroups (1: undersaturated wells. 2: trona precipitating springs. 3: dolomite  
685 precipitating springs).

686 Fig. 8. Stability diagrams for some minerals in the systems  $Na_2-Al_2O_3-SiO_2-H_2O$  (a) and  $CaO-$   
687  $Al_2O_3-SiO_2-H_2O$  (b) at 25°C

688

689 Fig. 9. The scanning electron microscope image (a), X-ray diffraction peaks (b), and electron  
690 probe microanalyzer mapping (c,d, e,f) of carbonate precipitate from Nyos cave spring

691 Fig. 10. The scanning electron microscope image (a), X-ray diffraction peaks (b), and electron  
692 probe microanalyzer mapping (c,d, e,f) of carbonate precipitate from the Sabga A spring

693 Fig. 11. The scanning electron microscope image (a), X-ray diffraction peaks (b), and electron  
694 probe microanalyzer mapping (c,d, e,f) of carbonate precipitate from the Sabga B spring

695 Fig.12. The scanning electron microscope image (a), X-ray diffraction peaks (b), and electron  
696 probe microanalyzer mapping (c,d, e,f) of carbonate precipitate from Bambui B spring

697 Fig. 13. Electron probe microanalyzer mapping of Na, Ca, Mg, and F of carbonate precipitate  
698 from Bambui B spring, showing enrichment of fluorine in the matrix of the carbonate

699 Fig. 14. The scanning electron microscope image (a), X-ray diffraction peaks (b), and electron  
700 probe microanalyzer mapping (c,d, e,f) of carbonate precipitate from Lobe D spring

1  
2  
3  
4  
5  
6  
7  
8  
9  
10  
11  
12  
13  
14  
15  
16  
17  
18  
19  
20  
21  
22  
23  
24  
25  
26  
27  
28  
29  
30  
31  
32  
33  
34  
35  
36  
37  
38  
39  
40  
41  
42  
43  
44  
45  
46  
47  
48  
49  
50  
51  
52  
53  
54  
55  
56  
57  
58  
59  
60  
61  
62  
63  
64  
65

701 Fig. 15. Carbonates-water oxygen isotopic fractionation temperature in observed soda springs  
702 along the CVL. Dolomites fractionated at relatively higher temperatures (35-43°C) than tronas  
703 (circum 20°C).

704  
705 Fig. 16. Plots of  $^{13}\text{C}$  and  $\delta^{18}\text{O}$  (PDB), showed observed tronas to be relatively depleted in  $^{13}\text{C}$   
706 and enriched in  $^{18}\text{O}$  (PDB).

707  
708 Fig. 17. Except for the Lobe springs that showed highest  $^{87}\text{Sr}/^{86}\text{Sr}$  ratio, in all the other observed  
709 springs the carbonate phases are relatively enriched in  $^{87}\text{Sr}/^{86}\text{Sr}$  ratio than the water phase (a),  
710 and  $^{87}\text{Sr}/^{86}\text{Sr}$  are relatively depleted in tronas than in dolomites (b)

711  
712 Fig. 18. Chloride versus fluoride cross plots showing volcanogenic contributions into the Lobe,  
713 Bambui and Nyos springs

714  
715  
716 **Table captions**

717  
718 Table 1. Laboratory analytical methods of the carbonates and water phases in observed springs

719  
720 Table 2. Chemical composition of water from the observed springs and shallow wells. ND: not  
721 detected. NM: not measured

722  
723 Table 3. Fractionation temperature and isotopic compositions of carbonates precipitating from  
724 the observed springs

725  
726  
727  
728

1 **Major ions,  $\delta^{18}\text{O}$ ,  $\delta^{13}\text{C}$  and  $^{87}\text{Sr}/^{86}\text{Sr}$  compositions of water and precipitates from springs**  
2 **along the Cameroon Volcanic Line (Cameroon, West Africa): Implications for provenance**  
3 **and volcanic hazards**

4

5 Wilson Yetoh FANTONG<sup>1</sup> $\Psi$ , Brice Tchakam KAMTCHUENG<sup>1</sup>, Yasuo ISHIZAKI<sup>2</sup>, Ernest Chi  
6 FRU<sup>3</sup>, Emilia Bi FANTONG<sup>4</sup>, Mengnjo Jude WIRMVEM<sup>1</sup>, Festus Tongwa AKA<sup>1</sup>, Bertil  
7 NLEND<sup>1</sup>, Didier HARMAN<sup>4</sup>, Akira UEDA<sup>5</sup>, Minoru KUSAKABE<sup>5</sup>, Gregory TANYILEKE<sup>1</sup>,  
8 Takeshi OHBA<sup>6</sup>

9 <sup>1</sup> Hydrological Research Center/ IRGM, Box 4110, Yaounde-Cameroon

10 <sup>2</sup> Graduate School of Science and Engineering and Research, Environmental and Energy  
11 Sciences, Earth and Environmental Systems

12 <sup>3</sup> School of Earth and Ocean Sciences, Cardiff University, Cardiff, [Park Place](#), Wales-United  
13 Kingdom

14 <sup>4</sup> Ministry of Secondary Education, Cameroon

15 <sup>5</sup>Laboratory of Environmental Biology and Chemistry, University of Toyama, Gofuku 3190,  
16 Toyama 930-8555 Japan

17 <sup>6</sup>Department of Chemistry, School of Science, Tokai University, Hiratsuka, 259-1211, Japan

18  $\Psi$  Corresponding author: [fyetoh@yahoo.com](mailto:fyetoh@yahoo.com); [fantongy@gmail.com](mailto:fantongy@gmail.com)

19 **Abstract**

20 A combined study of major ions,  $\delta^{18}\text{O}$ ,  $\delta\text{D}$ ,  $^{13}\text{C}$ ,  $^{87}\text{Sr}/^{86}\text{Sr}$  isotopes, X-ray diffraction, scanning  
21 electron [microscopy](#), and electron probe microanalyses on springs and spring mineral  
22 precipitates along the Cameroon Volcanic Line (CVL) was undertaken to understand water  
23 chemistry, and infer the type and origin of the precipitates. The waters are of evaporated Na+K-  
24 Cl and non-evaporated Ca+Mg-HCO<sub>3</sub> types, with the more mineralized (electrical conductivity-  
25 EC of 13130  $\mu\text{S}/\text{cm}$ ) Lobe spring inferred to result from interaction of circulating 49°C waters  
26 with magmatic volatiles of the active Mt. Cameroon. Water mineralization in the other springs  
27 follows the order: Sabga A > Sabga B > Bambui B > Bambui A > Nyos Cave. But for the Nyos  
28 Cave spring, all other springs contain fluoride (up to 0.5 - 35.6 mg/l above WHO potable water  
29 upper limit). The Sabga spring **contains** arsenic (up to 1.3 mg/l above the WHO limits). The  
30 springs show low [fractionation temperatures in the range of 19 – 43 °C](#). The Lobe and Sabga A  
31 springs are precipitating dolomite ( $\text{CaMg}(\text{CO}_3)_2$ ), while the Nyos Cave, Bambui A, Bambui B

32 and Sabga B springs precipitate trona ( $(\text{Na}_3\text{H}(\text{CO}_3)_2 \cdot \text{H}_2\text{O})$ ). Our data suggest a marine provenance  
33 for the carbonates, and point to a volcanic input for the Lobe, Nyos, Sabga A, and Bambui A  
34 springs. The latter springs are therefore proposed as proxies for monitoring volcanic activity for  
35 hazard mitigation along the CVL.

36 Key words: *Bubbling springs. Precipitates. Composition. Provenance. Volcanic activity.*  
37 *Hazards mitigation.*

38

39

## 40 **Introduction**

41 Mineral-depositing springs are natural systems that offer a good opportunity to study various  
42 mechanisms by which waters establish equilibrium with conditions at the Earth's surface  
43 (Amundson and Kelly, 1987; Omelon et al., 2006). For example, carbonate-precipitating waters  
44 provide an opportunity to evaluate a dynamic carbonate system and the major controls associated  
45 with calcite precipitation (Barnes, 1965; Jacobson and Usdowski, 1975), including; isotope  
46 fractionation associated with natural calcite precipitation from spring waters (McCrea, 1950;  
47 Friedman, 1970; Usdowski et al., 1979; Dandurand et al., 1982; Amundson and Kelly, 1987;  
48 Usdowski and Hoefs, 1990; Hamilton et al., 1991; Liu et al., 2003), as well as the types,  
49 morphologies, textures, and processes involved in the formation of various carbonate phases  
50 (Tucker and Bathurst, 1990; Bradley and Eugster, 1969; Ford and Pedley, 1996; Forti, 2005).

51

52 Many orifices of gas-water-carbonate interacting systems occur along the Cameroon Volcanic  
53 Line (CVL-Fig. 1). Based on carbonate enrichment studies on volcanic debris and springs in part  
54 of the continental sector of the CVL (Le Marechal, 1976; Verla et al., 2014); chemical and  
55 isotopic characteristics of fluids along the CVL (Tanyileke, 1994); the geochemistry of gases in  
56 springs around Mt. Cameroon and Lake Nyos (Kusakabe et al., 1989; Sano et al., 1990; Aka,  
57 1991); the sedimentology and geochemistry of the Bongongo and Ngol travertines along the  
58 CVL (Bisse et al., 2018), the following hypotheses have been proposed: (1) the bubbling mineral  
59 springs along the CVL contain abundant  $\text{CO}_2$ . (2) The  $\text{CO}_2$  in the bubbling springs is dominantly  
60 of magmatic origin. (3) Helium and carbon isotope ratios of gases from a few of the springs

61 along the CVL revealed a signature similar to hotspot type magma. (4) The precipitating  
62 minerals are travertines.

63 Although these studies provide initial data to understand the geochemical dynamics within the  
64 CVL gas-water-carbonate systems, gaps required to better understand the system include; a) a  
65 total absence of comprehensive information on the classification and genetic processes of the  
66 precipitating carbonates, which is exploited by the indigenes for preparation of traditional soup,  
67 b) high concentration ( $> 100$  mg/l) of geogenic fluoride has been reported (e.g., Kut et al., 2016;  
68 and references there-in) in thermal waters along the Ethiopian rift. Such concentrations of  
69 fluoride in water that is used for domestic purposes and livestock rearing can cause tremendous  
70 health effects (e.g., Fantong et al., 2010). Livestock rearing on the slopes of the CVL heavily  
71 consumes water from the springs (Fig. 2), so there is still a need to re-assess their chemical  
72 characteristics with focus on potential harmful elements like fluoride and arsenic, and c) the  
73 carbonate-water fractionation temperature remains unknown.

74 Against this backdrop, the objectives of this study are to 1) characterize the water chemistry with  
75 focus on health implications, 2) estimate the carbonate-water fractionation temperature, and 3)  
76 identify, describe and classify the carbonates that are precipitating from the springs.

77

## 78 **Study area**

79 Figure 1 shows, the sample sites along the CVL, a prominent 1600 km long Y-shaped chain of  
80 Tertiary to Recent, generally alkaline volcanoes that overlap an array of dextral faults called the  
81 Central Africa Shear Zone (CASZ) (Ngako et al., 2006) on the African continent, comparable  
82 only to the East Africa Rift System. The CVL follows a trend of crustal weakness that stretches  
83 from the Atlantic Island of Annobon, through the Gulf of Guinea, to the interior of the African  
84 continent (Fitton, 1980; Déruelle et al., 1987, Halliday et al., 1988;). It is unique amongst  
85 intraplate volcanic provinces in that it straddles the continental margin and includes both oceanic  
86 and continental intraplate volcanism. The oceanic sector constitutes a mildly alkaline volcanic  
87 series, which evolves towards phonolite, while the continental sector evolves towards rhyolite  
88 (e.g., Fitton, 1980). Isotopic studies of lavas (Halliday et al., 1988) divide the CVL into three  
89 sectors: an oceanic zone, ocean-continent boundary zone and a continental zone.

90 The study area overlaps two (coastal and tropical western highlands) of the five climatic zones in  
91 Cameroon, with mean annual rainfall of 5000 and 3000 mm, mean annual atmospheric

92 temperatures of 26°C and 21°C, humidity of 85% and 80%, and evaporation of 600 mm and 700  
93 mm, **respectively** (Sighomnou, 2004). Hydrologically, three (coastal, Sanaga, and Niger) of the  
94 five river basins in Cameroon drain the study area in a dendritic manner. According to Le  
95 Marechal (1968) and Tanyileke (1994), **riverine and in aquifer waters** encounter heat and mantle-  
96 derived CO<sub>2</sub> gas that emanate through the CASZ, **causing heating** and bubbling of the spring  
97 systems along the CVL. At each spring site the gas phase manifests as either bubbles or ‘rotten  
98 egg’ smell, while the precipitates occur as white films, white grains in volcanic ash, stalactite and  
99 stalactmite in caves, and mounds around orifices as shown in **Fig. 3**. At the sites of Sabga A in  
100 **Fig. 3**, animals consume the water as a source of salt, while humans exploit the precipitates **for**  
101 **food recipes**.

102

### 103 **Method of study**

104 Water and precipitate samples were collected from selected bubbling soda spring sites along the  
105 CVL (**Fig. 3**) in October 2015. Each water sample was collected in 3 acid-washed 250 ml  
106 polyethylene bottles after rinsing them thrice with the sample. At each sampling site, an  
107 unfiltered, unacidified and tightly **corked** sample was collected in one bottle for subsequent  
108 analyses for stable environmental isotopes **of hydrogen ( $\delta^2\text{H}$ ) and oxygen ( $\delta^{18}\text{O}$ )**. The second  
109 bottle contained un-acidified but filtered sample for anion analyses, and the third filtered and  
110 acidified sample for cations and trace elements analyses. Prior to sample collection, in-situ  
111 physicochemical measurements were **recorded** for pH (TOA-DKK HM-30P meter), electrical  
112 conductivity (TOA-DKK CM-31P EC meter), **reduction-oxidation** potential (TOA-DKK ORP  
113 meter), and water temperature. Geographical parameters (latitude, longitude and altitude) of each  
114 sample site were recorded **in** the field using a hand-held Garmin GPS. Alkalinity was measured  
115 using a ‘‘Hach’’ field titration kit, after addition of 0.16 N H<sub>2</sub>SO<sub>4</sub> to the sample to reach the  
116 endpoint titration (pH 4.5). Samples were filtered through 0.2  $\mu\text{m}$  filters prior to major ions and  
117 dissolved silica determination. Three kilograms chunks of massive carbonate was chipped off  
118 with a hammer at sites with consolidated precipitate, and 300 g scoped from sites with  
119 unconsolidated precipitate. Each precipitate was put in a clean plastic container, sealed and  
120 labelled.

121 Water samples and precipitates were transported to the University of Toyama, in Japan for  
122 chemical analyses.

123 The various chemical analyses that were done in various institutes in Japan are tabulated in Table  
124 1.

125

## 126 **Results and Discussions**

### 127 *Variation of water chemistry*

128 Chemical compositions and isotopic ratios of water samples and carbonate phases are presented  
129 in Tables 2 and 3. Measured in-situ parameters show values in the range of 54 - 13130  $\mu\text{S}/\text{cm}$  for  
130 EC, 4.3 - 7.5 for pH, and 19.3 - 47.4°C for water temperature.

131 The chemistry of the observed water resources determined with the use of the Piper's diagram  
132 (Piper, 1944) (Fig. 4a), shows that water from the Lobe soda springs and its nearby hand dug  
133 wells, located in the ocean-continent-boundary (OCB) and close to the ocean (Fig. 4a), have a  
134 dominant Na+K-Cl signature. On the other hand, water from the soda springs in Sabga, Bambui,  
135 and Nyos have dominantly Ca+Mg-HCO<sub>3</sub> signature. The observed disparity in water facies may  
136 be due to the proximity of the Lobe springs to the ocean, which impacts the sodium chloride  
137 characteristics as accorded in Le Marechal (1976). Whilst in the other springs, an interaction  
138 between primary and secondary minerals in rocks and water could be the dominant explanation  
139 as also explained by other researchers (Kamctung et al., 2014; Fantong et al., 2015). The Stiff  
140 diagrams for the water chemistry (Fig. 4b), also depict similar water facies like the Piper's  
141 diagram, but they further suggest varying degree of mineralization of the water sources. In the  
142 OCB, the larger sizes of the stiff diagram for the Lobe soda springs indicate more mineralization  
143 than for water from the wells. Likewise in the samples from the continental sector (CS) the water  
144 in the Sabga soda springs are most mineralized, followed by those in Bambui and the least  
145 mineralized is that from the Nyos soda spring. The observed variation in degree of mineralisation  
146 could in part be indicating variation in residence time, where the older springs are enriched in  
147 elements from aquifer minerals than in younger springs (e.g., Fantong et al., 2010a; Kamctung  
148 et al., 2015) that are renewed through a local and short recharge-discharge flow paths.

149

### 150 *Recharge mechanisms and evaporation of the sampled waters*

151 Isotopic ratios of hydrogen and oxygen, which are used in this study to infer recharge and  
152 evaporation mechanisms in the waters are also shown in Table 2 and graphically presented in Fig.  
153 5. The  $\delta\text{D}$  values ranged from -41.8 in Sabga A soda spring to -26 ‰ in water from well 5.

154 Oxygen isotope ( $\delta^{18}\text{O}$ ) values range from -6.3 ‰ in Sabga A spring to -3.1 ‰ in water from well  
155 3. Due to the paucity of isotope data on local rainfall, the Global Meteoric Water Line (GMWL)  
156 of Craig (1961), which is defined by the line  $\delta\text{D} = 8\delta^{18}\text{O} + 10$  is also presented as a reference.  
157 Distribution of sample water in the  $\delta\text{D}$ - $\delta^{18}\text{O}$  graph suggests that water in the Bambui and Sabga  
158 soda springs are subject to little or no evaporation, while the Lobe soda springs suggest slight  
159 evaporation, but water from the wells and Nyos soda springs show remarkable evaporation  
160 tendencies. Such a pattern depicts that the Bambui and Sabga soda springs are subject to the  
161 mechanism of preferential flow pass, which is caused by rapid recharge (e.g., Tsujimura et al.,  
162 2007; Asai et al., 2009), that is favored by the highly altered and jointed lavas as opposed to the  
163 Lobe and Nyos cave soda springs, and the wells. Except for the Lobe soda springs, the other  
164 springs are sources of drinking water for animals (cattle and goats), and a source of minerals  
165 (carbonate) for local manufacture of soup for consumption by the nearby population, thus it is  
166 important to assess at a preliminary scale the medical hydrogeochemical characteristics of the  
167 springs.

#### 168 *Health implications of the water chemistry*

169 Given that the gas bubbling springs are located in the area of livestock rearing and human  
170 activities, their chemistry is here preliminarily evaluated to assess potential health implications.  
171 With respect to fluoride, Figure 6a shows that except for the Nyos cave soda spring, all the other  
172 soda springs contain fluoride at concentrations that are above the WHO optimal limit (1.5 mg/l  
173 e.g., Kut et al., 2016). This indicates that the animals and the population that exploit these  
174 springs are potentially exposed to fluoride poisoning as reported by Fantong et al. (2010b) in the  
175 Far Northern Region of Cameroon. **The potential geogenic and volcanic provenance (Davies,  
176 2013), and actual epidemic effects of such high concentrations of fluoride are not within the  
177 scope of this study, and need further investigation.**

178 With respect to arsenic (As), Figure 6b shows that the Sabga soda springs contain As at  
179 concentrations as high as 1.33 ppm that are above the WHO upper limit (0.03 ppm in drinking  
180 water). Based on the field observations that water from the Sabga soda springs is heavily  
181 consumed by cattle, and carbonate there-from is exploited for consumption by the population, it  
182 is also a challenge for medical geochemists to carry out a comprehensive investigation into the  
183 incidence, origin, mobilization and epidemiological effects of arsenic in these areas.

184

185 ***Impact of volcanic volatile or magmatic input on chemistry of the spring water***

186 The dissolved state of elements and saturation state of compounds observed in the springs are to  
187 **an extent determined by their saturation indices and stoichiometry (e.g., Faure, 1991).**

188

189 ***Saturation indices and activity diagrams***

190 The saturation index (SI) of a given mineral in an aqueous system is defined as (Lloyd and  
191 **Heathcoat, 1985; and Deutch, 1997):**

192 
$$SI = \log \left( \frac{IAP}{K_{sp}} \right) \quad (1)$$

193 where IAP is the ion activity product and  $K_{sp}$  is the solubility product of the mineral in the  
194 system. A  $SI > 0$  points to supersaturation, and a tendency for the mineral to precipitate from the  
195 water. Saturation can be produced by factors like incongruent dissolution, common ion effect,  
196 evaporation, and rapid increase in temperature and  $CO_2$  exsolution (Appelo and Postma, 2005).  
197 A  $SI < 0$  points toward undersaturation, and implies that water dissolves the minerals from  
198 surrounding rocks. Negative SI value might also reflect that the character of water is either from  
199 a formation with insufficient concentrations of the mineral for precipitation to occur (Garrels and  
200 **Mackenzie, 1967).**

201 The thermodynamic data used in this computation are those contained in the database of  
202 'Phreeqc for Windows'. A plot of the calculated SI (with respect to quartz, anhydrite, aragonite,  
203 calcite and dolomite) versus TDS (Fig.7) groups the water samples into three subgroups:  
204 subgroup 1, which consists of water from the shallow wells is undersaturated with respect to all  
205 the selected phases and has the lowest TDS values that ranged from 63-83 mg/l. The  
206 undersaturation of subgroup 1 suggests that no mineral precipitates in the wells as observed on  
207 the field. Subgroup 2, which consists of Nyos cave soda spring, Bambui soda spring B and Sabga  
208 soda spring B, show supersaturation with respect to quartz, dolomite. On the field, this subgroup  
209 is found to be dominantly precipitating trona (a Na-rich carbonate) and dolomite to a lesser  
210 extent. Subgroup 3 that consists of the Lobe and Sabga A soda springs, are supersaturated with  
211 respect to dolomite, quartz and calcite, and it is actually precipitating more of dolomite, and  
212 trona to a lesser extent.

213 The stability of secondary minerals (Na and Ca montmorillonites, kaolinite, gibbsite) and  
214 amorphous quartz in the springs and wells were evaluated by plotting  $\log (a_{Na}/a_H)$  vs  $\log (a_{H_4SiO_4})$

215 (the albite system) (Fig. 8a) and  $\log (a_{\text{Ca}2}/a_{\text{H}})$  versus  $\log (a_{\text{H}_4\text{SiO}_4})$  (the anorthite system) (Fig.  
216 8b). These diagrams were drawn with the assumption that aluminum was preserved in the  
217 weathering product (Appelo and Postma,1993), because the amount of alumina will remain  
218 constant in fresh rocks and its altered equivalent. The constant amount in alumina ( $\text{Al}_2\text{O}_3$ ) is  
219 because an apparent increase in its weight % is actually always caused by a reduction in the  
220 weight of the fresh rock to some smaller amount (Faure, 1991). End member compositions were  
221 also assumed using equilibrium relationship for standard temperature ( $25^\circ\text{C}$ ) and pressure (1  
222 atmosphere), which approximately reflect the springs and groundwater conditions. Activities of  
223 the species were computed using the analytical concentrations and activity coefficient  
224 determined by Phreeqc for Windows version 2.1 under the above conditions (Appelo and  
225 Postma, 1993). According to the figures, groundwater from the wells span the stability field of  
226 kaolinite, while all the soda springs with exception of the Nyos soda spring are in equilibrium  
227 within the Na and Ca -montmorillonite stability fields. This concurs with the incidence of clay  
228 minerals in the study area (Fantong et al., 2015). Moreover, the presence of kaolinite and  
229 montmorillonite in the study area occur as groundmass in the XRD (X-Ray Defraction) peaks of  
230 Figures 9b,10b, 11b, 12b, and 14b. A combination of information from the saturation indices and  
231 stability diagrams is supported by the presence of precipitating carbonate phases in the soda  
232 springs as shown in Fig. 1.

233

### 234 *Typology of carbonate phases*

235 The typology of the carbonate phases that precipitate from the observed soda springs is done by  
236 describing the morphology by using SEM images, and identifying the carbonate phase by using  
237 XRD diagrams and EPMA elemental mapping.

238

### 239 **Carbonate from the Nyos cave soda spring**

240 The SEM image in Fig. 9a shows that the carbonate is an association of cluster of powdery  
241 amorphous groundmass upon which sub-euhedral crystals developed. This carbonate is identified  
242 with XRD peaks (Fig.9b) as a trona (low- syn trisodium hydrogen dehydrate carbonate). To  
243 accentuate the trona phase, an elemental EPMA mapping (Fig.9 c, d, e and f) shows the  
244 dominance of sodium, traces of calcium and total absence of magnesium.

245

246 **Carbonate from Sabga A soda spring**

247 The SEM image of [Fig. 10a](#) shows that the carbonate is nail-shaped stalactite crystals protruding  
248 from a cluster of powdery amorphous groundmass. This carbonate is identified with XRD peaks  
249 (Fig.10b) as a dolomite (calcium-magnesium bicarbonate). Dolomite precipitate in this spring is  
250 supported by an elemental EPMA mapping (Fig. 10 c, d, e and f), which shows a dominance and  
251 remarkable presence of both calcium and magnesium, with traces of sodium.

252

253 **Carbonate from Sabga B soda spring**

254 The SEM image of [Fig. 11a](#) shows that the carbonate is made up of radiating tabular columns of  
255 crystals whose faces are edged by bacteria. This carbonate is identified with XRD peaks (Fig.  
256 11b) as a trona (low-syn trisodium hydrogen dehydrate carbonate). The presence of this trona  
257 precipitating in this spring is justified by an elemental EPMA mapping (Fig. 11c, d, e and f),  
258 which shows a dominance of sodium and an almost absence of calcium and magnesium.

259

260 **Carbonate from Bambui B soda spring**

261 The SEM image of [Fig. 12a](#) shows that the morphology of the carbonate is an intersecting  
262 mosaic of tabular crystals whose faces are edged by bacteria. This carbonate is identified with  
263 XRD peaks (Fig. 12b) as a trona similar to that of Sabga B. The presence of this trona  
264 precipitating in this spring is supported by an elemental EPMA mapping (Fig. 12 c, d, e and f),  
265 which shows a dominance of sodium and **low content** of calcium and magnesium. The  
266 disseminated distribution of fluorine, which almost coincide with the distribution of faint calcite  
267 suggest the presence of fluorite (CaF<sub>2</sub>), which could be dissolving to enrich the water phase with  
268 fluoride as seen in [Fig. 13e](#).

269

270 **Carbonate from Lobe D soda spring**

271 The SEM image of [Fig. 14a](#) shows that the carbonate is a coliform flower-shape radiating  
272 crystals, which is colonized by bacteria. This carbonate is identified with XRD peaks (Fig. 14b)  
273 as a dolomite. The occurrence of dolomite as the precipitate in this spring is supported by an  
274 elemental EPMA mapping (Fig. 14c, d, e and f), which shows high content of both calcium and  
275 magnesium, and **low content** of sodium.

276 Summarily, the carbonate phases that are precipitating from the studied soda springs along the  
277 CVL are dominantly dolomite and trona. The pristine geochemical attributes and characteristics  
278 of the carbonate are at a later phase altered (Demeny, 2016) by diatoms and bacteria as shown in  
279 Figure 11a and 12a. The incidence of bacteria in such a hydrogeochemical system leaves  
280 biogeochemists with another opportunity to assess the incidence and role of bacteria in the soda  
281 spring systems.

282

### 283 **Origin of the fluids and carbonates**

284 In a bid to identify the formation (sources and paleo temperature) processes that led to the  
285 formation of the observed carbonates, we used  $^{13}\text{C}$  isotopes,  $^{87}\text{Sr}/^{86}\text{Sr}$ , carbonate-water  
286 fractionation temperatures, and  $\text{Cl}^-$  versus  $\text{F}^-$  plot as geochemical tracers.

287

### 288 *Carbonate-water fractionation temperature*

289 Although oxygen-isotope thermometry based on isotopic fractionation of oxygen between  
290 carbonates and water dates back to the **Mid-1900s**, the carbonate-water oxygen isotopic  
291 fractionation equations are still being discussed. The use of isotope thermometry is based on  
292 several criteria: (i) the temperature dependence of the isotopic fractionation between the  
293 investigated compounds (in our case dolomite/trona and water) and (ii) the isotopic compositions  
294 of the compounds are known, (iii) the isotopic equilibrium between the compounds can be  
295 proven or at least reasonably assumed, and (iv) no subsequent isotopic alteration occurred after  
296 the deposition of carbonates. These considerations are valid for inorganic carbonate formation, as  
297 biogenic carbonate is severely affected by the organisms' metabolism, resulting in a species-  
298 dependent ‘‘vital effect’’ (Demeny et al., 2010 and references therein)

299 The temperatures at which the carbonate phases precipitate from the springs were calculated by  
300 using the empirical equation for the temperature dependence of calcite-water oxygen isotope  
301 fractionation from 10 to 70 °C as shown in equations 2 and 3 that were reported by Demeny et al.  
302 (2010).

$$303 \quad 1000 \cdot \ln \alpha = 17599/T - 29.64 \quad [\text{for travertines with a temperature range of } 30 \text{ to } 70^\circ\text{C}] \quad (2)$$

$$304 \quad 1000 \cdot \ln \alpha = 17500/T - 29.89 \quad [\text{for cave deposits for the range } 10 \text{ to } 25^\circ\text{C}] \quad (3)$$

305 **The variable T are in °C.**

306 The values obtained suggest that carbonates precipitate from soda springs along the CVL at  
307 temperature that varied from 18.5 - 43°C. The lowest fractionation temperatures (18.5 - 18.6°C)  
308 occurred in the Sabga soda springs, while the highest (35 - 43°C), occurred in the Lobe soda  
309 springs (Table 3). A plot (Fig. 15), shows that with the exception of the dolomite in the ‘Sabga  
310 A soda spring’, the tronas fractionated at lower temperature (~18.5 - 20 °C) than the dolomites,  
311 which fractionated at temperature ranging from 35.2 - 43°C. Based on Figure 15, the oxygen  
312 isotopes in carbonates precipitating along the Cameroon Volcanic Line yielded an empirical  
313 fractionation– temperature equations of:

$$314 \quad 1000.\ln\alpha = -0.2153T + 35.3 \quad (4)$$

315

### 316 *Stable isotopes of $^{13}\text{C}$ , $^{87}\text{Sr}/^{86}\text{Sr}$ , and $^{18}\text{O}$*

317 The observed carbonates (dolomite and trona) facies in the samples showed broad ranges in  
318  $^{87}\text{Sr}/^{86}\text{Sr}$ ,  $^{13}\text{C}$  and  $\delta^{18}\text{O}$ . The  $^{87}\text{Sr}/^{86}\text{Sr}$  ratio varied from 0.706 - 0.713, the  $^{13}\text{C}$  varied from -3.09 to  
319 5.22 VPDB and  $\delta^{18}\text{O}$  from -8.4 to -1.4 VPDB as shown in Table 3. Their  $\delta^{13}\text{C}$  values of observed  
320 dolomites are close to the range of values reported for carbonates precipitating from seawater (0  
321 -4 VPDB; Veizer et al., 1999; Shah et al., 2012). Indication of marine origin of the dolomites  
322 corroborates with field observation, because the dolomite precipitates from the Lobe soda spring  
323 located in the **OCB** of the study area. However, the carbonates (trona) identified in our study  
324 area showed relatively depleted  $\delta^{13}\text{C}$  signatures, which may indicate a possible external source of  
325 carbon during trona precipitation (Fig. 16) or a temperature dependent fractionation effect (Shah  
326 et al., 2012). The depleted  $\delta^{18}\text{O}$  in dolomite from the 49°C Lobe soda springs, may be due to its  
327 higher temperatures (thermogenic type) (Bisse et al., 2018), given that precipitation of dolomite  
328 from hot springs leads to relatively depleted  $\delta^{18}\text{O}$  ratios (Land, 1983).

329 With exception of the Lobe soda springs, where  $^{87}\text{Sr}/^{86}\text{Sr}$  value did not vary between the  
330 carbonate and water phases, in the other soda springs (Bambui soda springs A and B, Sabga soda  
331 springs A and B, and Nyos cave soda spring), the  $^{87}\text{Sr}/^{86}\text{Sr}$  ratio shows a decoupling tendency  
332 where the water phases contain relatively higher values than the carbonate phases (Fig. 17a). The  
333 relatively higher  $^{87}\text{Sr}/^{86}\text{Sr}$  ratio in the Lobe soda springs may indicate interaction of dolomitizing  
334 fluids with radiogenic lithologies (Shah et al., 2012), which commonly occur along the CVL  
335 (e.g., Aka et al., 2000; 2001). Moreover, the  $^{87}\text{Sr}/^{86}\text{Sr}$  versus  $^{18}\text{O}$  cross plot (Fig. 17b), shows that  
336 the dolomites are richer in  $^{87}\text{Sr}/^{86}\text{Sr}$  ratio than the tronas. However, the signatures in the dolomite

337 of the Sabga soda spring “A” together with those in the tronas are closer to those of the marine  
338 signatures (McArthur et al., 2001). Such marine signatures in tronas (Na-rich carbonate) within  
339 the continental sector of the Cameroon Volcanic Line, may suggest the presence of paleo-  
340 continental sabkha environments, where various sodium carbonates have been recorded in  
341 tropical regions (Whitten and Brooks, 1972). This suggestion, however, requires further  
342 investigation.

343

#### 344 **Implications for monitoring and hazard mitigation**

345 Volcanogenic sources of fluorine (e.g., Symonds et al., 1987; Symonds et al., 1988; Bellomo et  
346 al., 2003) and chlorine (e.g., Keene and Graedel 1995) containing gasses have been reported in  
347 active and passive volcanic areas, and recently in the Nyiragongo volcano in Congo (Liotta et al.,  
348 2017). As used by the later, we also used a cross plot of chloride versus fluoride (Fig. 18) to infer  
349 volcanogenic contribution in the observed springs along the CVL. The figure suggests  
350 volcanogenic inputs into the Lobe, Nyos, Sabga A, and Bambui A springs. The implication of a  
351 volcanic input to these fluids suggests that they can be used to monitor volcanic activity and thus  
352 mitigate hazards, especially in the vicinity of the Lobe spring located close to the currently active  
353 Mt. Cameroon. Moreover, the dominant fluids in the Lobe, Nyos, Sabga A, and Bambui A  
354 springs are magmatic CO<sub>2</sub> and H<sub>2</sub>O (Sano 1990). Water dissolves slightly more in silicic melts  
355 than in basaltic melts, whereas CO<sub>2</sub> dissolves more in basaltic than in silicic melts. Kusakabe  
356 (2017) reports that the solubility of CO<sub>2</sub> and H<sub>2</sub>O in basaltic melts at 1200°C is a function of the  
357 total pressure of the volatiles, whose composition in the melt changes as the decompression  
358 proceeds. For example, at low pressure the mole fraction of H<sub>2</sub>O equals 0.2 and that of CO<sub>2</sub> is  
359 0.8, implying that basaltic melt becomes rich in CO<sub>2</sub> as the magma ascends and the confining  
360 pressure reduces, resulting to degassing. If degassing takes place in an open system, CO<sub>2</sub>-rich  
361 fluid leaves the magma. This solubility-controlled behavior of CO<sub>2</sub> in basaltic magma may  
362 explain a CO<sub>2</sub>-rich nature of fluids separated from the magma. The ultimate source of CO<sub>2</sub> in the  
363 Nyos, Lobe, Sabga A, and Bambui A springs may therefore be derived from the decarbonation of  
364 crystallized metasomatic fluids in the subcontinental lithosphere (Aka, 2015; Asaah et al., 2015).  
365 The **low** (-2 to -3 ‰) <sup>13</sup>C values of carbonates in the Nyos and Sabga soda spring may also  
366 indicate magmatic origin of the **CO<sub>2</sub>** that contributes in precipitating the carbonates. Thus, the

367 permanent supply of such CO<sub>2</sub> in the springs provides good sites for monitoring volcanic activity  
368 for hazard mitigation.

369

### 370 **Conclusions**

371 The chemistry of water in the bubbling soda springs observed along the Cameroon Volcanic Line  
372 shows an evaporated Na+K-Cl and non-evaporated Ca+Mg-HCO<sub>3</sub> facies in the ocean continental  
373 boundary sector (OCB) and continental sector (CS), respectively. In the OCB, the Lobe soda  
374 springs shows more mineralization than water from nearby hand dug wells. This may indicate  
375 that spring water (T=49°C) is circulating deeper than the well water. In the continental sector  
376 (CS) the water in the Sabga soda springs are the most mineralized, followed by those in Bambui  
377 soda spring and the least mineralized is the Nyos soda spring. With exception of the soda springs  
378 in the Nyos area, all other studied soda springs contain fluoride from geogenic fluorine at  
379 concentrations above the WHO upper limit, whilst concentrations of arsenic (> 0.3 mg/l) that  
380 also call for health concern occur in the Sabga soda springs. The observed soda springs are either  
381 saturated or super-saturated with respect to quartz, and carbonate phases, which are actually  
382 precipitating as dolomite and trona. The carbonate-water fractionation temperature varies from  
383 18.5 - 43°C. X-ray diffraction spectra and chemical mapping by electron probe microanalyzer  
384 unraveled that the precipitating carbonates occur as dolomite in the Lobe and Sabga A soda  
385 springs, and as trona in the Nyos, Bambui and Sabga B soda springs. Scanning electron  
386 microscope (SEM), reveals various morphologies of the carbonates, including amorphous to  
387 tabular euhedral tronas, and nail shaped to bacteria-colonized coliform dolomites. Geochemical  
388 tracers of <sup>13</sup>C, <sup>87</sup>Sr/<sup>86</sup>Sr, and <sup>18</sup>O indicate a dominantly marine provenance of the carbonate.  
389 Chloride versus fluoride cross plot suggest a contribution from volcanic volatiles in the Lobe,  
390 Nyos, Sabga A, and Bambui A springs. This contribution of a volcanic input to these fluids  
391 suggests that they can be used to monitor volcanic activity and thus mitigate hazards, especially  
392 in the vicinity of the Lobe spring that is located close to the currently active Mt. Cameroon.

393

### 394 **Acknowledgements**

395 We thank the Institute of Geological and Mining Research (IRGM), Yaoundé, for financial and  
396 logistical support during sampling. Thanks to the funders (JICA and JST) of SATREPS-IRGM  
397 project that provided field and laboratory equipment that were used to generate the data during

398 this study. We thank all the members of the Department of Environmental Biology and  
399 Chemistry, University of Toyama, Japan, for their enriching comments during the preparation of  
400 this manuscript. We are also grateful to Prof. Suh Emmanuel and Prof. Loic Peiffer for their  
401 review comments that enriched the content of the manuscript.

402

403

404

405

406

407

408

409

410

## 411 **References**

412

413 Aka, F.T., 1991. Volcano Monitoring by Geochemical Analyses of Volcanic Gases. Thesis, The  
414 University of Leeds, LS2 9JT. 94 pp.

415

416

417 Aka, F.T., 2000. Noble gas systematics and K–Ar Chronology: implications on the geotectonic  
418 evolution of the Cameroon Volcanic Line, West Africa, PhD thesis, Univ. Okayama, Japan.  
419 175 pp.

420 Aka, F. T. (2015) Depth of melt segregation below the Nyos maar-diatreme volcano (Cameroon,  
421 West Africa): Major trace element evidence and their bearing on the origin of CO<sub>2</sub> in Lake  
422 Nyos. Volcanic Lakes (Rouwet, D., Christenson, B., Tassi, F. and Vandemeulebrouck, J.,  
423 eds.), Springer-Heidelberg.

424

425

426 Aka, F.T., Kusakabe, M.K., Nagao, K., Tanyileke, G., 2001. Noble gas isotopic compositions  
427 and water/gas chemistry of soda springs from the islands of Bioko, Saõ Tome' and  
428 Annobon, along the Cameroon Volcanic Line, West Africa. Appl. Geochem.16, 323–338.

429

430 Amundson, R., Kelly, E., 1987. The chemistry and mineralogy of a CO<sub>2</sub>-rich travertine  
431 depositing spring in the California Coast Range. Geochim. Cosmochim. Acta 51, 2883–2890.

432

433 Appelo, C.A.J., Postma, D., 2005. Geochemistry, groundwater, and pollution. 2nd edn. Balkema  
434 Publishers, Rotterdam, 649 pp

435 Asai, K., Satake, H., and Tsujimura, M., 2009. Isotopic approach to understanding the

436 groundwater flow system within the andesitic strato-volcano in a temperate humid  
437 region: case study of Ontake volcano, Central Japan. *Hydrol. Processes*. 23, 559-571.  
438

439 Asaah, A. N. E., Yokoyama, T., Aka, F. T., Usui, T., Kuritani, T., Wirmvem, M. J., Iwamori, H.,  
440 Fozing, E. M., Tamen, J., Mofor, G. J., Ohba, T., Tanyileke, G. and Hell, J. V. (2015)  
441 Geochemistry of lavas from maar-bearing volcanoes in the Oku Volcanic Group of the  
442 Cameroon Volcanic Line. *Chem. Geol.* 406, 55–69.  
443

444 Barnes, I., 1965. Geochemistry of Birch Creek, Inyo County, California: a travertine depositing  
445 creek in an arid climate. *Geochim. Cosmochim. Acta* 29, 85–112.  
446

447

448 Bellomo, S., D'Alessandro, W., and Longo, M., 2003. Volcanogenic fluorine in rainwater around  
449 active degassing volcanoes: Mt.Etna and Stromboli Island, Italy. *Sci. Total Environ.* 301,  
450 175–185.  
451

452 Bisse, S. B., Ekomané, E., Eyong, J.T., Ollivier, V., Douville, E., Nganne, M.J.M., Bokanda,  
453 E.E., Bitom, L.D., 2018. Sedimentological and geochemical study of the Bongongo and  
454 Ngol travertines located at the Cameroon Volcanic Line. *Journal of African Earth Sciences*.  
455 DOI.org/10.1016/j.jafrearsci.2018.03.028  
456

457 Craig, H., 1961. Isotopic variations in meteoric waters. *Science* 133:1702–1703  
458

459 Dandurand, J.L., Gout, R., Hoefs, J., Menschel, G., Schott, J., Usdowski, E., 1982. Kinetically  
460 controlled variations of major components and carbon and oxygen isotopes in a calcite  
461 precipitating spring. *Chem. Geol.* 36, 299–315.  
462

463 Davies, T.C., 2013. Geochemical variables as plausible aetiological cofactors in the incidence of  
464 some common environmental diseases in Africa. *Journ. African Earth Sciences.* 79, 24-49  
465

466

467 Demeny, A., Kele, S., and Siklosy, Z., 2010. Empirical equations for the temperature  
468 dependence of calcite-water oxygen isotope fractionation from 10 to 70°C. *Rapid Commun.*  
469 *Mass Spectro.* 24, 3521-3526

470 Demeny, A., Nemeth, P., Czuppon, G., Leel-Ossy, S., Szabo, M., Judik, K., Nemeth, T., Steiber,  
471 J., 2016. Formation of amorphous calcium carbonate in caves and its implications for  
472 speleothem research. *Scientific Report.* 6, 39602  
473

474 Deruelle, B., Nni, J., and Kambou, R., 1987. Mount Cameroon: An active volcano of the  
475 Cameroon Volcanic Line. *J. African Earth Sciences.* 6, 197-214  
476

477 Deutsch, W.J., 1997. Groundwater geochemistry: fundamentals and application to  
478 contamination. CRC, Boca Raton  
479

480 Bradley, W.H., and Eugster, H.P., 1969. Geochemistry and paleolimnology of the trona deposits  
481 and associated authigenic minerals of green river formation of Wyoming. Geological Survey  
482 Professional Paper 496-B, US Government Printing office, Washington, 66 pp  
483

484 Fantong, W.Y., Satake, H., Ayonghe, S.N., Suh, C.E., Adelana, S.M.A., Fantong, E.B.S.,  
485 Banseka, H.S., Gwanfogbe, C.D., Woincham, L.N., Uehara, Y., Zhang, J., 2010b.  
486 Geochemical provenance and spatial distribution of fluoride in groundwater of Mayo  
487 Tsanaga River Basin, Far north Region, Cameroon: implications for incidence of fluorosis  
488 and optimal consumption dose. *Environ Geochem Health*. Vol. 32: 147-163  
489

490 Fantong, W.Y., Kamtchueng, B.T., Yamaguchi, K., Ueda, A., Issa, Ntchantcho, R., Wirmvem,  
491 M.J., Kusakabe, M., Ohba, T., Zhang, J., Aka, F.T., Tanyileke, G.Z., Hell, J.V., 2015.  
492 Characteristics of Chemical weathering and water-rock interaction in Lake Nyos dam  
493 (Cameroon): Implications for vulnerability to failure and re-enforcement. *Journal of African  
494 Earth Sciences*: 101:42-55  
495

496 Fantong, W.Y., Satake, H., Aka, F.T., Ayonghe, S.N., Kazuyoshi, A., Mandal, A.K., Ako, A.A.,  
497 2010a. Hydrochemical and isotopic evidence of recharge, apparent age, and flow direction  
498 of groundwater in Mayo Tsanaga River Basin, Cameroon: Bearings on contamination.  
499 *Journal of Environ Earth Sci*. Vol. 60: 107-120  
500

501 Faure, G., 1991. Principles and Applications of Inorganic Geochemistry. *Macmillan Publishing  
502 Company*, New York, 626 p.  
503  
504

505 Fitton, J.D., 1980. The Benue Trough and the Cameroon Line – A Migrating Rift System in  
506 West Africa. *Earth Planet. Sci. Lett.* 51, 132-138  
507

508 Ford, T.D., Pedley, H.M. 1996. A Review of Tufa and Travertine Deposits of the World. *Earth  
509 Science Reviews* 41, 117-175.  
510

511 Forti, P., 2005. Genetic processes of cave minerals in volcanic environments: an overview.  
512 *Journal of Cave and Karst Studies*. Vol 67:1, 3-13.  
513  
514

515 Friedman, I., 1970. Some investigations of the deposition of travertine from Hot Springs – I. The  
516 isotopic chemistry of a travertine-depositing spring. *Geochim. Cosmochim. Acta* 34, 1303–  
517 1315.

518  
519

520 Garrels, R.M., Mackenzie, F.T., 1967. Origin of the chemical composition of some springs and  
521 lakes. In: RF Gould (ed.). *Equilibrium concepts in natural water systems*. Washington, DC:  
522 American Chemical Society, pp 222-242.

523

524 Halliday, A.N., Dicken, A.P., Fallice, A.E., and Fitton, J.T., 1988. Mantle dynamics. A Nd, Sr,  
525 Pb, and O isotope study of the Cameroon Volcanic Line. *J. Petrol.* 29, 181-211

526  
527

528 Hamilton, S.M., Michel, F.A., Jefferson, C.W., 1991. CO<sub>2</sub>-rich ground waters of the Flat River  
529 Valley, N.W.T. In: Prowse, T., Ommanney, C. (Eds.), *Northern Hydrology Selected  
530 Perspectives, Proceedings of the Northern Hydrology Symposium, 10–12 July 1990,*  
531 *Saskatoon, Saskatchewan, NHRI Paper #6*, pp. 105–199.

532

533 Jacobson, R.L., Usdowski, E., 1975. Geochemical controls on a calcite precipitating spring.  
534 *Contrib. Mineral. Petrol.* 51, 65–74.

535  
536

537 Kamtchueng, B. T., Fantong, W.Y., Wirmvem, M.J., Tiodjio, R.E., Takounjou, A.F., Asai, K.,  
538 Serges L. Djomou, S.L.B., Kusakabe, M., Ohba, T., Tanyileke, G., Hell, J.V., Ueda A.,  
539 2015. A multi-tracer approach for assessing the origin, apparent age and recharge  
540 mechanism of shallow groundwater in the Lake Nyos catchment, Northwest, Cameroon.  
541 *Journal of Hydrology*, 523:790–803.

542

543 Kamtchueng, B.T., Fantong, W.Y., Ueda, A., Tiodjio, E.R., Anazawa, K., Wirmvem, J.,  
544 Mvondo, J.O., Nkamdjou, L., Kusakabe, M., Ohba, T., Tanyileke, G.Z., Joseph, V. H.,  
545 2014. Assessment of shallow groundwater in Lake Nyos catchment (Cameroon, Central-  
546 Africa): implications for hydrogeochemical controls and uses. *Environmental Earth  
547 Sciences*, 72:3663–3678.

548 Kusakabe, M., 2017. Lakes Nyos and Monoun gas disasters (Cameroon)—Limnic eruptions  
549 caused by excessive accumulation of magmatic CO<sub>2</sub> in crater lakes. *GEOchem. Monogr.*  
550 *Ser. 1*, 1–50, doi:10.5047/gems.2017.00101.0001.

551

552 Kusakabe, M., Ohsumi, T., and Arakami, S., 1989. The Lake Nyos gas disaster: chemical and  
553 isotopic evidence in waters and dissolved gases in three Cameroonian Lakes, Nyos,  
554 Monoun and Wum. In: Le Guern, F., and Sigvaldason, G., (Editors), The Lake Nyos Event  
555 and Natural Carbon dioxide Degassing, 1. J. Volcanol. Geothermal Res., 39, 167-185.  
556

557 Kut, K.M.K., Sarsevat, A., Srivastava, A., Pitmann, C.U., Moham, D., 2016. A review of  
558 Fluoride in African Groundwater and Local Remediation Methods. Groundwater for  
559 Sustainable Development 2, 190-175  
560

561 Land, L.S., 1983. The application of stable isotopes to studies of the origin of dolomite and to  
562 problems of diagenesis of clastic sediments, in: Arthur M.A., Anderson T.F. (eds), Stable  
563 isotopes in Sedimentary Geology, Soc. Econ. Paleont. Miner. Short Course No. 10, 4.1-  
564 4.22.  
565

566 Le Marechal, A., 1976. Geologie et Geochemie des sources thermominerales du Cameroun.  
567 ORSTOM, Paris  
568

569

570 Liotta, M., Shamavu, P., Scaglione, S., D'Alessandra, W., Bobrowski, N., Giuffrida, G.B.,  
571 Tedesco, D., Calabrese, S., 2017. Mobility of plume-derived volcanogenic elements in  
572 meteoric water at Nyiragongo volcano (Congo) inferred from the chemical composition of  
573 single rainfall events. *Geochimica et Cosmochimica Acta*. 217, 254-272  
574

575 Liu, Z., Zhang, M., Li, Q., You, S., 2003. Hydrochemical and isotope characteristics of spring  
576 water and travertine in the Baishuitai area (SW China) and their meaning for  
577 paleoenvironmental reconstruction. *Environ. Geol.* 44, 698-704.  
578

579 Lloyd, J.W., Heathcoat, J.A., 1985. Natural inorganic hydrochemistry in relation to groundwater:  
580 an introduction. Oxford University Press, New York, p 296  
581

582

583 McArthur, J.M., Howarth, R.J., Bailey, T.R., 2001. Strontium isotope stratigraphy: LOWESS  
584 Version 3. Best-fit line to the marine Sr-isotope curve for 0 to 509 Ma and accompanying  
585 look-up table for deriving numerical age, *J. Geol.* **109**, 155-169.  
586

587 McCrea, 1950. On the Isotope Chemistry of Carbonates and a Paleotemperature Scale. The  
588 Journal of Chemical Physics. 18, 6.  
589  
590

591 Ngako, V., Njonfang, E., Aka, F. T., Affaton, P., & Nnange, J. M., 2006. The north–south  
592 Paleozoic to Quaternary trend of alkaline magmatism from Niger-Nigeria to Cameroon:  
593 complex interaction between hotspots and Precambrian faults. *Journal of African Earth*  
594 *Sciences*, 45, 241–256. doi:10.1016/j.jafrearsci.2006.03.003.  
595

596 Omelon CR, Pollard WH, Anderson DT (2006) A geochemical evaluation of perennial spring  
597 activity and associated mineral precipitates at Expedition Fjord, Axel Heiberg Island,  
598 Canadian High Arctic. *Applied geochemistry* 21,1-15  
599

600

601 Piper, A.M., 1944. A graphic procedure in the geochemical interpretation of water analyses. *Am*  
602 *Geophys Union Trans* 25:914–923  
603

604 Sano, Y., Kusakabe, M., Hirabayashi, J., Nojiri, Y., Shinohara, H., Njini, T., Tanyileke, G.Z.,  
605 1990. Helium and Carbon Fluxes in Lake Nyos, Cameroon: Constraints on next gas burst.  
606 *Earth and Planetary Science Letters*. 99, 303-314  
607

608

609 Shah, M.M., Nader, F.H., Garcia, D., Swennen, R., Ellam, R., 2012. Hydrothermal dolomites in  
610 the Early Albian (Cretaceous) platform carbonates: (NW Spain): Nature and origin of  
611 dolomite and dolomitizing fluids. *Oil & Gas Science and Technology-Rev. IFP Energies*  
612 *nouvelles* 67:1, 88-122  
613

614 Sighomnou, D., 2004. Analyse et Redefinition des Regimes Climatiques et Hydrologiques du  
615 Cameroun: Perspectives d'évolution des Ressources en Eau. Ph.D Thesis, University of  
616 Yaounde 1. 292 pp.  
617

618

619 Symonds, R. B., Rose, W. I., Reed, M. H., Lichte, F. E., and Finnegan, D. L., 1987.  
620 Volatilization, transport and sublimation of metallic and non-metallic elements in high  
621 temperature gases at Merapi Volcano, Indonesia. *Geochim. Cosmochim.Acta* 51, 2083–  
622 2101.  
623

624 Symonds, R.B., Rose, W.I., Reed, M.H., 1988. Contribution of Cl<sup>-</sup> and F<sup>-</sup> bearing gases to the  
625 atmosphere by volcanoes, *Nature*, 334, 415-418.  
626

627 Tanyileke, G.Z., 1994. Fluid Geochemistry of CO<sub>2</sub> – Rich Lakes and Soda Springs Along the  
628 Cameroon Volcanic Line. Dissertation, Okayama University, Japan.  
629

- 630 Tsujimura, M., Abe, Y., Tanaka, T., Shimada, J., Higuchi, S., Yamanaka, T., Davaa, G.,  
631 Oyunbaatar, D., 2007. Stable isotopic and geochemical characteristics of groundwater in  
632 Kherlin River Basin: a semiarid region in Eastern Mongolia. *J Hydrol* 333:47–57  
633
- 634 Tucker, M. E., and Bathurst, R.G.C., 1990. Carbonate Diagenesis. Reprint series volume 1 of the  
635 International Association of Sedimentologists. Blackwell Scientific Publications. 312 pages  
636  
637
- 638 Usdowski, E., Hoefs, J., Menschel, G., 1979. Relationship between  $^{13}\text{C}$  and  $^{18}\text{O}$  fractionation and  
639 changes in major element composition in a recent calcite-depositing spring – a model of  
640 chemical variations with inorganic  $\text{CaCO}_3$  precipitation. *Earth Planet. Sci. Lett.* 42, 267–  
641 276.  
642
- 643 Usdowski, E., Hoefs, J., 1990. Kinetic  $^{13}\text{C}/^{12}\text{C}$  and  $^{18}\text{O}/^{16}\text{O}$  effects upon dissolution and  
644 outgassing of  $\text{CO}_2$  in the system  $\text{CO}_2\text{--H}_2\text{O}$ . *Chem. Geol.* 80, 109–118.  
645
- 646 Veizer, J., Ala, D., Azmy, K., Bruckschen, P., Buhl, D., Bruhn, F., Carden, G.A.F., Diener, A.,  
647 Ebner, S., Godderis, Y., Jasper, T., Korte, C., Pawellek, F., Podlaha, O., Strauss, H., 1999.  
648  $^{87}\text{Sr}/^{86}\text{Sr}$ ,  $\delta^{13}\text{C}$  and  $\delta^{18}\text{O}$  evolution of Phanerozoic seawater, *Chem. Geol.* **161**, 59-88.  
649  
650
- 651 Verla, R.B., Mboudou, G.M.M., Njoh, O., Ngoran, G.N., Afahnwie, A.N., 2014. Carbonate  
652 Enrichment in Volcanic Debris and Its Relationship with Carbonate Dissolution Signatures  
653 of Springs in the Sabga-Bamessing, North West, Cameroon. *International Journal of*  
654 *Geosciences*, 2014, 5, 107-121  
655
- 656 Whitten, D.G.A., and Brooks, J.R.V., 1972. *The Penguin Dictionary of Geology*. Penguin book  
657 limited, England-Great Britain. 493 pages  
658  
659

### 660 **Figures captions**

661 Fig. 1. Locations of sampled carbonate depositing soda springs along the Cameroon Volcanic  
662 Line (CVL). CS stands for the continental sector of the CVL, and OCB stands for the oceanic  
663 continental boundary of the CVL. The locations of Lake Monoun (L. Monoun), Lake Nyos (L.  
664 Nyos), and Mount Cameroon (Mt. Cameroon) are also shown. The black dots correspond to  
665 samples' locations

666

667 Fig.2. Herds of cattle consuming water from the carbonate depositing springs that have been  
668 harnessed

669

670 Fig. 3. Samples (deposited carbonates and water) collection sites from observed springs

671 Fig. 4. Water chemistry presented as Piper's diagram (a), and Stiff diagrams (b) for the observed  
672 springs

673 Fig. 5. Plot of  $\delta\text{H}$  and  $\delta^{18}\text{O}$  in water from observed springs. The Sabga and Bambui springs  
674 showed no evaporation effect, while the Lobe springs, the Nyos spring and water in shallow  
675 wells around Lobe spring were subjected to evaporation relative to the meteoric water lines.  
676 Zone 1 represents the soda springs and zone 2 represents shallow groundwater in the Lobe spring  
677 neighborhood. LMWL: Local meteoric water line. GMWL: Global meteoric water line

678 Fig. 6. With respect to fluoride concentrations (a), all the observed soda springs with exception  
679 of that in Nyos, contain fluoride above the WHO upper limit of 1.5 mg/l. With respect to Arsenic  
680 (As) concentrations (b), the springs in the continental sector contain As above the WHO upper  
681 limit

682 Fig. 7. The plots of saturation indices (SI; with respect to quartz, anhydrite, aragonite, calcite and  
683 dolomite) versus total dissolved solid (TDS) for investigated water samples (wells and springs),  
684 show three subgroups (1: undersaturated wells. 2: trona precipitating springs. 3: dolomite  
685 precipitating springs).

686 Fig. 8. Stability diagrams for some minerals in the systems  $\text{Na}_2\text{-Al}_2\text{O}_3\text{-SiO}_2\text{-H}_2\text{O}$  (a) and  $\text{CaO-}$   
687  $\text{Al}_2\text{O}_3\text{-SiO}_2\text{-H}_2\text{O}$  (b) at 25°C

688

689 Fig. 9. The scanning electron microscope image (a), X-ray diffraction peaks (b), and electron  
690 probe microanalyzer mapping (c,d, e,f) of carbonate precipitate from Nyos cave spring

691 Fig. 10. The scanning electron microscope image (a), X-ray diffraction peaks (b), and electron  
692 probe microanalyzer mapping (c,d, e,f) of carbonate precipitate from the Sabga A spring

693 Fig. 11. The scanning electron microscope image (a), X-ray diffraction peaks (b), and electron  
694 probe microanalyzer mapping (c,d, e,f) of carbonate precipitate from the Sabga B spring

695 Fig.12. The scanning electron microscope image (a), X-ray diffraction peaks (b), and electron  
696 probe microanalyzer mapping (c,d, e,f) of carbonate precipitate from Bambui B spring

697 Fig. 13. Electron probe microanalyzer mapping of Na, Ca, Mg, and F of carbonate precipitate  
698 from Bambui B spring, showing enrichment of fluorine in the matrix of the carbonate

699 Fig. 14. The scanning electron microscope image (a), X-ray diffraction peaks (b), and electron  
700 probe microanalyzer mapping (c,d, e,f) of carbonate precipitate from Lobe D spring

701 Fig. 15. Carbonates-water oxygen isotopic fractionation temperature in observed soda springs  
702 along the CVL. Dolomites fractionated at relatively higher temperatures (35-43°C) than tronas  
703 (circum 20°C).

704  
705 Fig. 16. Plots of  $^{13}\text{C}$  and  $\delta^{18}\text{O}$  (PDB), showed observed tronas to be relatively depleted in  $^{13}\text{C}$   
706 and enriched in  $^{18}\text{O}$  (PDB).

707  
708 Fig. 17. Except for the Lobe springs that showed highest  $^{87}\text{Sr}/^{86}\text{Sr}$  ratio, in all the other observed  
709 springs the carbonate phases are relatively enriched in  $^{87}\text{Sr}/^{86}\text{Sr}$  ratio than the water phase (a),  
710 and  $^{87}\text{Sr}/^{86}\text{Sr}$  are relatively depleted in tronas than in dolomites (b)

711  
712 Fig. 18. Chloride versus fluoride cross plots showing volcanogenic contributions into the Lobe,  
713 Bambui and Nyos springs

714

715

### 716 **Table captions**

717

718 Table 1. Laboratory analytical methods of the carbonates and water phases in observed springs

719

720 Table 2. Chemical composition of water from the observed springs and shallow wells. ND: not  
721 detected. NM: not measured

722

723 Table 3. Fractionation temperature and isotopic compositions of carbonates precipitating from  
724 the observed springs

725

726

727

728

1 **Major ions,  $\delta^{18}\text{O}$ ,  $\delta^{13}\text{C}$  and  $^{87}\text{Sr}/^{86}\text{Sr}$  compositions of water and precipitates from springs**  
2 **along the Cameroon Volcanic Line (Cameroon, West Africa): Implications for provenance**  
3 **and volcanic hazards**

4

5 Wilson Yetoh FANTONG<sup>1</sup> $\Psi$ , Brice Tchakam KAMTCHUENG<sup>1</sup>, Yasuo ISHIZAKI<sup>2</sup>, Ernest Chi  
6 FRU<sup>3</sup>, Emilia Bi FANTONG<sup>4</sup>, Mengnjo Jude WIRMVEM<sup>1</sup>, Festus Tongwa AKA<sup>1</sup>, Bertil  
7 NLEND<sup>1</sup>, Didier HARMAN<sup>4</sup>, Akira UEDA<sup>5</sup>, Minoru KUSAKABE<sup>5</sup>, Gregory TANYILEKE<sup>1</sup>,  
8 Takeshi OHBA<sup>6</sup>

9 <sup>1</sup> Hydrological Research Center/ IRGM, Box 4110, Yaounde-Cameroon

10 <sup>2</sup> Graduate School of Science and Engineering and Research, Environmental and Energy  
11 Sciences, Earth and Environmental Systems

12 <sup>3</sup> School of Earth and Ocean Sciences, Cardiff University, Cardiff, Park Place, Wales-United  
13 Kingdom

14 <sup>4</sup> Ministry of Secondary Education, Cameroon

15 <sup>5</sup>Laboratory of Environmental Biology and Chemistry, University of Toyama, Gofuku 3190,  
16 Toyama 930-8555 Japan

17 <sup>6</sup>Department of Chemistry, School of Science, Tokai University, Hiratsuka, 259-1211, Japan

18  $\Psi$  Corresponding author: [fyetoh@yahoo.com](mailto:fyetoh@yahoo.com); [fantongy@gmail.com](mailto:fantongy@gmail.com)

19 **Abstract**

20 A combined study of major ions,  $\delta^{18}\text{O}$ ,  $\delta\text{D}$ ,  $^{13}\text{C}$ ,  $^{87}\text{Sr}/^{86}\text{Sr}$  isotopes, X-ray diffraction, scanning  
21 electron microscopy, and electron probe microanalyses on springs and spring mineral  
22 precipitates along the Cameroon Volcanic Line (CVL) was undertaken to understand water  
23 chemistry, and infer the type and origin of the precipitates. The waters are of evaporated Na+K-  
24 Cl and non-evaporated Ca+Mg-HCO<sub>3</sub> types, with the more mineralized (electrical conductivity-  
25 EC of 13130  $\mu\text{S}/\text{cm}$ ) Lobe spring inferred to result from interaction of circulating 49°C waters  
26 with magmatic volatiles of the active Mt. Cameroon. Water mineralization in the other springs  
27 follows the order: Sabga A > Sabga B > Bambui B > Bambui A > Nyos Cave. But for the Nyos  
28 Cave spring, all other springs contain fluoride (up to 0.5 - 35.6 mg/l above WHO potable water  
29 upper limit). The Sabga spring contains arsenic (up to 1.3 mg/l above the WHO limits). The  
30 springs show low fractionation temperatures in the range of 19 – 43 °C. The Lobe and Sabga A  
31 springs are precipitating dolomite (CaMg(CO<sub>3</sub>)<sub>2</sub>), while the Nyos Cave, Bambui A, Bambui B

32 and Sabga B springs precipitate trona ( $(\text{Na}_3\text{H}(\text{CO}_3)_2 \cdot \text{H}_2\text{O})$ ). Our data suggest a marine provenance  
33 for the carbonates, and point to a volcanic input for the Lobe, Nyos, Sabga A, and Bambui A  
34 springs. The latter springs are therefore proposed as proxies for monitoring volcanic activity for  
35 hazard mitigation along the CVL.

36 Key words: *Bubbling springs. Precipitates. Composition. Provenance. Volcanic activity.*  
37 *Hazards mitigation.*

38

39

## 40 **Introduction**

41 Mineral-depositing springs are natural systems that offer a good opportunity to study various  
42 mechanisms by which waters establish equilibrium with conditions at the Earth's surface  
43 (Amundson and Kelly, 1987; Omelon et al., 2006). For example, carbonate-precipitating waters  
44 provide an opportunity to evaluate a dynamic carbonate system and the major controls associated  
45 with calcite precipitation (Barnes, 1965; Jacobson and Usdowski, 1975), including; isotope  
46 fractionation associated with natural calcite precipitation from spring waters (McCrea, 1950;  
47 Friedman, 1970; Usdowski et al., 1979; Dandurand et al., 1982; Amundson and Kelly, 1987;  
48 Usdowski and Hoefs, 1990; Hamilton et al., 1991; Liu et al., 2003), as well as the types,  
49 morphologies, textures, and processes involved in the formation of various carbonate phases  
50 (Tucker and Bathurst, 1990; Bradley and Eugster, 1969; Ford and Pedley, 1996; Forti, 2005).

51

52 Many orifices of gas-water-carbonate interacting systems occur along the Cameroon Volcanic  
53 Line (CVL-Fig. 1). Based on carbonate enrichment studies on volcanic debris and springs in part  
54 of the continental sector of the CVL (Le Marechal, 1976; Verla et al., 2014); chemical and  
55 isotopic characteristics of fluids along the CVL (Tanyileke, 1994); the geochemistry of gases in  
56 springs around Mt. Cameroon and Lake Nyos (Kusakabe et al., 1989; Sano et al., 1990; Aka,  
57 1991); the sedimentology and geochemistry of the Bongongo and Ngol travertines along the  
58 CVL (Bisse et al., 2018), the following hypotheses have been proposed: (1) the bubbling mineral  
59 springs along the CVL contain abundant  $\text{CO}_2$ . (2) The  $\text{CO}_2$  in the bubbling springs is dominantly  
60 of magmatic origin. (3) Helium and carbon isotope ratios of gases from a few of the springs

61 along the CVL revealed a signature similar to hotspot type magma. (4) The precipitating  
62 minerals are travertines.

63 Although these studies provide initial data to understand the geochemical dynamics within the  
64 CVL gas-water-carbonate systems, gaps required to better understand the system include; a) a  
65 total absence of comprehensive information on the classification and genetic processes of the  
66 precipitating carbonates, which is exploited by the indigenes for preparation of traditional soup,  
67 b) high concentration ( $> 100$  mg/l) of geogenic fluoride has been reported (e.g., Kut et al., 2016;  
68 and references there-in) in thermal waters along the Ethiopian rift. Such concentrations of  
69 fluoride in water that is used for domestic purposes and livestock rearing can cause tremendous  
70 health effects (e.g., Fantong et al., 2010). Livestock rearing on the slopes of the CVL heavily  
71 consumes water from the springs (Fig. 2), so there is still a need to re-assess their chemical  
72 characteristics with focus on potential harmful elements like fluoride and arsenic, and c) the  
73 carbonate-water fractionation temperature remains unknown.

74 Against this backdrop, the objectives of this study are to 1) characterize the water chemistry with  
75 focus on health implications, 2) estimate the carbonate-water fractionation temperature, and 3)  
76 identify, describe and classify the carbonates that are precipitating from the springs.

77

## 78 **Study area**

79 Figure 1 shows, the sample sites along the CVL, a prominent 1600 km long Y-shaped chain of  
80 Tertiary to Recent, generally alkaline volcanoes that overlap an array of dextral faults called the  
81 Central Africa Shear Zone (CASZ) (Ngako et al., 2006) on the African continent, comparable  
82 only to the East Africa Rift System. The CVL follows a trend of crustal weakness that stretches  
83 from the Atlantic Island of Annobon, through the Gulf of Guinea, to the interior of the African  
84 continent (Fitton, 1980; Déruelle et al., 1987, Halliday et al., 1988;). It is unique amongst  
85 intraplate volcanic provinces in that it straddles the continental margin and includes both oceanic  
86 and continental intraplate volcanism. The oceanic sector constitutes a mildly alkaline volcanic  
87 series, which evolves towards phonolite, while the continental sector evolves towards rhyolite  
88 (e.g., Fitton, 1980). Isotopic studies of lavas (Halliday et al., 1988) divide the CVL into three  
89 sectors: an oceanic zone, ocean-continent boundary zone and a continental zone.

90 The study area overlaps two (coastal and tropical western highlands) of the five climatic zones in  
91 Cameroon, with mean annual rainfall of 5000 and 3000 mm, mean annual atmospheric

92 temperatures of 26°C and 21°C, humidity of 85% and 80%, and evaporation of 600 mm and 700  
93 mm, respectively (Sighomnou, 2004). Hydrologically, three (coastal, Sanaga, and Niger) of the  
94 five river basins in Cameroon drain the study area in a dendritic manner. According to Le  
95 Marechal (1968) and Tanyileke (1994), riverine and in aquifer waters encounter heat and mantle-  
96 derived CO<sub>2</sub> gas that emanate through the CASZ, causing heating and bubbling of the spring  
97 systems along the CVL. At each spring site the gas phase manifests as either bubbles or ‘rotten  
98 egg’ smell, while the precipitates occur as white films, white grains in volcanic ash, stalactite and  
99 stalactmite in caves, and mounds around orifices as shown in Fig. 3. At the sites of Sabga A in  
100 Fig. 3, animals consume the water as a source of salt, while humans exploit the precipitates for  
101 food recipes.

102

### 103 **Method of study**

104 Water and precipitate samples were collected from selected bubbling soda spring sites along the  
105 CVL (Fig. 3) in October 2015. Each water sample was collected in 3 acid-washed 250 ml  
106 polyethylene bottles after rinsing them thrice with the sample. At each sampling site, an  
107 unfiltered, unacidified and tightly corked sample was collected in one bottle for subsequent  
108 analyses for stable environmental isotopes of hydrogen ( $\delta^2\text{H}$ ) and oxygen ( $\delta^{18}\text{O}$ ). The second  
109 bottle contained un-acidified but filtered sample for anion analyses, and the third filtered and  
110 acidified sample for cations and trace elements analyses. Prior to sample collection, in-situ  
111 physicochemical measurements were recorded for pH (TOA-DKK HM-30P meter), electrical  
112 conductivity (TOA-DKK CM-31P EC meter), reduction-oxidation potential (TOA-DKK ORP  
113 meter), and water temperature. Geographical parameters (latitude, longitude and altitude) of each  
114 sample site were recorded in the field using a hand-held Garmin GPS. Alkalinity was measured  
115 using a ‘‘Hach’’ field titration kit, after addition of 0.16 N H<sub>2</sub>SO<sub>4</sub> to the sample to reach the  
116 endpoint titration (pH 4.5). Samples were filtered through 0.2  $\mu\text{m}$  filters prior to major ions and  
117 dissolved silica determination. Three kilograms chunks of massive carbonate was chipped off  
118 with a hammer at sites with consolidated precipitate, and 300 g scoped from sites with  
119 unconsolidated precipitate. Each precipitate was put in a clean plastic container, sealed and  
120 labelled.

121 Water samples and precipitates were transported to the University of Toyama, in Japan for  
122 chemical analyses.

123 The various chemical analyses that were done in various institutes in Japan are tabulated in Table  
124 1.

125

## 126 **Results and Discussions**

### 127 *Variation of water chemistry*

128 Chemical compositions and isotopic ratios of water samples and carbonate phases are presented  
129 in Tables 2 and 3. Measured in-situ parameters show values in the range of 54 - 13130  $\mu\text{S}/\text{cm}$  for  
130 EC, 4.3 - 7.5 for pH, and 19.3 - 47.4°C for water temperature.

131 The chemistry of the observed water resources determined with the use of the Piper's diagram  
132 (Piper, 1944) (Fig. 4a), shows that water from the Lobe soda springs and its nearby hand dug  
133 wells, located in the ocean-continent-boundary (OCB) and close to the ocean (Fig. 4a), have a  
134 dominant Na+K-Cl signature. On the other hand, water from the soda springs in Sabga, Bambui,  
135 and Nyos have dominantly Ca+Mg-HCO<sub>3</sub> signature. The observed disparity in water facies may  
136 be due to the proximity of the Lobe springs to the ocean, which impacts the sodium chloride  
137 characteristics as accorded in Le Marechal (1976). Whilst in the other springs, an interaction  
138 between primary and secondary minerals in rocks and water could be the dominant explanation  
139 as also explained by other researchers (Kamctung et al., 2014; Fantong et al., 2015). The Stiff  
140 diagrams for the water chemistry (Fig. 4b), also depict similar water facies like the Piper's  
141 diagram, but they further suggest varying degree of mineralization of the water sources. In the  
142 OCB, the larger sizes of the stiff diagram for the Lobe soda springs indicate more mineralization  
143 than for water from the wells. Likewise in the samples from the continental sector (CS) the water  
144 in the Sabga soda springs are most mineralized, followed by those in Bambui and the least  
145 mineralized is that from the Nyos soda spring. The observed variation in degree of mineralisation  
146 could in part be indicating variation in residence time, where the older springs are enriched in  
147 elements from aquifer minerals than in younger springs (e.g., Fantong et al., 2010a; Kamctung  
148 et al., 2015) that are renewed through a local and short recharge-discharge flow paths.

149

### 150 *Recharge mechanisms and evaporation of the sampled waters*

151 Isotopic ratios of hydrogen and oxygen, which are used in this study to infer recharge and  
152 evaporation mechanisms in the waters are also shown in Table 2 and graphically presented in Fig.  
153 5. The  $\delta\text{D}$  values ranged from -41.8 in Sabga A soda spring to -26 ‰ in water from well 5.

154 Oxygen isotope ( $\delta^{18}\text{O}$ ) values range from -6.3 ‰ in Sabga A spring to -3.1 ‰ in water from well  
155 3. Due to the paucity of isotope data on local rainfall, the Global Meteoric Water Line (GMWL)  
156 of Craig (1961), which is defined by the line  $\delta\text{D} = 8\delta^{18}\text{O} + 10$  is also presented as a reference.  
157 Distribution of sample water in the  $\delta\text{D}$ - $\delta^{18}\text{O}$  graph suggests that water in the Bambui and Sabga  
158 soda springs are subject to little or no evaporation, while the Lobe soda springs suggest slight  
159 evaporation, but water from the wells and Nyos soda springs show remarkable evaporation  
160 tendencies. Such a pattern depicts that the Bambui and Sabga soda springs are subject to the  
161 mechanism of preferential flow pass, which is caused by rapid recharge (e.g., Tsujimura et al.,  
162 2007; Asai et al., 2009), that is favored by the highly altered and jointed lavas as opposed to the  
163 Lobe and Nyos cave soda springs, and the wells. Except for the Lobe soda springs, the other  
164 springs are sources of drinking water for animals (cattle and goats), and a source of minerals  
165 (carbonate) for local manufacture of soup for consumption by the nearby population, thus it is  
166 important to assess at a preliminary scale the medical hydrogeochemical characteristics of the  
167 springs.

#### 168 ***Health implications of the water chemistry***

169 Given that the gas bubbling springs are located in the area of livestock rearing and human  
170 activities, their chemistry is here preliminarily evaluated to assess potential health implications.  
171 With respect to fluoride, Figure 6a shows that except for the Nyos cave soda spring, all the other  
172 soda springs contain fluoride at concentrations that are above the WHO optimal limit (1.5 mg/l  
173 e.g., Kut et al., 2016). This indicates that the animals and the population that exploit these  
174 springs are potentially exposed to fluoride poisoning as reported by Fantong et al. (2010b) in the  
175 Far Northern Region of Cameroon. The potential geogenic and volcanic provenance (Davies,  
176 2013), and actual epidemic effects of such high concentrations of fluoride are not within the  
177 scope of this study, and need further investigation.

178 With respect to arsenic (As), Figure 6b shows that the Sabga soda springs contain As at  
179 concentrations as high as 1.33 ppm that are above the WHO upper limit (0.03 ppm in drinking  
180 water). Based on the field observations that water from the Sabga soda springs is heavily  
181 consumed by cattle, and carbonate there-from is exploited for consumption by the population, it  
182 is also a challenge for medical geochemists to carry out a comprehensive investigation into the  
183 incidence, origin, mobilization and epidemiological effects of arsenic in these areas.

184

185 ***Impact of volcanic volatile or magmatic input on chemistry of the spring water***

186 The dissolved state of elements and saturation state of compounds observed in the springs are to  
187 an extent determined by their saturation indices and stoichiometry (e.g., Faure, 1991).

188

189 ***Saturation indices and activity diagrams***

190 The saturation index (SI) of a given mineral in an aqueous system is defined as (Lloyd and  
191 Heathcoat, 1985; and Deutch, 1997):

192 
$$SI = \log \left( \frac{IAP}{K_{sp}} \right) \quad (1)$$

193 where IAP is the ion activity product and  $K_{sp}$  is the solubility product of the mineral in the  
194 system. A  $SI > 0$  points to supersaturation, and a tendency for the mineral to precipitate from the  
195 water. Saturation can be produced by factors like incongruent dissolution, common ion effect,  
196 evaporation, and rapid increase in temperature and  $CO_2$  exsolution (Appelo and Postma, 2005).  
197 A  $SI < 0$  points toward undersaturation, and implies that water dissolves the minerals from  
198 surrounding rocks. Negative SI value might also reflect that the character of water is either from  
199 a formation with insufficient concentrations of the mineral for precipitation to occur (Garrels and  
200 Mackenzie, 1967).

201 The thermodynamic data used in this computation are those contained in the database of  
202 'Phreeqc for Windows'. A plot of the calculated SI (with respect to quartz, anhydrite, aragonite,  
203 calcite and dolomite) versus TDS (Fig.7) groups the water samples into three subgroups:  
204 subgroup 1, which consists of water from the shallow wells is undersaturated with respect to all  
205 the selected phases and has the lowest TDS values that ranged from 63-83 mg/l. The  
206 undersaturation of subgroup 1 suggests that no mineral precipitates in the wells as observed on  
207 the field. Subgroup 2, which consists of Nyos cave soda spring, Bambui soda spring B and Sabga  
208 soda spring B, show supersaturation with respect to quartz, dolomite. On the field, this subgroup  
209 is found to be dominantly precipitating trona (a Na-rich carbonate) and dolomite to a lesser  
210 extent. Subgroup 3 that consists of the Lobe and Sabga A soda springs, are supersaturated with  
211 respect to dolomite, quartz and calcite, and it is actually precipitating more of dolomite, and  
212 trona to a lesser extent.

213 The stability of secondary minerals (Na and Ca montmorillonites, kaolinite, gibbsite) and  
214 amorphous quartz in the springs and wells were evaluated by plotting  $\log (a_{Na}/a_H)$  vs  $\log (a_{H_4SiO_4})$

215 (the albite system) (Fig. 8a) and  $\log (a_{Ca2}/a_{2H})$  versus  $\log (a_{H4SiO4})$  (the anorthite system) (Fig.  
216 8b). These diagrams were drawn with the assumption that aluminum was preserved in the  
217 weathering product (Appelo and Postma,1993), because the amount of alumina will remain  
218 constant in fresh rocks and its altered equivalent. The constant amount in alumina ( $Al_2O_3$ ) is  
219 because an apparent increase in its weight % is actually always caused by a reduction in the  
220 weight of the fresh rock to some smaller amount (Faure, 1991). End member compositions were  
221 also assumed using equilibrium relationship for standard temperature ( $25^\circ C$ ) and pressure (1  
222 atmosphere), which approximately reflect the springs and groundwater conditions. Activities of  
223 the species were computed using the analytical concentrations and activity coefficient  
224 determined by Phreeqc for Windows version 2.1 under the above conditions (Appelo and  
225 Postma, 1993). According to the figures, groundwater from the wells span the stability field of  
226 kaolinite, while all the soda springs with exception of the Nyos soda spring are in equilibrium  
227 within the Na and Ca -montmorillonite stability fields. This concurs with the incidence of clay  
228 minerals in the study area (Fantong et al., 2015). Moreover, the presence of kaolinite and  
229 montmorillonite in the study area occur as groundmass in the XRD (X-Ray Defraction) peaks of  
230 Figures 9b,10b, 11b, 12b, and 14b. A combination of information from the saturation indices and  
231 stability diagrams is supported by the presence of precipitating carbonate phases in the soda  
232 springs as shown in Fig. 1.

233

### 234 *Typology of carbonate phases*

235 The typology of the carbonate phases that precipitate from the observed soda springs is done by  
236 describing the morphology by using SEM images, and identifying the carbonate phase by using  
237 XRD diagrams and EPMA elemental mapping.

238

### 239 **Carbonate from the Nyos cave soda spring**

240 The SEM image in Fig. 9a shows that the carbonate is an association of cluster of powdery  
241 amorphous groundmass upon which sub-euhedral crystals developed. This carbonate is identified  
242 with XRD peaks (Fig.9b) as a trona (low- syn trisodium hydrogen dehydrate carbonate). To  
243 accentuate the trona phase, an elemental EPMA mapping (Fig.9 c, d, e and f) shows the  
244 dominance of sodium, traces of calcium and total absence of magnesium.

245

246 **Carbonate from Sabga A soda spring**

247 The SEM image of Fig. 10a shows that the carbonate is nail-shaped stalactite crystals protruding  
248 from a cluster of powdery amorphous groundmass. This carbonate is identified with XRD peaks  
249 (Fig.10b) as a dolomite (calcium-magnesium bicarbonate). Dolomite precipitate in this spring is  
250 supported by an elemental EPMA mapping (Fig. 10 c, d, e and f), which shows a dominance and  
251 remarkable presence of both calcium and magnesium, with traces of sodium.

252

253 **Carbonate from Sabga B soda spring**

254 The SEM image of Fig. 11a shows that the carbonate is made up of radiating tabular columns of  
255 crystals whose faces are edged by bacteria. This carbonate is identified with XRD peaks (Fig.  
256 11b) as a trona (low-syn trisodium hydrogen dehydrate carbonate). The presence of this trona  
257 precipitating in this spring is justified by an elemental EPMA mapping (Fig. 11c, d, e and f),  
258 which shows a dominance of sodium and an almost absence of calcium and magnesium.

259

260 **Carbonate from Bambui B soda spring**

261 The SEM image of Fig. 12a shows that the morphology of the carbonate is an intersecting  
262 mosaic of tabular crystals whose faces are edged by bacteria. This carbonate is identified with  
263 XRD peaks (Fig. 12b) as a trona similar to that of Sabga B. The presence of this trona  
264 precipitating in this spring is supported by an elemental EPMA mapping (Fig. 12 c, d, e and f),  
265 which shows a dominance of sodium and low content of calcium and magnesium. The  
266 disseminated distribution of fluorine, which almost coincide with the distribution of faint calcite  
267 suggest the presence of fluorite (CaF<sub>2</sub>), which could be dissolving to enrich the water phase with  
268 fluoride as seen in Fig. 13e.

269

270 **Carbonate from Lobe D soda spring**

271 The SEM image of Fig. 14a shows that the carbonate is a coliform flower-shape radiating  
272 crystals, which is colonized by bacteria. This carbonate is identified with XRD peaks (Fig. 14b)  
273 as a dolomite. The occurrence of dolomite as the precipitate in this spring is supported by an  
274 elemental EPMA mapping (Fig. 14c, d, e and f), which shows high content of both calcium and  
275 magnesium, and low content of sodium.

276 Summarily, the carbonate phases that are precipitating from the studied soda springs along the  
277 CVL are dominantly dolomite and trona. The pristine geochemical attributes and characteristics  
278 of the carbonate are at a later phase altered (Demeny, 2016) by diatoms and bacteria as shown in  
279 Figure 11a and 12a. The incidence of bacteria in such a hydrogeochemical system leaves  
280 biogeochemists with another opportunity to assess the incidence and role of bacteria in the soda  
281 spring systems.

282

### 283 **Origin of the fluids and carbonates**

284 In a bid to identify the formation (sources and paleo temperature) processes that led to the  
285 formation of the observed carbonates, we used  $^{13}\text{C}$  isotopes,  $^{87}\text{Sr}/^{86}\text{Sr}$ , carbonate-water  
286 fractionation temperatures, and  $\text{Cl}^-$  versus  $\text{F}^-$  plot as geochemical tracers.

287

### 288 *Carbonate-water fractionation temperature*

289 Although oxygen-isotope thermometry based on isotopic fractionation of oxygen between  
290 carbonates and water dates back to the Mid-1900s, the carbonate-water oxygen isotopic  
291 fractionation equations are still being discussed. The use of isotope thermometry is based on  
292 several criteria: (i) the temperature dependence of the isotopic fractionation between the  
293 investigated compounds (in our case dolomite/trona and water) and (ii) the isotopic compositions  
294 of the compounds are known, (iii) the isotopic equilibrium between the compounds can be  
295 proven or at least reasonably assumed, and (iv) no subsequent isotopic alteration occurred after  
296 the deposition of carbonates. These considerations are valid for inorganic carbonate formation, as  
297 biogenic carbonate is severely affected by the organisms' metabolism, resulting in a species-  
298 dependent ‘‘vital effect’’ (Demeny et al., 2010 and references therein)

299 The temperatures at which the carbonate phases precipitate from the springs were calculated by  
300 using the empirical equation for the temperature dependence of calcite-water oxygen isotope  
301 fractionation from 10 to 70 °C as shown in equations 2 and 3 that were reported by Demeny et al.  
302 (2010).

$$303 \quad 1000 \cdot \ln \alpha = 17599/T - 29.64 \quad [\text{for travertines with a temperature range of } 30 \text{ to } 70^\circ\text{C}] \quad (2)$$

$$304 \quad 1000 \cdot \ln \alpha = 17500/T - 29.89 \quad [\text{for cave deposits for the range } 10 \text{ to } 25^\circ\text{C}] \quad (3)$$

305 The variable T are in °C.

306 The values obtained suggest that carbonates precipitate from soda springs along the CVL at  
307 temperature that varied from 18.5 - 43°C. The lowest fractionation temperatures (18.5 - 18.6°C)  
308 occurred in the Sabga soda springs, while the highest (35 - 43°C), occurred in the Lobe soda  
309 springs (Table 3). A plot (Fig. 15), shows that with the exception of the dolomite in the 'Sabga  
310 A soda spring', the tronas fractionated at lower temperature (~18.5 - 20 °C) than the dolomites,  
311 which fractionated at temperature ranging from 35.2 - 43°C. Based on Figure 15, the oxygen  
312 isotopes in carbonates precipitating along the Cameroon Volcanic Line yielded an empirical  
313 fractionation– temperature equations of:

$$314 \quad 1000.\ln\alpha = -0.2153T + 35.3 \quad (4)$$

315

### 316 *Stable isotopes of $^{13}\text{C}$ , $^{87}\text{Sr}/^{86}\text{Sr}$ , and $^{18}\text{O}$*

317 The observed carbonates (dolomite and trona) facies in the samples showed broad ranges in  
318  $^{87}\text{Sr}/^{86}\text{Sr}$ ,  $^{13}\text{C}$  and  $\delta^{18}\text{O}$ . The  $^{87}\text{Sr}/^{86}\text{Sr}$  ratio varied from 0.706 - 0.713, the  $^{13}\text{C}$  varied from -3.09 to  
319 5.22 VPDB and  $\delta^{18}\text{O}$  from -8.4 to -1.4 VPDB as shown in Table 3. Their  $\delta^{13}\text{C}$  values of observed  
320 dolomites are close to the range of values reported for carbonates precipitating from seawater (0  
321 -4 VPDB; Veizer et al., 1999; Shah et al., 2012). Indication of marine origin of the dolomites  
322 corroborates with field observation, because the dolomite precipitates from the Lobe soda spring  
323 located in the OCB of the study area. However, the carbonates (trona) identified in our study  
324 area showed relatively depleted  $\delta^{13}\text{C}$  signatures, which may indicate a possible external source of  
325 carbon during trona precipitation (Fig. 16) or a temperature dependent fractionation effect (Shah  
326 et al., 2012). The depleted  $\delta^{18}\text{O}$  in dolomite from the 49°C Lobe soda springs, may be due to its  
327 higher temperatures (thermogenic type) (Bisse et al., 2018), given that precipitation of dolomite  
328 from hot springs leads to relatively depleted  $\delta^{18}\text{O}$  ratios (Land, 1983).

329 With exception of the Lobe soda springs, where  $^{87}\text{Sr}/^{86}\text{Sr}$  value did not vary between the  
330 carbonate and water phases, in the other soda springs (Bambui soda springs A and B, Sabga soda  
331 springs A and B, and Nyos cave soda spring), the  $^{87}\text{Sr}/^{86}\text{Sr}$  ratio shows a decoupling tendency  
332 where the water phases contain relatively higher values than the carbonate phases (Fig. 17a). The  
333 relatively higher  $^{87}\text{Sr}/^{86}\text{Sr}$  ratio in the Lobe soda springs may indicate interaction of dolomitizing  
334 fluids with radiogenic lithologies (Shah et al., 2012), which commonly occur along the CVL  
335 (e.g., Aka et al., 2000; 2001). Moreover, the  $^{87}\text{Sr}/^{86}\text{Sr}$  versus  $^{18}\text{O}$  cross plot (Fig. 17b), shows that  
336 the dolomites are richer in  $^{87}\text{Sr}/^{86}\text{Sr}$  ratio than the tronas. However, the signatures in the dolomite

337 of the Sabga soda spring “A” together with those in the tronas are closer to those of the marine  
338 signatures (McArthur et al., 2001). Such marine signatures in tronas (Na-rich carbonate) within  
339 the continental sector of the Cameroon Volcanic Line, may suggest the presence of paleo-  
340 continental sabkha environments, where various sodium carbonates have been recorded in  
341 tropical regions (Whitten and Brooks, 1972). This suggestion, however, requires further  
342 investigation.

343

#### 344 **Implications for monitoring and hazard mitigation**

345 Volcanogenic sources of fluorine (e.g., Symonds et al., 1987; Symonds et al., 1988; Bellomo et  
346 al., 2003) and chlorine (e.g., Keene and Graedel 1995) containing gasses have been reported in  
347 active and passive volcanic areas, and recently in the Nyiragongo volcano in Congo (Liotta et al.,  
348 2017). As used by the later, we also used a cross plot of chloride versus fluoride (Fig. 18) to infer  
349 volcanogenic contribution in the observed springs along the CVL. The figure suggests  
350 volcanogenic inputs into the Lobe, Nyos, Sabga A, and Bambui A springs. The implication of a  
351 volcanic input to these fluids suggests that they can be used to monitor volcanic activity and thus  
352 mitigate hazards, especially in the vicinity of the Lobe spring located close to the currently active  
353 Mt. Cameroon. Moreover, the dominant fluids in the Lobe, Nyos, Sabga A, and Bambui A  
354 springs are magmatic CO<sub>2</sub> and H<sub>2</sub>O (Sano 1990). Water dissolves slightly more in silicic melts  
355 than in basaltic melts, whereas CO<sub>2</sub> dissolves more in basaltic than in silicic melts. Kusakabe  
356 (2017) reports that the solubility of CO<sub>2</sub> and H<sub>2</sub>O in basaltic melts at 1200°C is a function of the  
357 total pressure of the volatiles, whose composition in the melt changes as the decompression  
358 proceeds. For example, at low pressure the mole fraction of H<sub>2</sub>O equals 0.2 and that of CO<sub>2</sub> is  
359 0.8, implying that basaltic melt becomes rich in CO<sub>2</sub> as the magma ascends and the confining  
360 pressure reduces, resulting to degassing. If degassing takes place in an open system, CO<sub>2</sub>-rich  
361 fluid leaves the magma. This solubility-controlled behavior of CO<sub>2</sub> in basaltic magma may  
362 explain a CO<sub>2</sub>-rich nature of fluids separated from the magma. The ultimate source of CO<sub>2</sub> in the  
363 Nyos, Lobe, Sabga A, and Bambui A springs may therefore be derived from the decarbonation of  
364 crystallized metasomatic fluids in the subcontinental lithosphere (Aka, 2015; Asaah et al., 2015).  
365 The low (-2 to -3 ‰) <sup>13</sup>C values of carbonates in the Nyos and Sabga soda spring may also  
366 indicate magmatic origin of the CO<sub>2</sub> that contributes in precipitating the carbonates. Thus, the

367 permanent supply of such CO<sub>2</sub> in the springs provides good sites for monitoring volcanic activity  
368 for hazard mitigation.

369

### 370 **Conclusions**

371 The chemistry of water in the bubbling soda springs observed along the Cameroon Volcanic Line  
372 shows an evaporated Na+K-Cl and non-evaporated Ca+Mg-HCO<sub>3</sub> facies in the ocean continental  
373 boundary sector (OCB) and continental sector (CS), respectively. In the OCB, the Lobe soda  
374 springs shows more mineralization than water from nearby hand dug wells. This may indicate  
375 that spring water (T=49°C) is circulating deeper than the well water. In the continental sector  
376 (CS) the water in the Sabga soda springs are the most mineralized, followed by those in Bambui  
377 soda spring and the least mineralized is the Nyos soda spring. With exception of the soda springs  
378 in the Nyos area, all other studied soda springs contain fluoride from geogenic fluorine at  
379 concentrations above the WHO upper limit, whilst concentrations of arsenic (> 0.3 mg/l) that  
380 also call for health concern occur in the Sabga soda springs. The observed soda springs are either  
381 saturated or super-saturated with respect to quartz, and carbonate phases, which are actually  
382 precipitating as dolomite and trona. The carbonate-water fractionation temperature varies from  
383 18.5 - 43°C. X-ray diffraction spectra and chemical mapping by electron probe microanalyzer  
384 unraveled that the precipitating carbonates occur as dolomite in the Lobe and Sabga A soda  
385 springs, and as trona in the Nyos, Bambui and Sabga B soda springs. Scanning electron  
386 microscope (SEM), reveals various morphologies of the carbonates, including amorphous to  
387 tabular euhedral tronas, and nail shaped to bacteria-colonized coliform dolomites. Geochemical  
388 tracers of <sup>13</sup>C, <sup>87</sup>Sr/<sup>86</sup>Sr, and <sup>18</sup>O indicate a dominantly marine provenance of the carbonate.  
389 Chloride versus fluoride cross plot suggest a contribution from volcanic volatiles in the Lobe,  
390 Nyos, Sabga A, and Bambui A springs. This contribution of a volcanic input to these fluids  
391 suggests that they can be used to monitor volcanic activity and thus mitigate hazards, especially  
392 in the vicinity of the Lobe spring that is located close to the currently active Mt. Cameroon.

393

### 394 **Acknowledgements**

395 We thank the Institute of Geological and Mining Research (IRGM), Yaoundé, for financial and  
396 logistical support during sampling. Thanks to the funders (JICA and JST) of SATREPS-IRGM  
397 project that provided field and laboratory equipment that were used to generate the data during

398 this study. We thank all the members of the Department of Environmental Biology and  
399 Chemistry, University of Toyama, Japan, for their enriching comments during the preparation of  
400 this manuscript. We are also grateful to Prof. Suh Emmanuel and Prof. Loic Peiffer for their  
401 review comments that enriched the content of the manuscript.

402

403

404

405

406

407

408

409

410

## 411 **References**

412

413 Aka, F.T., 1991. Volcano Monitoring by Geochemical Analyses of Volcanic Gases. Thesis, The  
414 University of Leeds, LS2 9JT. 94 pp.

415

416

417 Aka, F.T., 2000. Noble gas systematics and K–Ar Chronology: implications on the geotectonic  
418 evolution of the Cameroon Volcanic Line, West Africa, PhD thesis, Univ. Okayama, Japan.  
419 175 pp.

420 Aka, F. T. (2015) Depth of melt segregation below the Nyos maar-diatreme volcano (Cameroon,  
421 West Africa): Major trace element evidence and their bearing on the origin of CO<sub>2</sub> in Lake  
422 Nyos. Volcanic Lakes (Rouwet, D., Christenson, B., Tassi, F. and Vandemeulebrouck, J.,  
423 eds.), Springer-Heidelberg.

424

425

426 Aka, F.T., Kusakabe, M.K., Nagao, K., Tanyileke, G., 2001. Noble gas isotopic compositions  
427 and water/gas chemistry of soda springs from the islands of Bioko, Saõ Tome' and  
428 Annobon, along the Cameroon Volcanic Line, West Africa. Appl. Geochem.16, 323–338.

429

430 Amundson, R., Kelly, E., 1987. The chemistry and mineralogy of a CO<sub>2</sub>-rich travertine  
431 depositing spring in the California Coast Range. Geochim. Cosmochim. Acta 51, 2883–2890.

432

433 Appelo, C.A.J., Postma, D., 2005. Geochemistry, groundwater, and pollution. 2nd edn. Balkema  
434 Publishers, Rotterdam, 649 pp

435 Asai, K., Satake, H., and Tsujimura, M., 2009. Isotopic approach to understanding the

436 groundwater flow system within the andesitic strato-volcano in a temperate humid  
437 region: case study of Ontake volcano, Central Japan. *Hydrol. Processes*. 23, 559-571.  
438

439 Asaah, A. N. E., Yokoyama, T., Aka, F. T., Usui, T., Kuritani, T., Wirmvem, M. J., Iwamori, H.,  
440 Fozing, E. M., Tamen, J., Mofor, G. J., Ohba, T., Tanyileke, G. and Hell, J. V. (2015)  
441 Geochemistry of lavas from maar-bearing volcanoes in the Oku Volcanic Group of the  
442 Cameroon Volcanic Line. *Chem. Geol.* 406, 55–69.  
443

444 Barnes, I., 1965. Geochemistry of Birch Creek, Inyo County, California: a travertine depositing  
445 creek in an arid climate. *Geochim. Cosmochim. Acta* 29, 85–112.  
446

447

448 Bellomo, S., D’Alessandro, W., and Longo, M., 2003. Volcanogenic fluorine in rainwater around  
449 active degassing volcanoes: Mt.Etna and Stromboli Island, Italy. *Sci. Total Environ.* 301,  
450 175–185.  
451

452 Bisse, S. B., Ekomané, E., Eyong, J.T., Ollivier, V., Douville, E., Nganne, M.J.M., Bokanda,  
453 E.E., Bitom, L.D., 2018. Sedimentological and geochemical study of the Bongongo and  
454 Ngol travertines located at the Cameroon Volcanic Line. *Journal of African Earth Sciences*.  
455 DOI.org/10.1016/j.jafrearsci.2018.03.028  
456

457 Craig, H., 1961. Isotopic variations in meteoric waters. *Science* 133:1702–1703  
458

459 Dandurand, J.L., Gout, R., Hoefs, J., Menschel, G., Schott, J., Usdowski, E., 1982. Kinetically  
460 controlled variations of major components and carbon and oxygen isotopes in a calcite  
461 precipitating spring. *Chem. Geol.* 36, 299–315.  
462

463 Davies, T.C., 2013. Geochemical variables as plausible aetiological cofactors in the incidence of  
464 some common environmental diseases in Africa. *Journ. African Earth Sciences.* 79, 24-49  
465

466

467 Demeny, A., Kele, S., and Siklosy, Z., 2010. Empirical equations for the temperature  
468 dependence of calcite-water oxygen isotope fractionation from 10 to 70°C. *Rapid Commun.*  
469 *Mass Spectro.* 24, 3521-3526

470 Demeny, A., Nemeth, P., Czuppon, G., Leel-Ossy, S., Szabo, M., Judik, K., Nemeth, T., Steiber,  
471 J., 2016. Formation of amorphous calcium carbonate in caves and its implications for  
472 speleothem research. *Scientific Report.* 6, 39602  
473

474 Deruelle, B., Nni, J., and Kambou, R., 1987. Mount Cameroon: An active volcano of the  
475 Cameroon Volcanic Line. *J. African Earth Sciences.* 6, 197-214  
476

477 Deutsch, W.J., 1997. Groundwater geochemistry: fundamentals and application to  
478 contamination. CRC, Boca Raton  
479

480 Bradley, W.H., and Eugster, H.P., 1969. Geochemistry and paleolimnology of the trona deposits  
481 and associated authigenic minerals of green river formation of Wyoming. Geological Survey  
482 Professional Paper 496-B, US Government Printing office, Washington, 66 pp  
483

484 Fantong, W.Y., Satake, H., Ayonghe, S.N., Suh, C.E., Adelana, S.M.A., Fantong, E.B.S.,  
485 Banseka, H.S., Gwanfogbe, C.D., Woincham, L.N., Uehara, Y., Zhang, J., 2010b.  
486 Geochemical provenance and spatial distribution of fluoride in groundwater of Mayo  
487 Tsanaga River Basin, Far north Region, Cameroon: implications for incidence of fluorosis  
488 and optimal consumption dose. *Environ Geochem Health*. Vol. 32: 147-163  
489

490 Fantong, W.Y., Kamtchueng, B.T., Yamaguchi, K., Ueda, A., Issa, Ntchantcho, R., Wirmvem,  
491 M.J., Kusakabe, M., Ohba, T., Zhang, J., Aka, F.T., Tanyileke, G.Z., Hell, J.V., 2015.  
492 Characteristics of Chemical weathering and water-rock interaction in Lake Nyos dam  
493 (Cameroon): Implications for vulnerability to failure and re-enforcement. *Journal of African  
494 Earth Sciences*: 101:42-55  
495

496 Fantong, W.Y., Satake, H., Aka, F.T., Ayonghe, S.N., Kazuyoshi, A., Mandal, A.K., Ako, A.A.,  
497 2010a. Hydrochemical and isotopic evidence of recharge, apparent age, and flow direction  
498 of groundwater in Mayo Tsanaga River Basin, Cameroon: Bearings on contamination.  
499 *Journal of Environ Earth Sci*. Vol. 60: 107-120  
500

501 Faure, G., 1991. Principles and Applications of Inorganic Geochemistry. *Macmillan Publishing  
502 Company*, New York, 626 p.  
503  
504

505 Fitton, J.D., 1980. The Benue Trough and the Cameroon Line – A Migrating Rift System in  
506 West Africa. *Earth Planet. Sci. Lett.* 51, 132-138  
507

508 Ford, T.D., Pedley, H.M. 1996. A Review of Tufa and Travertine Deposits of the World. *Earth  
509 Science Reviews* 41, 117-175.  
510

511 Forti, P., 2005. Genetic processes of cave minerals in volcanic environments: an overview.  
512 *Journal of Cave and Karst Studies*. Vol 67:1, 3-13.  
513  
514

515 Friedman, I., 1970. Some investigations of the deposition of travertine from Hot Springs – I. The  
516 isotopic chemistry of a travertine-depositing spring. *Geochim. Cosmochim. Acta* 34, 1303–  
517 1315.

518  
519

520 Garrels, R.M., Mackenzie, F.T., 1967. Origin of the chemical composition of some springs and  
521 lakes. In: RF Gould (ed.). *Equilibrium concepts in natural water systems*. Washington, DC:  
522 American Chemical Society, pp 222-242.

523

524 Halliday, A.N., Dicken, A.P., Fallice, A.E., and Fitton, J.T., 1988. Mantle dynamics. A Nd, Sr,  
525 Pb, and O isotope study of the Cameroon Volcanic Line. *J. Petrol.* 29, 181-211

526  
527

528 Hamilton, S.M., Michel, F.A., Jefferson, C.W., 1991. CO<sub>2</sub>-rich ground waters of the Flat River  
529 Valley, N.W.T. In: Prowse, T., Ommanney, C. (Eds.), *Northern Hydrology Selected  
530 Perspectives, Proceedings of the Northern Hydrology Symposium, 10–12 July 1990,*  
531 *Saskatoon, Saskatchewan, NHRI Paper #6*, pp. 105–199.

532

533 Jacobson, R.L., Usdowski, E., 1975. Geochemical controls on a calcite precipitating spring.  
534 *Contrib. Mineral. Petrol.* 51, 65–74.

535  
536

537 Kamtchueng, B. T., Fantong, W.Y., Wirmvem, M.J., Tiodjio, R.E., Takounjou, A.F., Asai, K.,  
538 Serges L. Djomou, S.L.B., Kusakabe, M., Ohba, T., Tanyileke, G., Hell, J.V., Ueda A.,  
539 2015. A multi-tracer approach for assessing the origin, apparent age and recharge  
540 mechanism of shallow groundwater in the Lake Nyos catchment, Northwest, Cameroon.  
541 *Journal of Hydrology*, 523:790–803.

542

543 Kamtchueng, B.T., Fantong, W.Y., Ueda, A., Tiodjio, E.R., Anazawa, K., Wirmvem, J.,  
544 Mvondo, J.O., Nkamdjou, L., Kusakabe, M., Ohba, T., Tanyileke, G.Z., Joseph, V. H.,  
545 2014. Assessment of shallow groundwater in Lake Nyos catchment (Cameroon, Central-  
546 Africa): implications for hydrogeochemical controls and uses. *Environmental Earth  
547 Sciences*, 72:3663–3678.

548 Kusakabe, M., 2017. Lakes Nyos and Monoun gas disasters (Cameroon)—Limnic eruptions  
549 caused by excessive accumulation of magmatic CO<sub>2</sub> in crater lakes. *GEOchem. Monogr.*  
550 *Ser. 1*, 1–50, doi:10.5047/gems.2017.00101.0001.

551

552 Kusakabe, M., Ohsumi, T., and Arakami, S., 1989. The Lake Nyos gas disaster: chemical and  
553 isotopic evidence in waters and dissolved gases in three Cameroonian Lakes, Nyos,  
554 Monoun and Wum. In: Le Guern, F., and Sigvaldason, G., (Editors), The Lake Nyos Event  
555 and Natural Carbon dioxide Degassing, 1. J. Volcanol. Geothermal Res., 39, 167-185.  
556

557 Kut, K.M.K., Sarsevat, A., Srivastava, A., Pitmann, C.U., Moham, D., 2016. A review of  
558 Fluoride in African Groundwater and Local Remediation Methods. Groundwater for  
559 Sustainable Development 2, 190-175  
560

561 Land, L.S., 1983. The application of stable isotopes to studies of the origin of dolomite and to  
562 problems of diagenesis of clastic sediments, in: Arthur M.A., Anderson T.F. (eds), Stable  
563 isotopes in Sedimentary Geology, Soc. Econ. Paleont. Miner. Short Course No. 10, 4.1-  
564 4.22.  
565

566 Le Marechal, A., 1976. Geologie et Geochemie des sources thermominerales du Cameroun.  
567 ORSTOM, Paris  
568

569

570 Liotta, M., Shamavu, P., Scaglione, S., D'Alessandra, W., Bobrowski, N., Giuffrida, G.B.,  
571 Tedesco, D., Calabrese, S., 2017. Mobility of plume-derived volcanogenic elements in  
572 meteoric water at Nyiragongo volcano (Congo) inferred from the chemical composition of  
573 single rainfall events. *Geochimica et Cosmochimica Acta*. 217, 254-272  
574

575 Liu, Z., Zhang, M., Li, Q., You, S., 2003. Hydrochemical and isotope characteristics of spring  
576 water and travertine in the Baishuitai area (SW China) and their meaning for  
577 paleoenvironmental reconstruction. *Environ. Geol.* 44, 698-704.  
578

579 Lloyd, J.W., Heathcoat, J.A., 1985. Natural inorganic hydrochemistry in relation to groundwater:  
580 an introduction. Oxford University Press, New York, p 296  
581

582

583 McArthur, J.M., Howarth, R.J., Bailey, T.R., 2001. Strontium isotope stratigraphy: LOWESS  
584 Version 3. Best-fit line to the marine Sr-isotope curve for 0 to 509 Ma and accompanying  
585 look-up table for deriving numerical age, *J. Geol.* **109**, 155-169.  
586

587 McCrea, 1950. On the Isotope Chemistry of Carbonates and a Paleotemperature Scale. The  
588 Journal of Chemical Physics. 18, 6.  
589  
590

591 Ngako, V., Njonfang, E., Aka, F. T., Affaton, P., & Nnange, J. M., 2006. The north–south  
592 Paleozoic to Quaternary trend of alkaline magmatism from Niger-Nigeria to Cameroon:  
593 complex interaction between hotspots and Precambrian faults. *Journal of African Earth*  
594 *Sciences*, 45, 241–256. doi:10.1016/j.jafrearsci.2006.03.003.  
595

596 Omelon CR, Pollard WH, Anderson DT (2006) A geochemical evaluation of perennial spring  
597 activity and associated mineral precipitates at Expedition Fjord, Axel Heiberg Island,  
598 Canadian High Arctic. *Applied geochemistry* 21,1-15  
599

600

601 Piper, A.M., 1944. A graphic procedure in the geochemical interpretation of water analyses. *Am*  
602 *Geophys Union Trans* 25:914–923  
603

604 Sano, Y., Kusakabe, M., Hirabayashi, J., Nojiri, Y., Shinohara, H., Njini, T., Tanyileke, G.Z.,  
605 1990. Helium and Carbon Fluxes in Lake Nyos, Cameroon: Constraints on next gas burst.  
606 *Earth and Planetary Science Letters*. 99, 303-314  
607

608

609 Shah, M.M., Nader, F.H., Garcia, D., Swennen, R., Ellam, R., 2012. Hydrothermal dolomites in  
610 the Early Albian (Cretaceous) platform carbonates: (NW Spain): Nature and origin of  
611 dolomite and dolomitizing fluids. *Oil & Gas Science and Technology-Rev. IFP Energies*  
612 *nouvelles* 67:1, 88-122  
613

614 Sighomnou, D., 2004. Analyse et Redefinition des Regimes Climatiques et Hydrologiques du  
615 Cameroun: Perspectives d'évolution des Ressources en Eau. Ph.D Thesis, University of  
616 Yaounde 1. 292 pp.  
617

618

619 Symonds, R. B., Rose, W. I., Reed, M. H., Lichte, F. E., and Finnegan, D. L., 1987.  
620 Volatilization, transport and sublimation of metallic and non-metallic elements in high  
621 temperature gases at Merapi Volcano, Indonesia. *Geochim. Cosmochim.Acta* 51, 2083–  
622 2101.  
623

624 Symonds, R.B., Rose, W.I., Reed, M.H., 1988. Contribution of Cl<sup>-</sup> and F<sup>-</sup> bearing gases to the  
625 atmosphere by volcanoes, *Nature*, 334, 415-418.  
626

627 Tanyileke, G.Z., 1994. Fluid Geochemistry of CO<sub>2</sub> – Rich Lakes and Soda Springs Along the  
628 Cameroon Volcanic Line. Dissertation, Okayama University, Japan.  
629

- 630 Tsujimura, M., Abe, Y., Tanaka, T., Shimade, J., Higuchi, S., Yamanaka, T., Davaa, G.,  
631 Oyunbaatar, D., 2007. Stable isotopic and geochemical characteristics of groundwater in  
632 Kherlin River Basin: a semiarid region in Eastern Mongolia. *J Hydrol* 333:47–57  
633
- 634 Tucker, M. E., and Bathurst, R.G.C., 1990. Carbonate Diagenesis. Reprint series volume 1 of the  
635 International Association of Sedimentologists. Blackwell Scientific Publications. 312 pages  
636  
637
- 638 Usdowski, E., Hoefs, J., Menschel, G., 1979. Relationship between  $^{13}\text{C}$  and  $^{18}\text{O}$  fractionation and  
639 changes in major element composition in a recent calcite-depositing spring – a model of  
640 chemical variations with inorganic  $\text{CaCO}_3$  precipitation. *Earth Planet. Sci. Lett.* 42, 267–  
641 276.  
642
- 643 Usdowski, E., Hoefs, J., 1990. Kinetic  $^{13}\text{C}/^{12}\text{C}$  and  $^{18}\text{O}/^{16}\text{O}$  effects upon dissolution and  
644 outgassing of  $\text{CO}_2$  in the system  $\text{CO}_2\text{--H}_2\text{O}$ . *Chem. Geol.* 80, 109–118.  
645
- 646 Veizer, J., Ala, D., Azmy, K., Bruckschen, P., Buhl, D., Bruhn, F., Carden, G.A.F., Diener, A.,  
647 Ebner, S., Godderis, Y., Jasper, T., Korte, C., Pawellek, F., Podlaha, O., Strauss, H., 1999.  
648  $^{87}\text{Sr}/^{86}\text{Sr}$ ,  $\delta^{13}\text{C}$  and  $\delta^{18}\text{O}$  evolution of Phanerozoic seawater, *Chem. Geol.* **161**, 59-88.  
649  
650
- 651 Verla, R.B., Mboudou, G.M.M., Njoh, O., Ngoran, G.N., Afahnwie, A.N., 2014. Carbonate  
652 Enrichment in Volcanic Debris and Its Relationship with Carbonate Dissolution Signatures  
653 of Springs in the Sabga-Bamessing, North West, Cameroon. *International Journal of*  
654 *Geosciences*, 2014, 5, 107-121  
655
- 656 Whitten, D.G.A., and Brooks, J.R.V., 1972. *The Penguin Dictionary of Geology*. Penguin book  
657 limited, England-Great Britain. 493 pages  
658  
659

### 660 **Figures captions**

661 Fig. 1. Locations of sampled carbonate depositing soda springs along the Cameroon Volcanic  
662 Line (CVL). CS stands for the continental sector of the CVL, and OCB stands for the oceanic  
663 continental boundary of the CVL. The locations of Lake Monoun (L. Monoun), Lake Nyos (L.  
664 Nyos), and Mount Cameroon (Mt. Cameroon) are also shown. The black dots correspond to  
665 samples' locations

666

667 Fig.2. Herds of cattle consuming water from the carbonate depositing springs that have been  
668 harnessed

669

670 Fig. 3. Samples (deposited carbonates and water) collection sites from observed springs

671 Fig. 4. Water chemistry presented as Piper's diagram (a), and Stiff diagrams (b) for the observed  
672 springs

673 Fig. 5. Plot of  $\delta\text{H}$  and  $\delta^{18}\text{O}$  in water from observed springs. The Sabga and Bambui springs  
674 showed no evaporation effect, while the Lobe springs, the Nyos spring and water in shallow  
675 wells around Lobe spring were subjected to evaporation relative to the meteoric water lines.  
676 Zone 1 represents the soda springs and zone 2 represents shallow groundwater in the Lobe spring  
677 neighborhood. LMWL: Local meteoric water line. GMWL: Global meteoric water line

678 Fig. 6. With respect to fluoride concentrations (a), all the observed soda springs with exception  
679 of that in Nyos, contain fluoride above the WHO upper limit of 1.5 mg/l. With respect to Arsenic  
680 (As) concentrations (b), the springs in the continental sector contain As above the WHO upper  
681 limit

682 Fig. 7. The plots of saturation indices (SI; with respect to quartz, anhydrite, aragonite, calcite and  
683 dolomite) versus total dissolved solid (TDS) for investigated water samples (wells and springs),  
684 show three subgroups (1: undersaturated wells. 2: trona precipitating springs. 3: dolomite  
685 precipitating springs).

686 Fig. 8. Stability diagrams for some minerals in the systems  $\text{Na}_2\text{-Al}_2\text{O}_3\text{-SiO}_2\text{-H}_2\text{O}$  (a) and  $\text{CaO-}$   
687  $\text{Al}_2\text{O}_3\text{-SiO}_2\text{-H}_2\text{O}$  (b) at 25°C

688

689 Fig. 9. The scanning electron microscope image (a), X-ray diffraction peaks (b), and electron  
690 probe microanalyzer mapping (c,d, e,f) of carbonate precipitate from Nyos cave spring

691 Fig. 10. The scanning electron microscope image (a), X-ray diffraction peaks (b), and electron  
692 probe microanalyzer mapping (c,d, e,f) of carbonate precipitate from the Sabga A spring

693 Fig. 11. The scanning electron microscope image (a), X-ray diffraction peaks (b), and electron  
694 probe microanalyzer mapping (c,d, e,f) of carbonate precipitate from the Sabga B spring

695 Fig.12. The scanning electron microscope image (a), X-ray diffraction peaks (b), and electron  
696 probe microanalyzer mapping (c,d, e,f) of carbonate precipitate from Bambui B spring

697 Fig. 13. Electron probe microanalyzer mapping of Na, Ca, Mg, and F of carbonate precipitate  
698 from Bambui B spring, showing enrichment of fluorine in the matrix of the carbonate

699 Fig. 14. The scanning electron microscope image (a), X-ray diffraction peaks (b), and electron  
700 probe microanalyzer mapping (c,d, e,f) of carbonate precipitate from Lobe D spring

701 Fig. 15. Carbonates-water oxygen isotopic fractionation temperature in observed soda springs  
702 along the CVL. Dolomites fractionated at relatively higher temperatures (35-43°C) than tronas  
703 (circum 20°C).

704  
705 Fig. 16. Plots of  $^{13}\text{C}$  and  $\delta^{18}\text{O}$  (PDB), showed observed tronas to be relatively depleted in  $^{13}\text{C}$   
706 and enriched in  $^{18}\text{O}$  (PDB).

707  
708 Fig. 17. Except for the Lobe springs that showed highest  $^{87}\text{Sr}/^{86}\text{Sr}$  ratio, in all the other observed  
709 springs the carbonate phases are relatively enriched in  $^{87}\text{Sr}/^{86}\text{Sr}$  ratio than the water phase (a),  
710 and  $^{87}\text{Sr}/^{86}\text{Sr}$  are relatively depleted in tronas than in dolomites (b)

711  
712 Fig. 18. Chloride versus fluoride cross plots showing volcanogenic contributions into the Lobe,  
713 Bambui and Nyos springs

714

715

### 716 **Table captions**

717

718 Table 1. Laboratory analytical methods of the carbonates and water phases in observed springs

719

720 Table 2. Chemical composition of water from the observed springs and shallow wells. ND: not  
721 detected. NM: not measured

722

723 Table 3. Fractionation temperature and isotopic compositions of carbonates precipitating from  
724 the observed springs

725

726

727

728

**Table 2**[Click here to download Table: Table 2.docx](#)

Table 2 :

Sample name	Code	Elevation	Temp	pH	EC	Na <sup>+</sup>	K <sup>+</sup>	Mg <sup>2+</sup>	Ca <sup>2+</sup>	SiO <sub>2</sub>	F <sup>-</sup>	Cl <sup>-</sup>	NO <sub>3</sub> <sup>-</sup>	SO <sub>4</sub> <sup>2-</sup>	HCO <sub>3</sub> <sup>-</sup>	As	δD	δ <sup>18</sup> O	<sup>87</sup> Sr/ <sup>86</sup> Sr
		m.asl	°C	-	µS/cm	mg/L	mg/L	mg/L	mg/L	mg/L	mg/L	mg/L	mg/L	mg/L	mg/L	mg/L	ppm	‰	‰
Bambui Bssp	WS12	1290	22.2	7.0	1650	214	22.2	95.9	248.1	49.12	2	4.8	2.03	4.8	994.4	ND	-36.21	-6.30	0.708618 ± 0.000017
Bambui Assp	WS14	2082	21.8	7.4	1010	351	16.51	21	277.7	17.7	6.78	31.1	1.8	0.36	147.7	ND	-39.41	-6.10	0.70873 ± 0.000021
Lobe Assp	WS10	30	47.4	6.4	12840	1650	70	95	28.2	24.5	35	2130	22.6	113.9	2118	0.009	-32.21	-4.68	0.713340 ± 0.000015
Lobe Dssp	WS9	30	49.0	6.4	13130	1630	66.6	78.64	382.85	25.1	37.1	2198	22.22	99.81	652.9	0.007	-34.76	-4.65	0.713343 ± 0.000013
SabgaA ssp	WS7	1456	20.0	7.5	10710	1240	46.7	13.1	224.4	20.5	3.7	1.59	0.19	6.52	3103	1.33	-41.82	-6.30	0.708808 ± 0.000024
SabgaB ssp	WS6	1535	19.3	7.2	5030	243	79	76.5	275	14.8	4.3	229	0.69	6.72	747	0.015	-39.84	-6.01	0.709314 ± 0.000026
Well 1	WW1	49	27.7	4.5	145	9.94	1.21	0.78	3.06	3.05	0.04	14.7	3.8	23	0.67	ND	-27.94	-3.35	NM
Well 2	WW2	39	28.0	4.9	87	15.69	0.59	1.13	2.79	4.22	0.5	24.95	5.01	5.09	7.32	ND	-30.55	-3.37	NM
Well 3	WW3	51	27.0	4.3	109	7.22	0.78	1.7	3.6	3.38	0.08	10.72	2.57	2.5	13.42	ND	-29.98	-3.1	NM
Well 4	WW4	54	26.0	5.2	54	9.89	1.99	0.5	7.6	5.99	0.19	17.75	8.06	2.33	3.72	ND	-26	-3.27	NM
Well 5	WW5	46	27.0	5.7	229	14.3	1.64	0.75	6.1	9.7	0.19	23.07	9.31	3.98	8.54	ND	NM	NM	NM
Well 6	WW6	51	28.0	6.0	482	322	10.2	46.1	62.4	6.54	1.8	87.33	5.81	261.9	567.4	ND	-31.67	-3.35	0.705157 ± 0.000014
Nyos sodaCssp	NS1	1000	24.0	5.4	198	11.7	422	15	13.2	3.4	0.09	0.6	0.24	1.6	137	ND	-31.12	-3.40	0.70746 ± 0.000029
Nyos soda	NS2	1000	23.0	5.7	536	26	8.11	43	28	4.1	0.01	1.26	0.04	4.15	346	ND	-31.22	-3.59	0.707 ± 0.000014





Figure 1  
[Click here to download high resolution image](#)

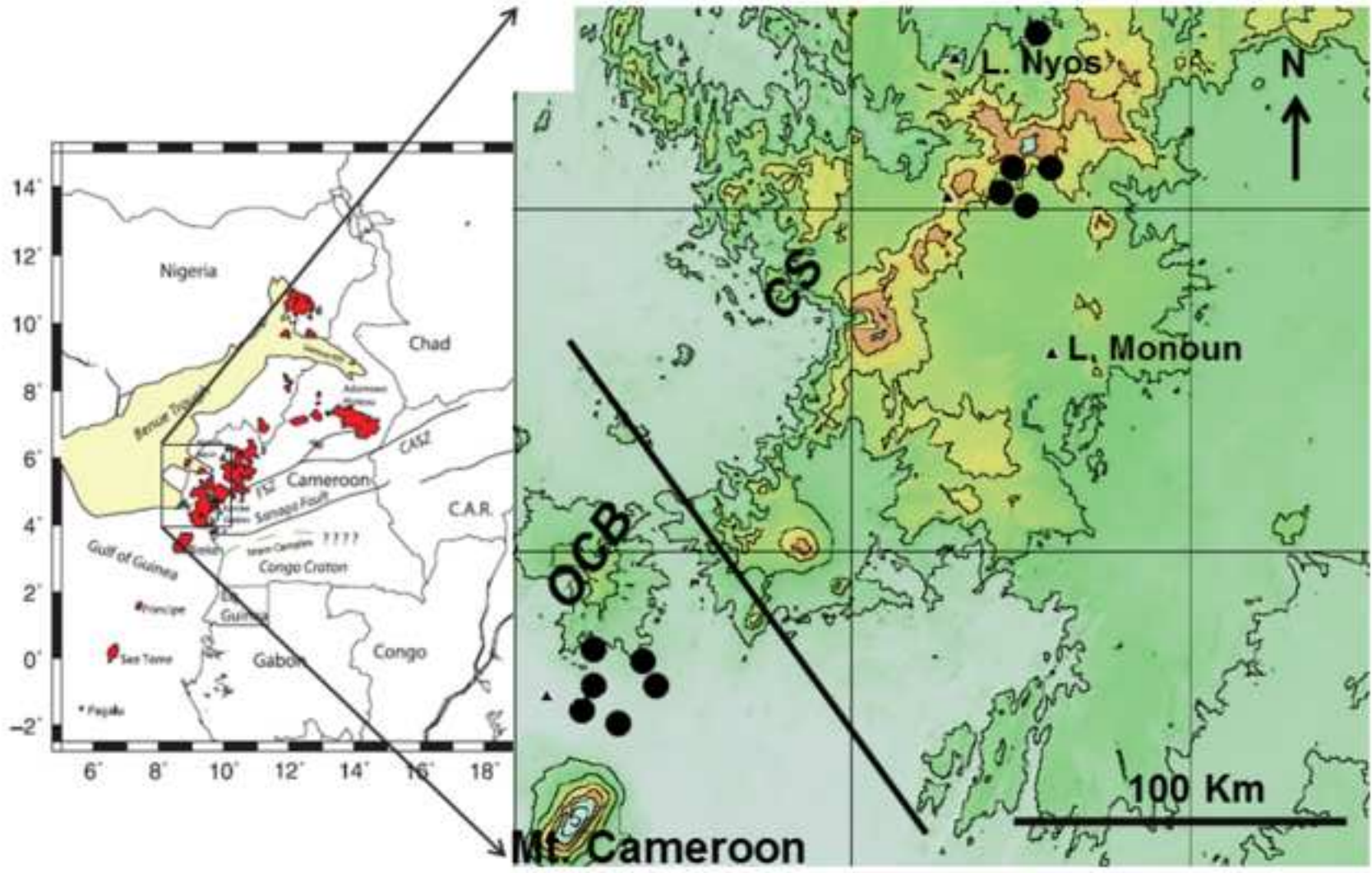


**Figure 2**  
[Click here to download high resolution image](#)



Figure 3  
[Click here to download high resolution image](#)

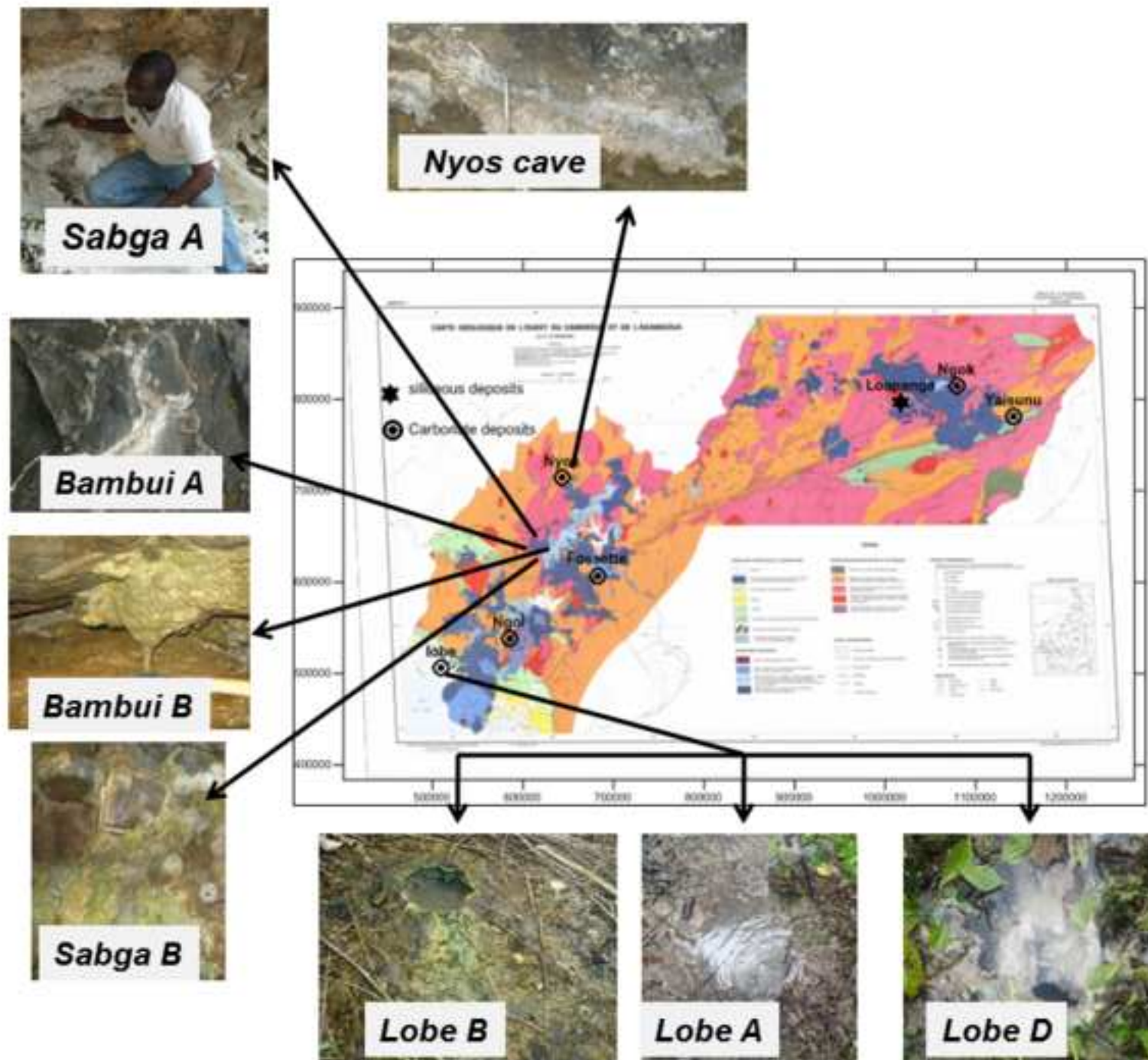


Figure 4  
[Click here to download high resolution image](#)

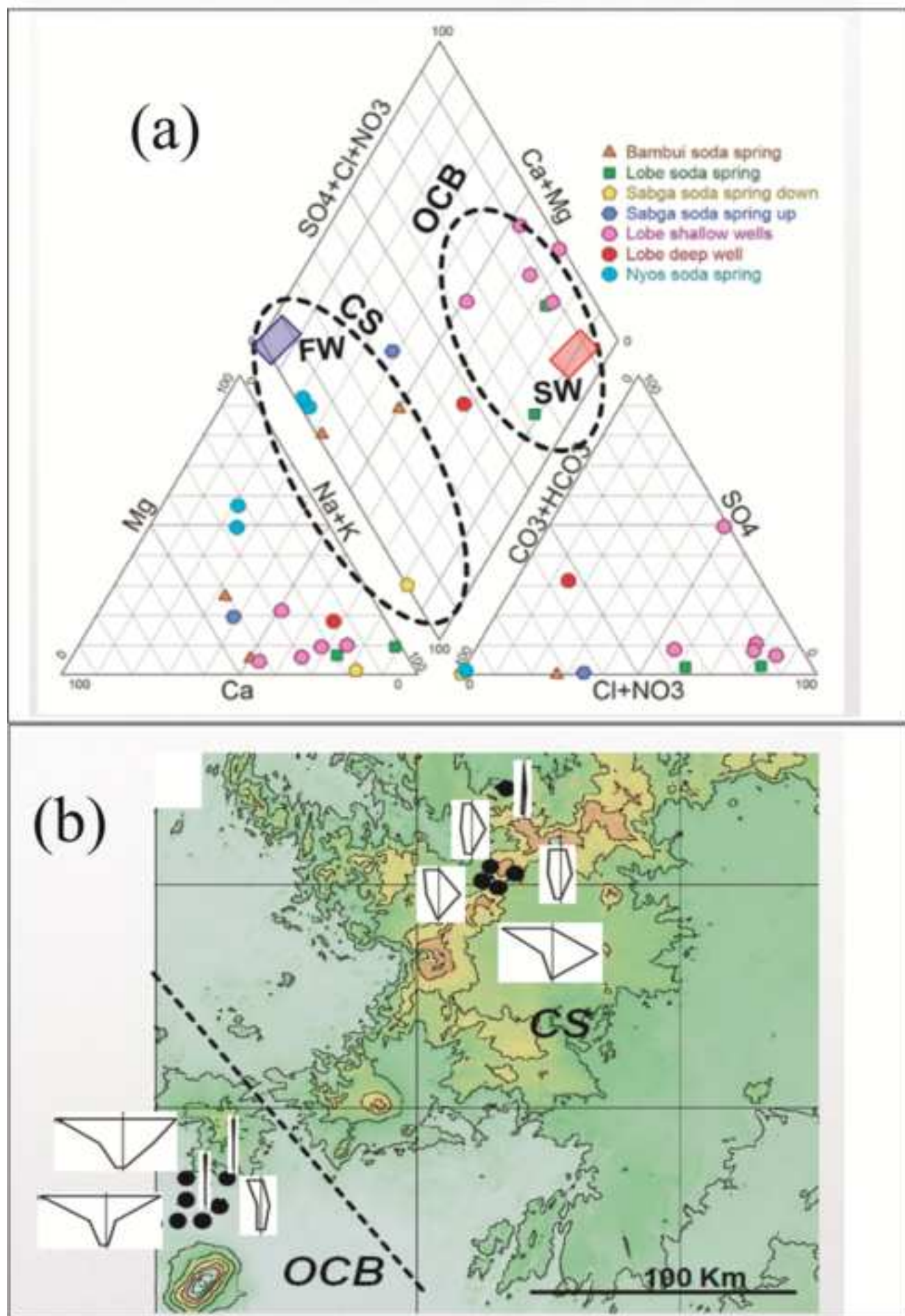


Figure 5  
[Click here to download high resolution image](#)

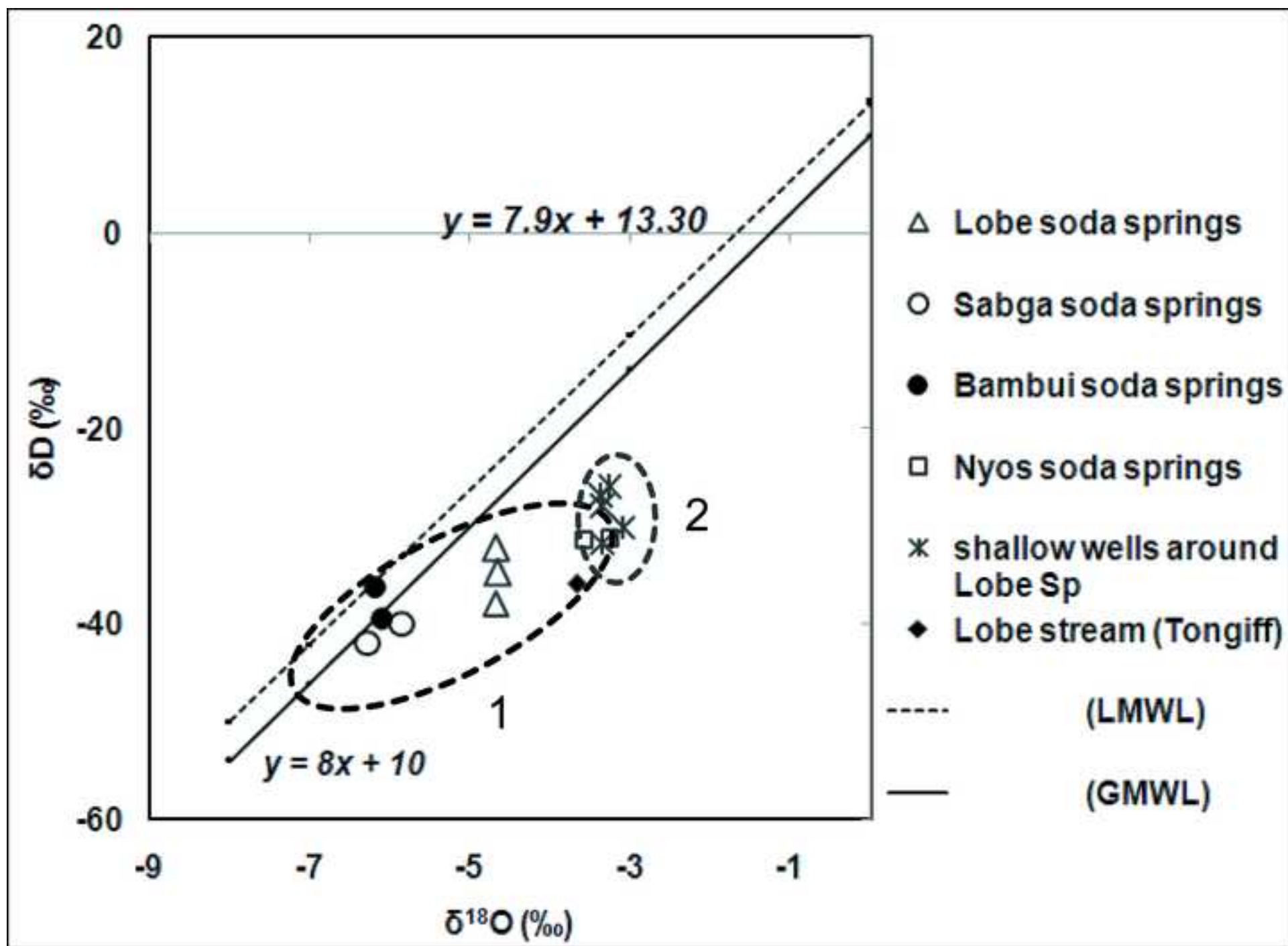


Figure 6  
[Click here to download high resolution image](#)

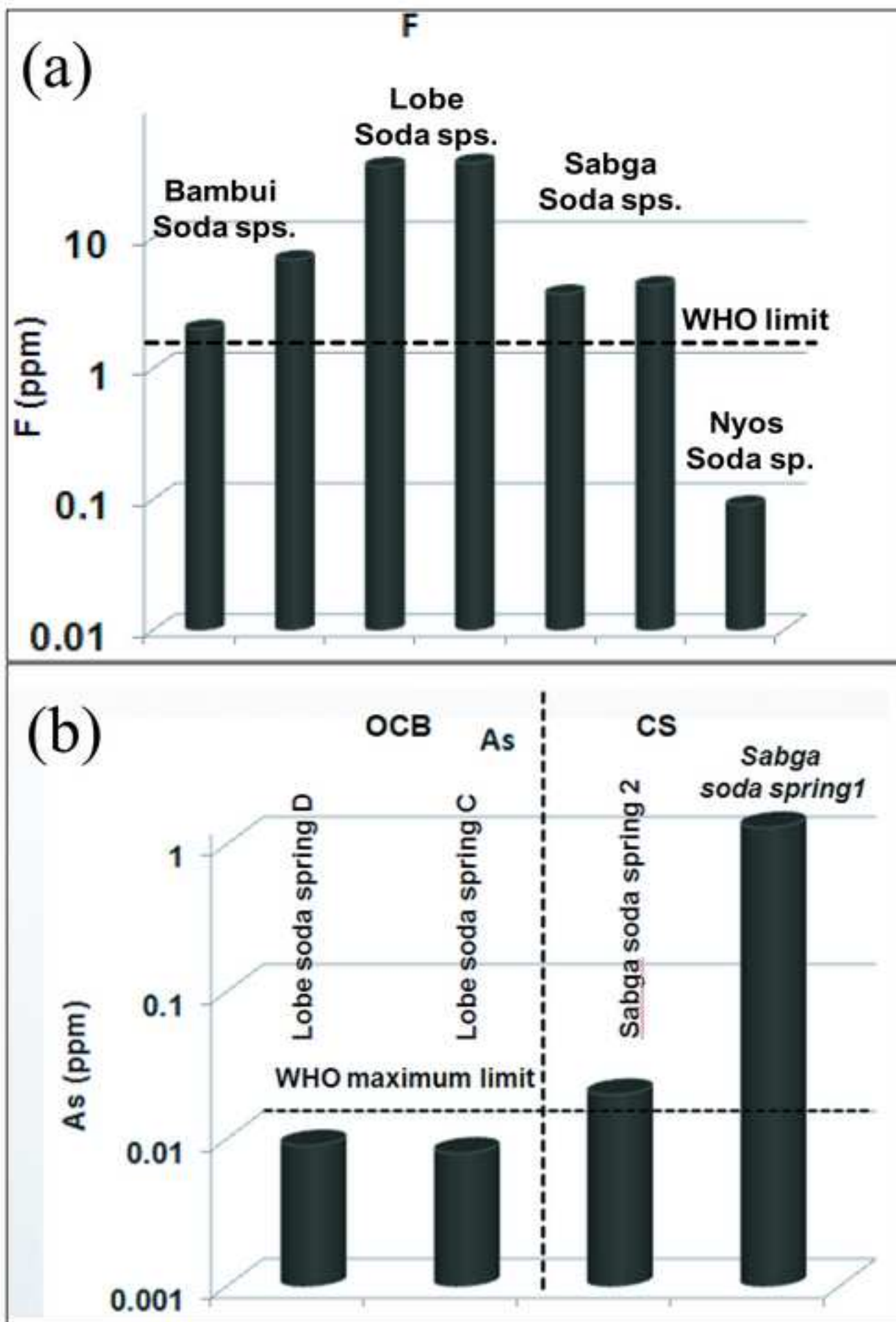


Figure 7  
[Click here to download high resolution image](#)

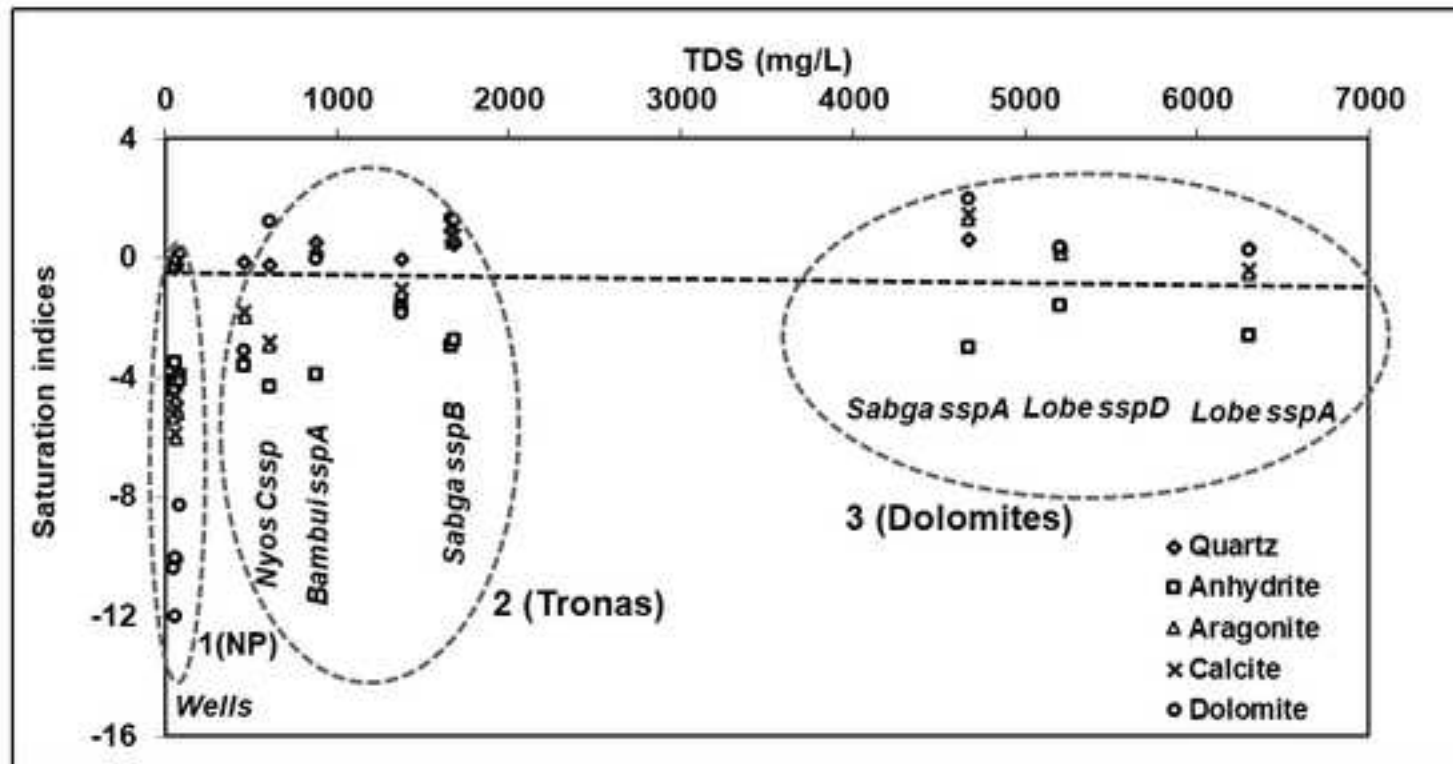


Figure 8  
[Click here to download high resolution image](#)

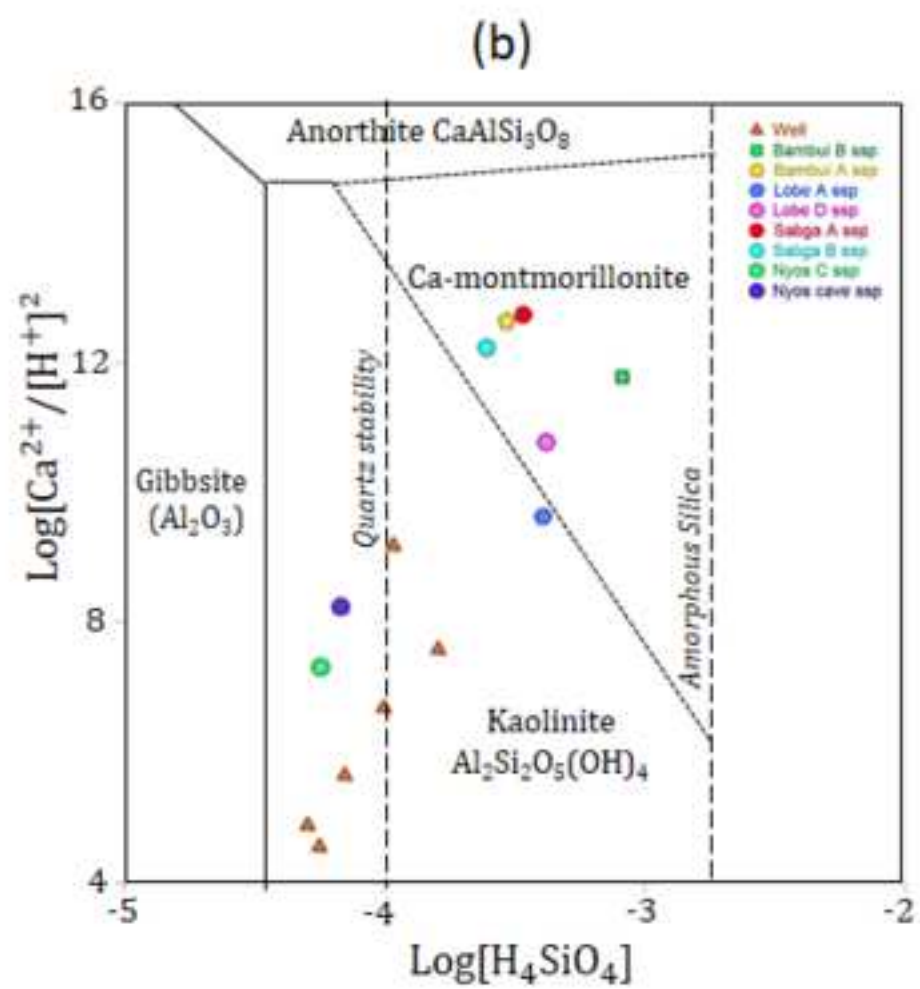
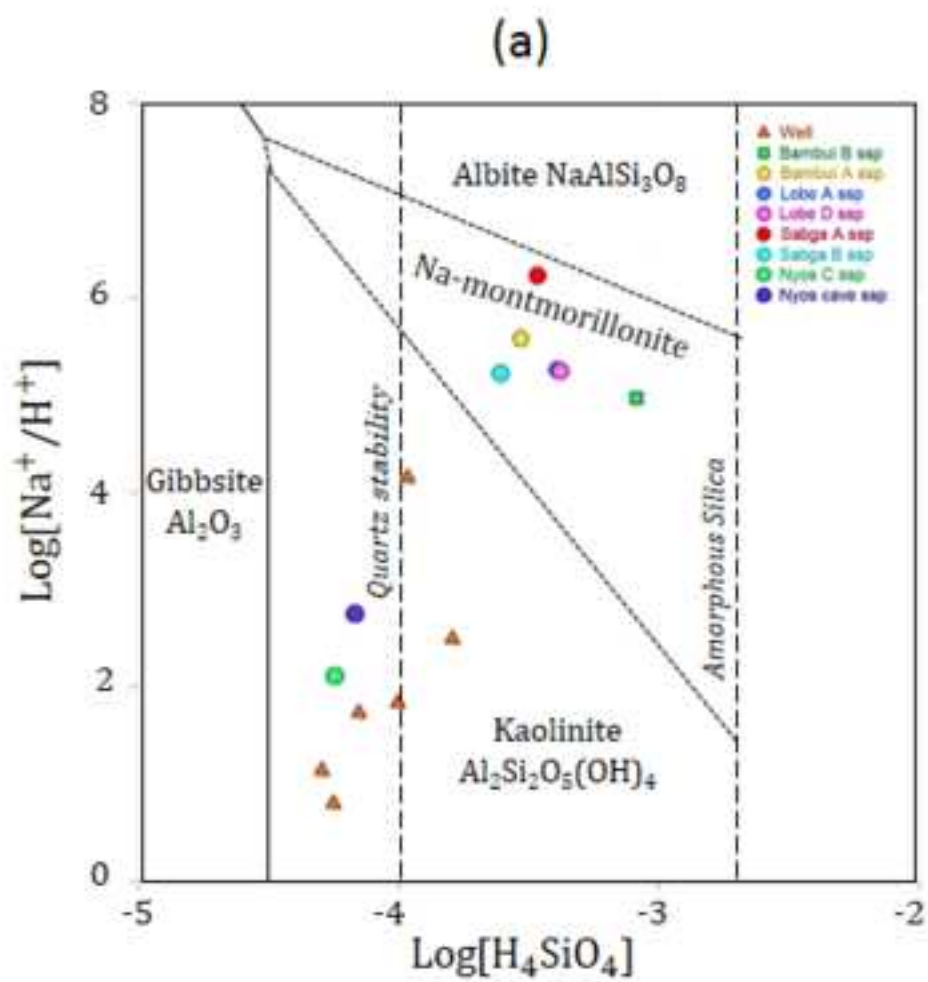




Figure 10  
[Click here to download high resolution image](#)

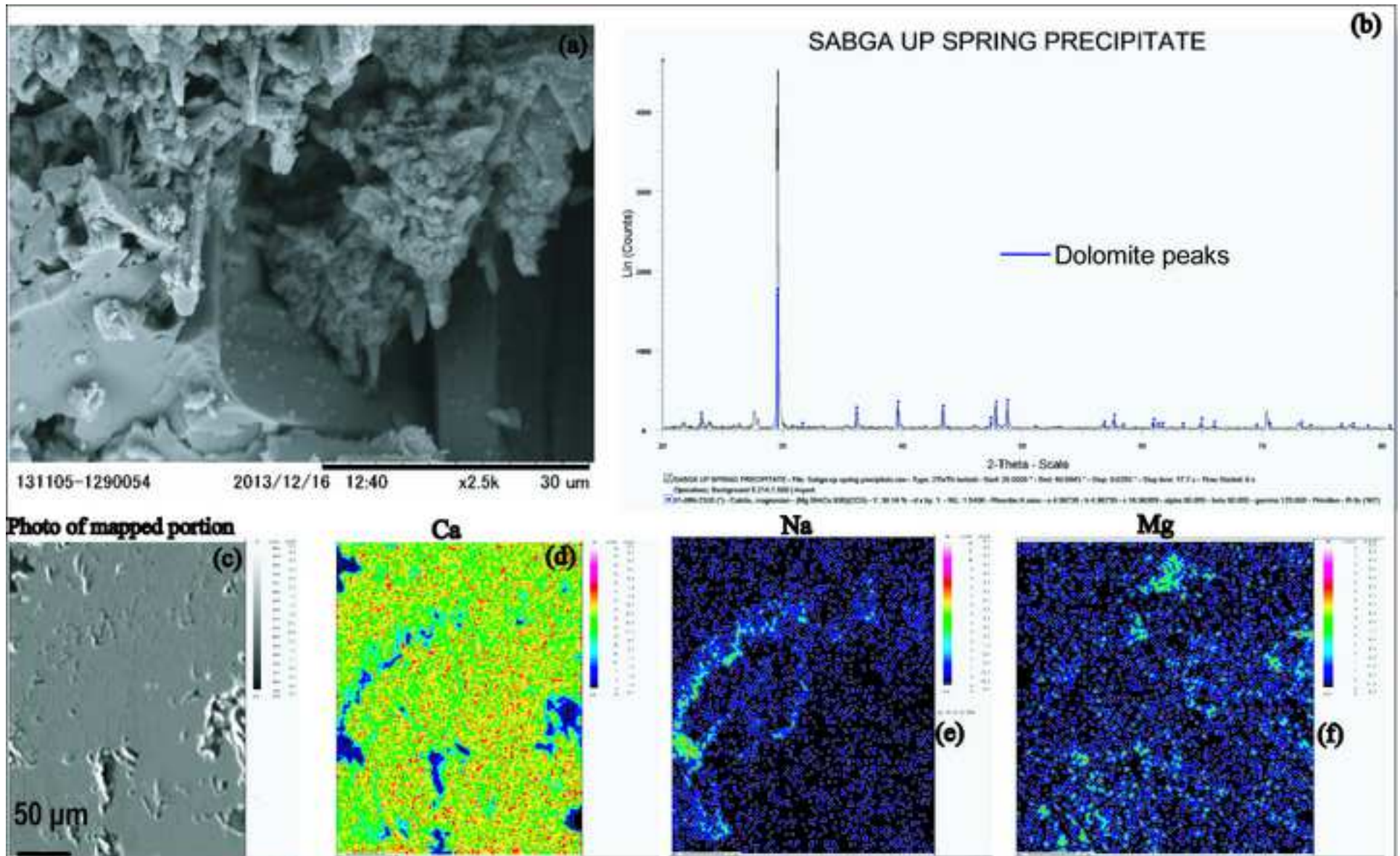


Figure 11

[Click here to download high resolution image](#)

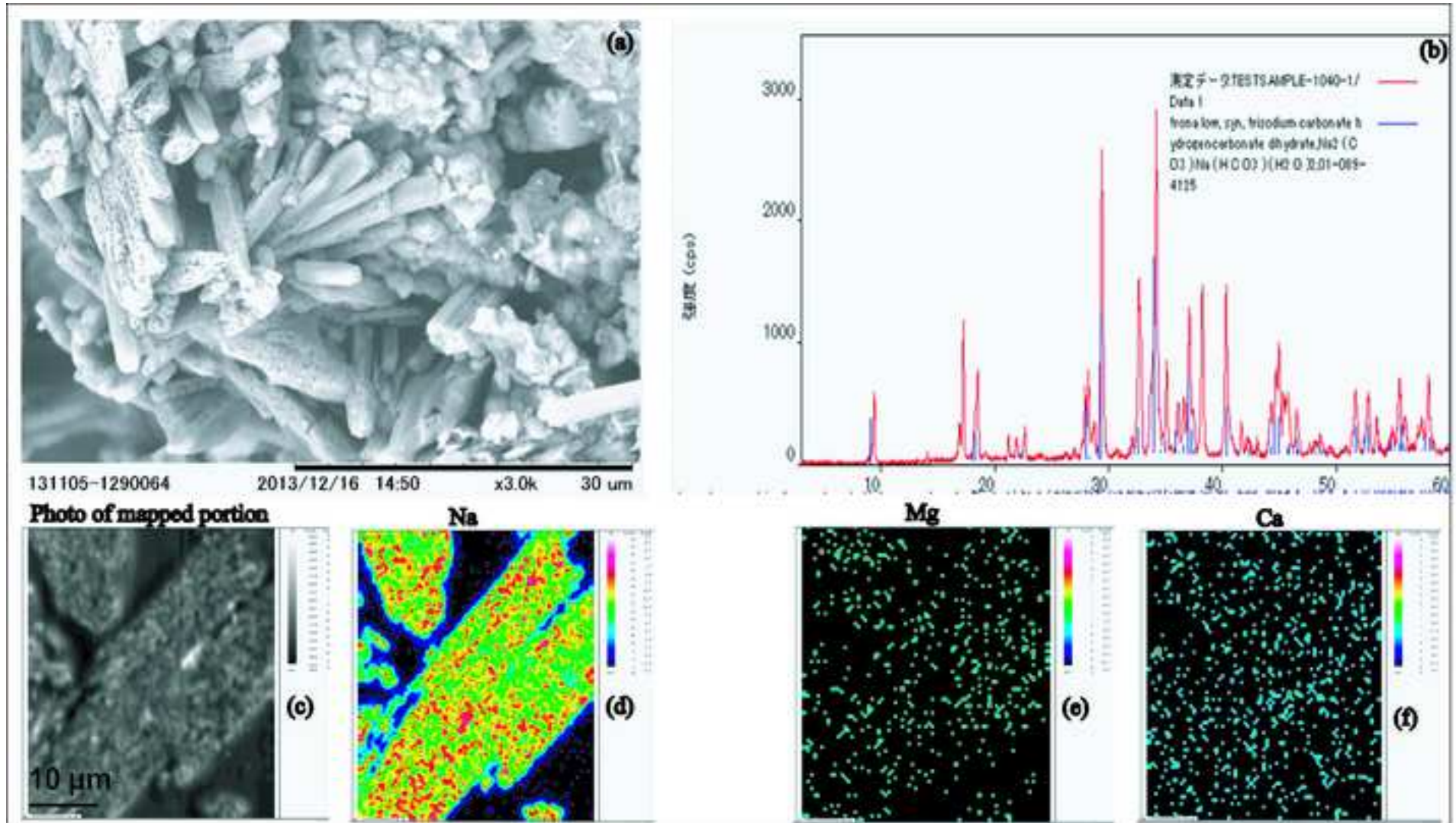




Figure 13  
[Click here to download high resolution image](#)

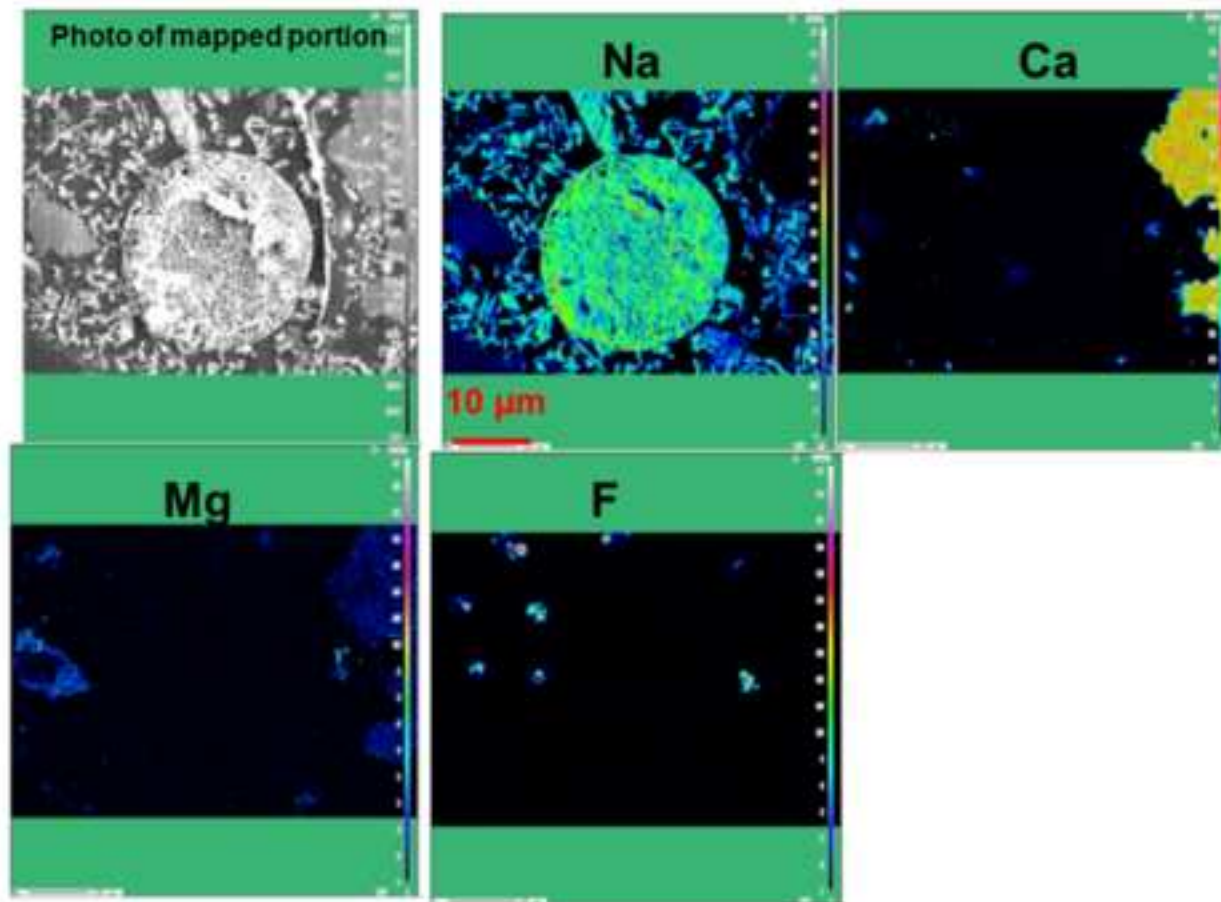




Figure 15

[Click here to download high resolution image](#)

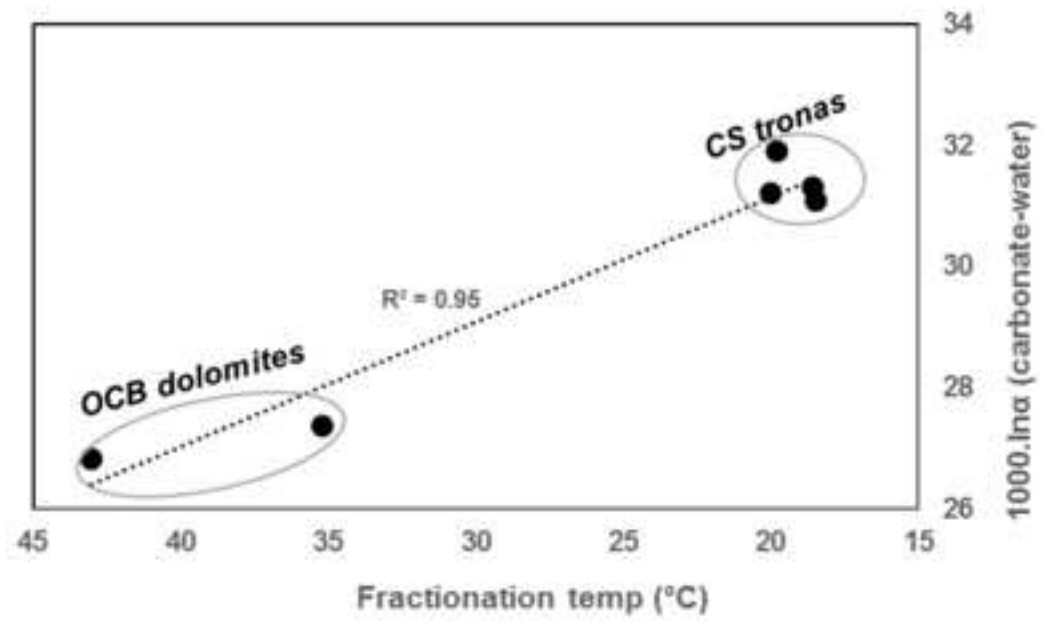


Figure 16  
[Click here to download high resolution image](#)

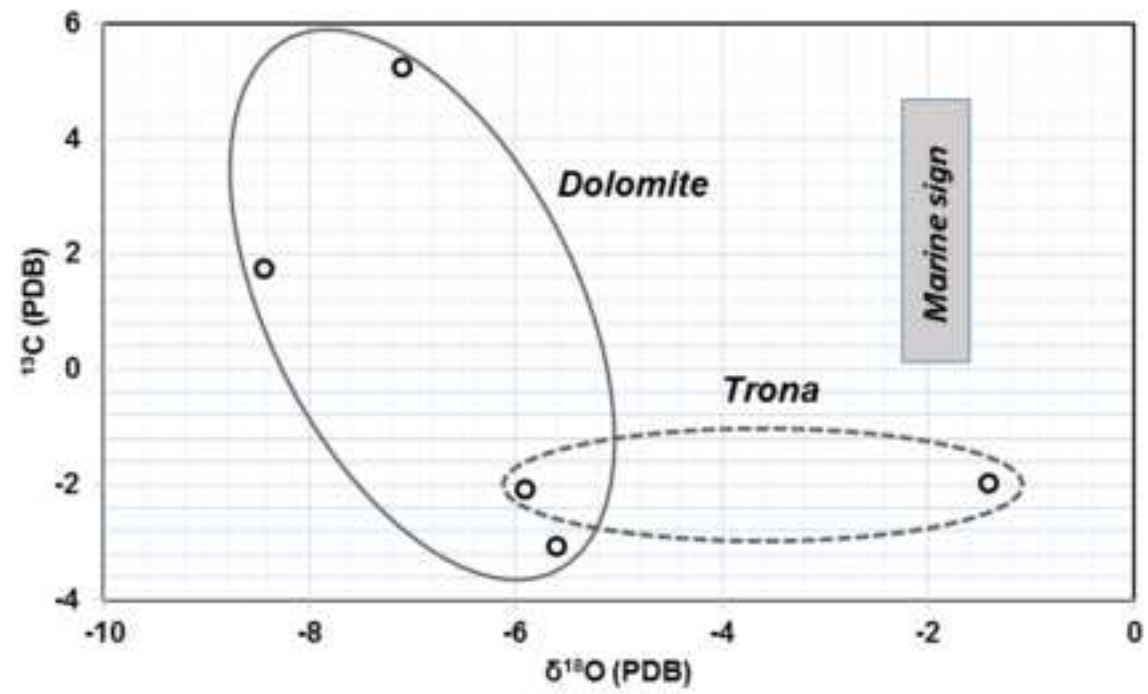


Figure 17a

[Click here to download high resolution image](#)

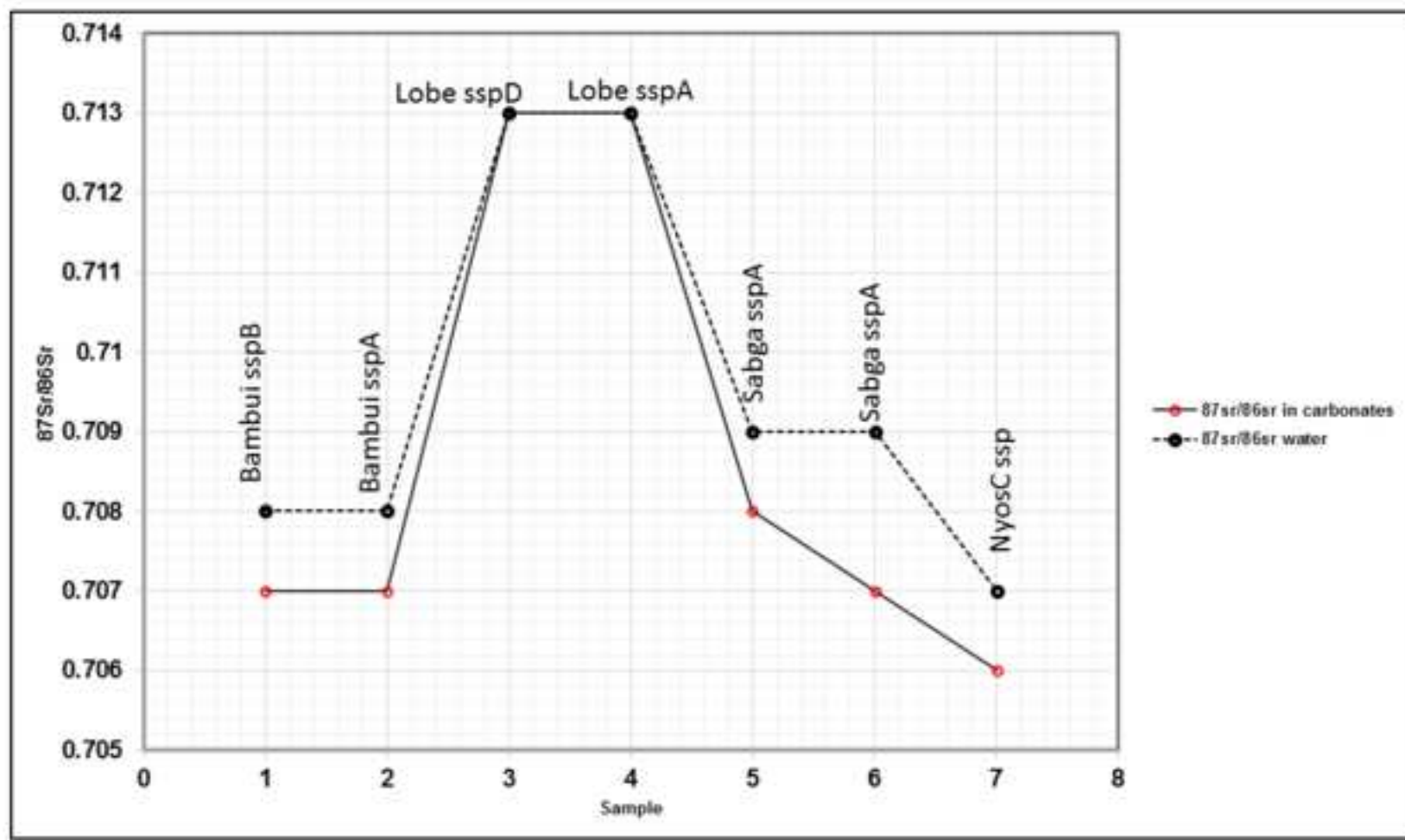


Figure 17b  
[Click here to download high resolution image](#)

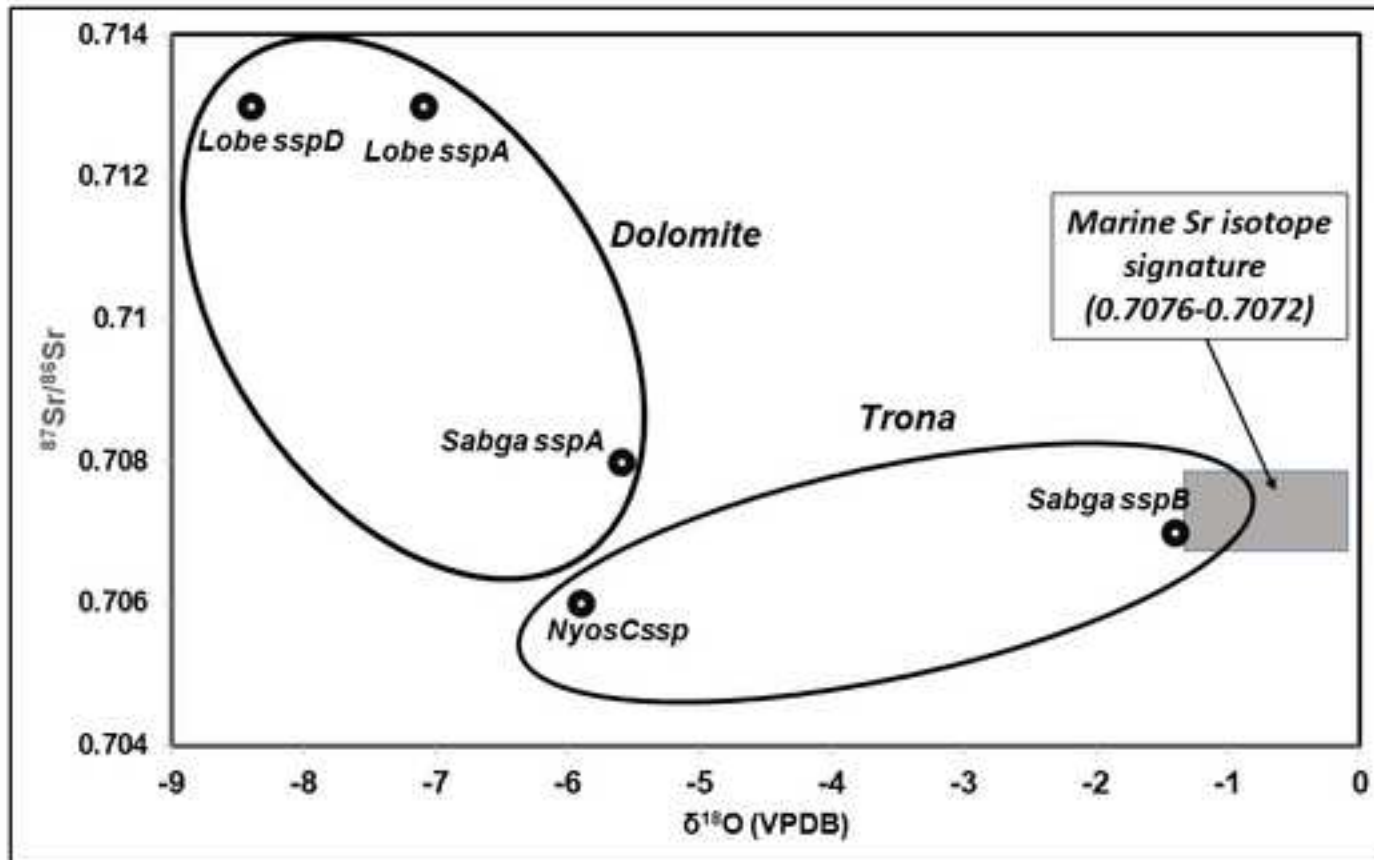
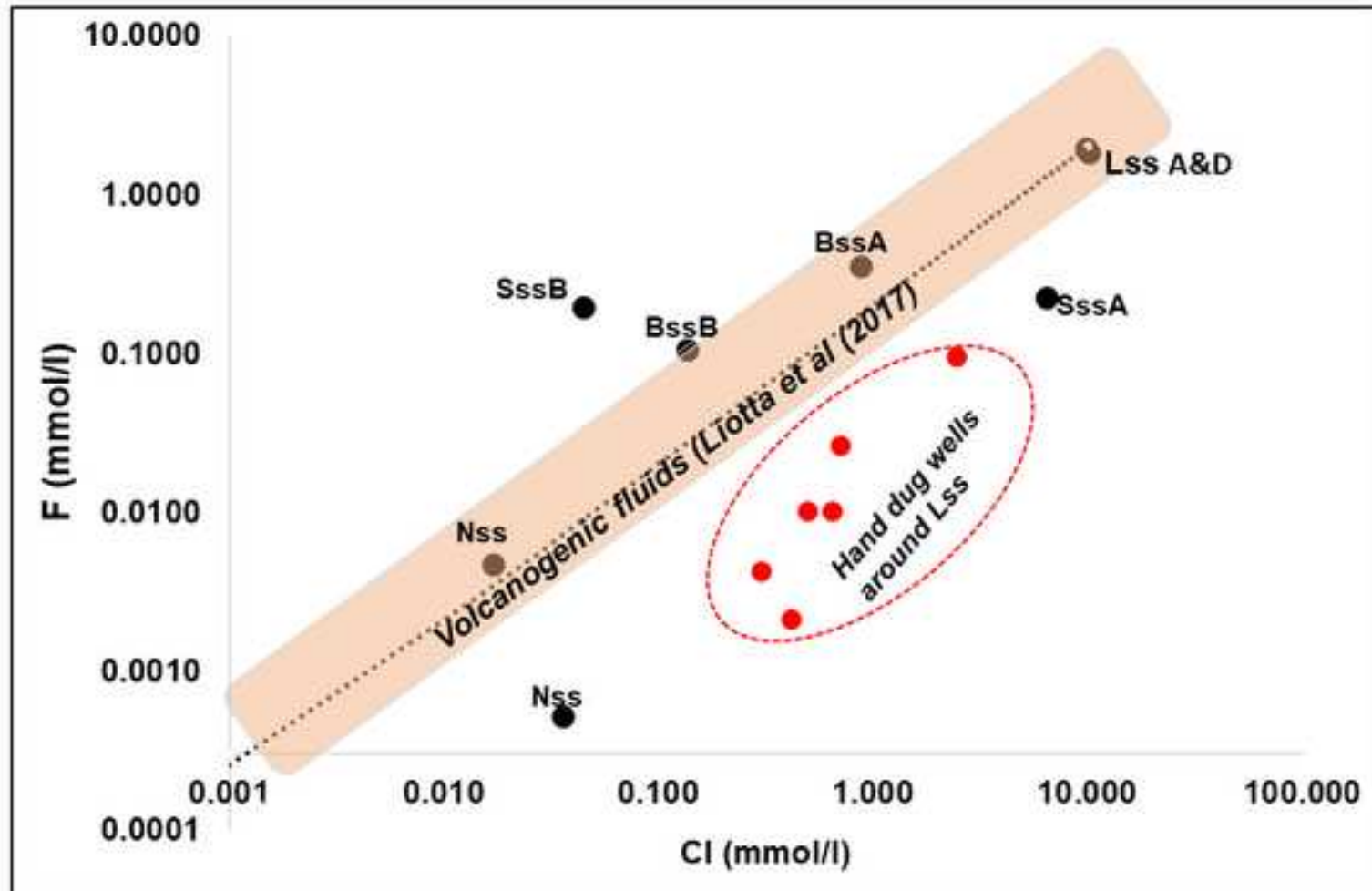


Figure 18 Revised

[Click here to download high resolution image](#)



**Major ions,  $\delta^{18}\text{O}$ ,  $\delta^{13}\text{C}$  and  $^{87}\text{Sr}/^{86}\text{Sr}$  compositions of water and precipitates from springs along the Cameroon Volcanic Line (Cameroon, West Africa): Implications for provenance and volcanic hazards**

Wilson Yetoh FANTONG<sup>1Ψ</sup>, Brice Tchakam KAMTCHUENG<sup>1</sup>, Yasuo ISHIZAKI<sup>2</sup>, Ernest Chi FRU<sup>3</sup>, Emilia Bi FANTONG<sup>4</sup>, Mengnjo Jude WIRMVEM<sup>1</sup>, Festus Tongwa AKA<sup>1</sup>, Bertil NLEND<sup>1</sup>, Didier HARMAN<sup>4</sup>, Akira UEDA<sup>5</sup>, Minoru KUSAKABE<sup>5</sup>, Gregory TANYILEKE<sup>1</sup>, Takeshi OHBA<sup>6</sup>

<sup>1</sup> Hydrological Research Center/ IRGM, Box 4110, Yaounde-Cameroon

<sup>2</sup> Graduate School of Science and Engineering and Research, Environmental and Energy Sciences, Earth and Environmental Systems

<sup>3</sup> School of Earth and Ocean Sciences, Cardiff University, Cardiff, Park Place, Wales-United Kingdom

<sup>4</sup> Ministry of Secondary Education, Cameroon

<sup>5</sup> Laboratory of Environmental Biology and Chemistry, University of Toyama, Gofuku 3190, Toyama 930-8555 Japan

<sup>6</sup> Department of Chemistry, School of Science, Tokai University, Hiratsuka, 259-1211, Japan

Ψ Corresponding author: [fyetoh@yahoo.com](mailto:fyetoh@yahoo.com); [fantongy@gmail.com](mailto:fantongy@gmail.com)